構造

小野 克彦

H7. 3

Studies on Novel Organic Redox Systems Containing Fused 1,2,5-Thiadiazole Rings

Katsuhiko Ono

DOCTOR OF PHILOSOPHY

Department of Structural Molecular Science
School of Mathematical and Physical Science
The Graduate University for Advanced Studies

1994

Contents

Chapter 1 Introduction

Introduction

Recently much attention has been focused on the development of organic conductors and superconductors.[1] For this purpose, syntheses of new electron donors and acceptors are very important. One of the important points for the molecular design is to extend π-conjugation in order to reduce on-site Coulombic repulsion.[2] The other is to form highly dimensional crystal structures with intermolecular interactions.[3] From these viewpoints, 1,2,5-thiadiazole rings are of interest since they have extended π-conjugation and polarized heteroatoms resulting in strong intermolecular interactions by heteroatom contacts. Introduction of fused thiadiazole rings into redox systems affords various new types of electron donors or acceptors. Furthermore, since thiadiazoles are electron-withdrawing heterocycles, compounds with both thiadiazole rings and electron-donating ones are expected to have a high polarizability, an intramolecular charge-transfer (CT) interaction, and an enhanced amphoteric redox ability. In my research work, I designed some new types of redox systems containing thiadiazole moieties, and investigated their electronic properties and crystal structures. In this chapter, I briefly describe some previous work relating to redox systems containing fused thiadiazole rings and the framework of the present thesis.

Redox Systems containing Fused Thiadiazole Rings

Syntheses of new electron acceptors comparable to tetracyanoquinodimethane (TCNQ) have been desirable. Bis([1,2,5]thiadiazolo)tetracyanoquinodimethane (BTDA)

was designed for this request.[4] It is a TCNQ derivative containing fused thiadiazole units and has a larger expanded π-electron system. Although the reduction potentials (E_1 = -0.02 V, E_2 = -0.49 V vs. SCE)[5] are a little lower than those of TCNQ (E_1 = +0.18 V, E_2 = -0.36 V)[5], the on-site Coulombic repulsion is decreased (BTDA: ΔE = 0.47, TCNQ: ΔE = 0.54). Therefore, BTDA is regarded as a good electron acceptor for organic conductors. In practice, BTDA reacted with tetrathiatetracene (TTT) or dimethyldihydrophenazine (DMPH) to give highly conductive CT complexes (TTT: σ_{rt} = 3.4 S cm^{-1}; DMPH: σ_{rt} = 6.7 S cm^{-1}).[6] Moreover, the CT complex of TSeT was found to show metallic behavior down to 1.5 K without a Peierls transition (σ_{rt} = 2000 S cm^{-1}).[7] Many kinds of anion radical salts were also prepared, and their properties were investigated in detail.[8]

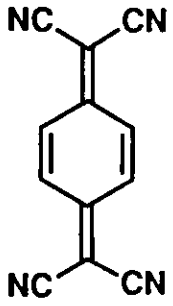

TCNQ

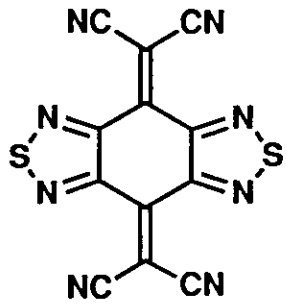

BTDA

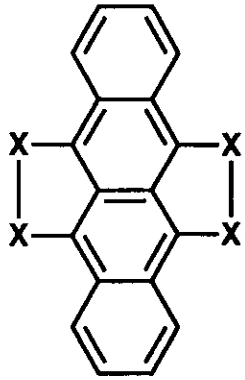

X = S TTT
X = Se TSeT

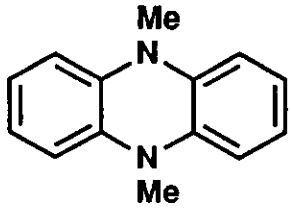

DMPH

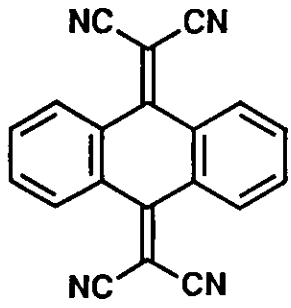

TCNAQ

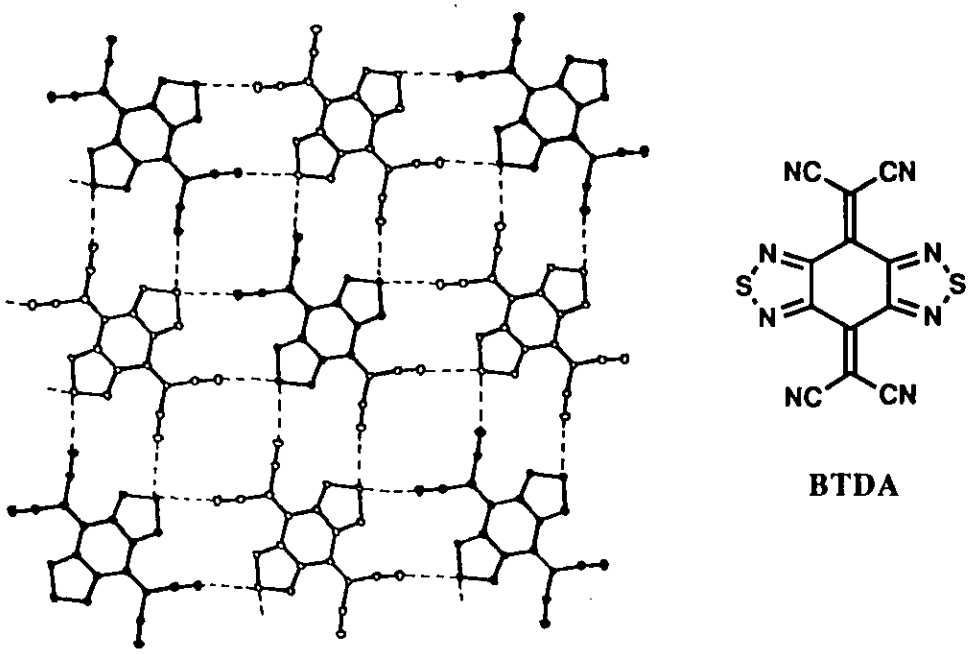

BTDA

Figure 1. View of the sheet-like network of BTDA. Broken lines reveal short S•••N interactions (3.03 Å). (*Chem. Lett.*, **1986**, 1433.)

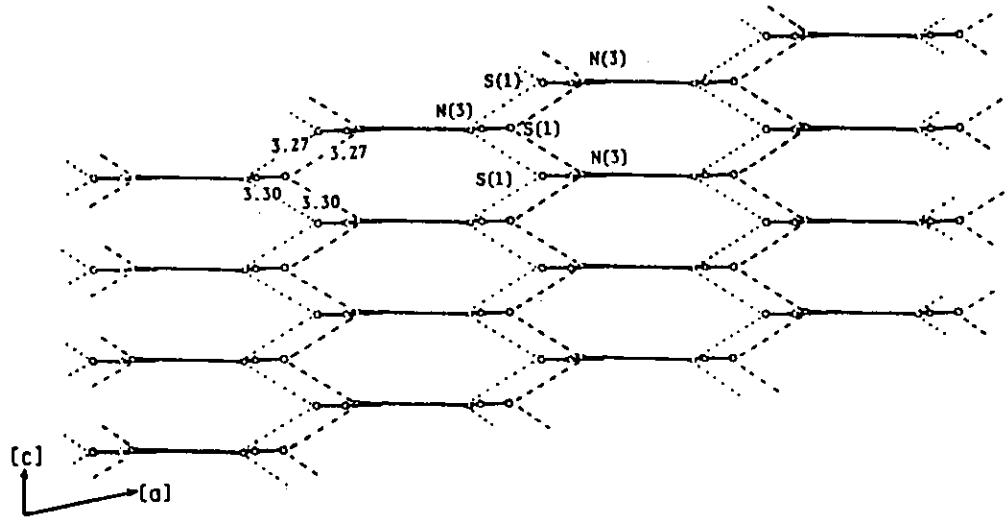

Figure 2. Honeycomb-like network of BTDA in the *n*-Bu_3NMe salt. Only BTDA molecules are shown for clarity. Broken lines reveal short S•••N contacts. (*Bull. Chem. Soc. Jpn.*, **1988**, *61*, 483.)

The molecular structure of BTDA is planar and fairly different from that of tetracyanoanthraquinodimethane (TCNAQ), which is butterfly-shaped because of the steric hindrance between the CN groups and the *peri*-hydrogen atoms.[9] The crystal structure is composed of a two-dimensionally expanded molecular sheet as shown in Figure 1.[10] The most important feature is the transverse interaction between the S atoms of the thiadiazole rings and the N atoms of the TCNQ skeleton. The contact distance of 3.03 Å is much shorter than the sum of their van der Waals radii (3.35 Å). These S•••N≡C contacts were also found in the anion radical salts and the CT complexes with several types of donors. In the *n*-Bu_3NMe salt, the BTDA molecules are arranged to form a ribbon-like network with short S•••N≡C contacts along the *a* axis, resulting in the formation of a three-dimensional honeycomb-like structure as shown in Figure 2.[8] The electrical conductivity of the single crystal was 6.3 x 10^{-2} S cm^{-1} and the small anisotropy was characterized (14 : 1 along the *c* and *a* axes).

BTDA interacts with donor molecules such as benzene, xylene, dimethylnaphthalene, and tetrathiafulvalene (TTF) to afford the inclusion crystals forming the tight network structures of BTDA.[11] Recently, it was demonstrated that the CT crystals of *o*-divinylbenzene give the optical pure adduct with 95% ee upon irradiation.[12] Such inclusion crystals derived from BTDA are attractive from the viewpoint of absolute asymmetric syntheses. 4,7-Bis(dicyanomethylene)-4,7-dihydro[2,1,3]benzothiadiazole

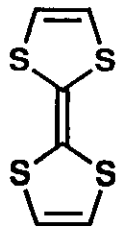

TTF

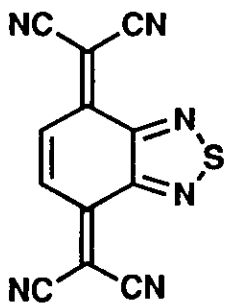

TDA

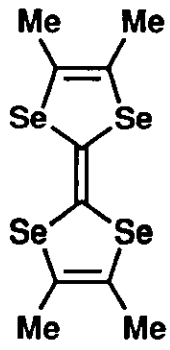

TMTSF

(TDA), which has one fused thiadiazole ring, does not supply such an inclusion crystal because of the failure to form a sheet-like network.[13] TDA afforded highly conductive CT complexes with TTF or tetramethyltetraselenafulvalene (TMTSF) (TTF: σ_{rt} = 1.3 S cm^{-1}; TMTSF: σ_{rt} = 0.71 S cm^{-1}).

Although 2,2′-*p*-quinobis(1,3-dithiole) (QBT) is of interest as a strong electron donor (E_1 = -0.11 V, E_2 = -0.04 V vs. SCE)[5] with decreased Coulombic repulsion (ΔE = 0.07), it is too unstable to give organic metals because of the strong quinoid character.[14] 4,7-Bis(1,3-dithiol-2-ylidene)-4,7-dihydro[2,1,3]benzothiadiazole (TQBT) was designed for an improvement of QBT.[15] The oxidation potentials (E_1 = +0.36 V, E_2 = +0.53 V vs. SCE)[16] are lower than that of TTF (E_1 = +0.46 V, E_2 = +0.87 V)[16], and the difference between the first and second oxidation potentials is small (TQBT: ΔE = 0.17, TTF: ΔE = 0.41). Thus, TQBT is a good electron donor with small on-site Coulombic repulsion. The complex of the tetramethyl-derivative and TCNQ showed highly conducting behavior (σ_{rt} = 0.56 S cm^{-1}). The cation radical salts with PF_6 or AsF_6 were both metallic down to 100 K (PF_6 salt: σ_{rt} = 100 S cm^{-1}; AsF_6 salt: σ_{rt} = 68 S cm^{-1}), although the ClO_4, BF_4, and ReO_4 salts showed semiconducting behavior.

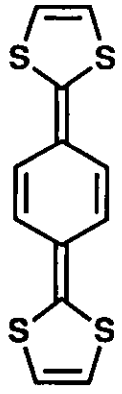

QBT

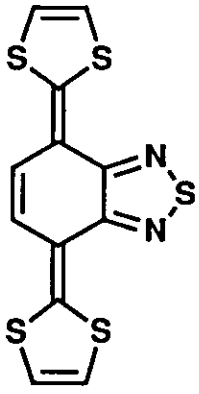

TQBT

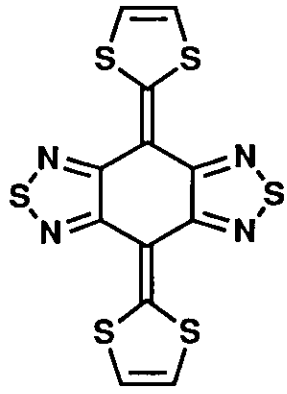

BTQBT

4*H*,8*H*-4,8-Bis(1,3-dithiol-2-ylidene)benzo[1,2-*c*:4,5-*c*´]bis([1,2,5]thiadiazole) (BTQBT), which has two fused thiadiazole rings, is not good as an electron donor because of its weak electron-donating ability and low solubility. However, BTQBT shows a high electrical conductivity as a single component.[17] Its electrical behavior is ascribable to short S•••S contacts and an intermolecular CT interaction in the crystal. Furthermore, donor molecules **1**[18], **2**[19], and **3**[20] were synthesized, and their electrical properties and crystal structures were investigated.

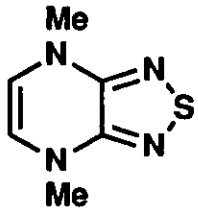

1

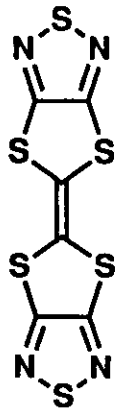

2

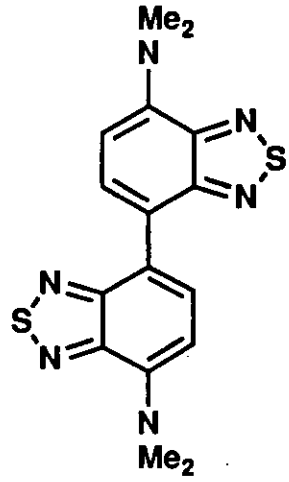

3

The advantages of introduction of fused thiadiazole rings for electron donors or acceptors are summarized as follows. (i) On-site Coulombic repulsion is decreased owing to the extended π-conjugation. (ii) Intermolecular interactions are increased through short S•••N contacts. (iii) Highly polarized molecules are obtained by combination with electron-donating parts. (iv) Anion species are stabilized by the electron-withdrawing property. (v) Molecular planarity is maintained due to no steric hindrance.

Framework of Present Thesis

My research work is characterized by the development of various novel types of redox systems containing 1,2,5-thiadiazole rings. The present thesis deals with electron donors and donor-π-acceptor molecules. Designed molecules for each chapter are as follows.

Chapter 2 describes the preparation, properties, and X-ray crystal structure analysis of 7-(1,3-dithiol-2-ylidene)-4-methyl-4,7-dihydro[1,2,5]thiadiazolo[3,4-*b*]pyridine **4**. Compound **4** and its derivatives are of interest as novel electron donors analogous to compound **1** and 4-(1,3-dithiol-2-ylidene)-1-methyl-1,4-dihydropyridine **5**, which has not been prepared except for the dibenzo-derivative.[21] The absorption spectra show the intramolecular CT bands owing to the donor-π-acceptor moiety, and the CV study demonstrates the strong electron-donating ability of **4**. The planar structure and the intramolecular S•••N contact are revealed by the X-ray crystal structure analysis. The crystal structure shows the effective overlap between the HOMO and LUMO and the columns connected by intermolecular short S•••S contacts. Molecular orbital (MO) calculations are used for characterization of their electronic properties and polarizability. The properties of their CT complexes and cation radical salts and their electrical conductivities are investigated.

Nonplanar donors or acceptors giving organic conductors are very few. Chapter 3 describes nonplanar donor molecule **6**, which contains fused benzene and fused thiadiazole rings. The X-ray crystal structure analysis reveals the unique butterfly-shaped structure and intramolecular short S•••N contacts. Uniform columnar stacking is also demonstrated, and the good electrical conductivity as a single component is attributable to the effective intermolecular overlap in the crystal. Furthermore, the structure is compared with that of its cation radical salt.

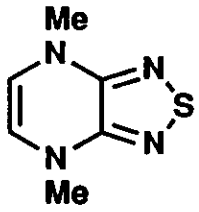

1

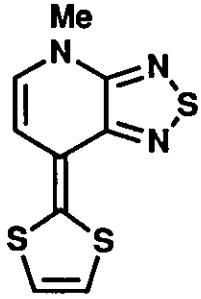

4

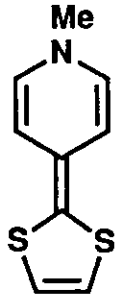

5

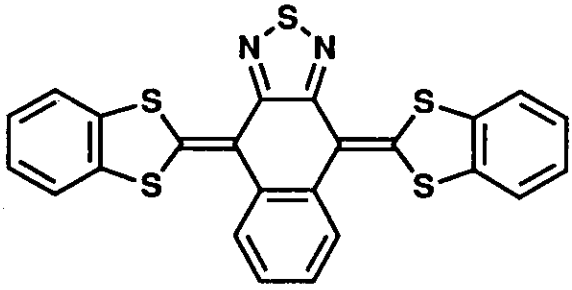

6

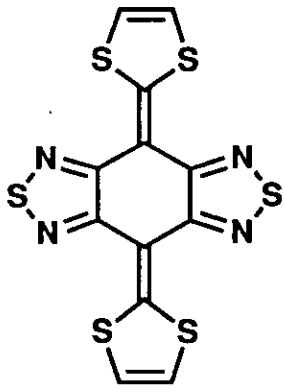

BTQBT

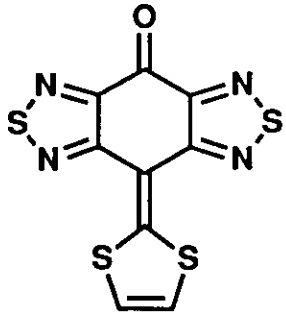

BTQT

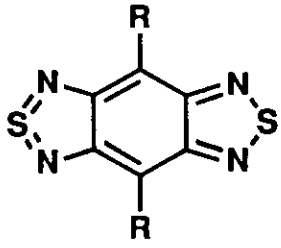

7

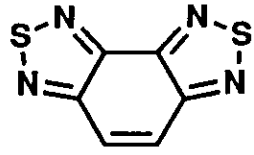

8

Molecules containing both donor and acceptor units are expected to exhibit unusual electrical properties owing to intramolecular CT interactions. BTQBT is one of the most electrical conducting materials as a single component.[17] Its electrical behavior is ascribable to strong intermolecular interactions in the crystal. One of the 1,3-dithiole groups of BTQBT is replaced with a carbonyl group to give BTQT, which has a more polarized structure than BTQBT. Chapter 4 deals with the X-ray crystal structure analysis and electrical behavior of BTQT. The molecular overlap is close to that of BTQBT, suggesting that an intermolecular CT interaction exists. On the other hand, the crystal structure is in sharp contrast with that of BTQBT. Three-dimensional intermolecular interactions through short S•••S, S•••N, and S•••O contacts are demonstrated. The MO calculations indicate that these S•••N and S•••O contacts are attributed to an electrostatic effect due to the highly polarized molecular structure. The electrical conducting behavior fails to obey Ohm's law. The non-ohmic behavior observed here is unprecedented as organic crystals.

Chapter 5 is concerned with novel heterocycles, benzo[1,2-*c*:4,5-*c*´]bis-([1,2,5]thiadiazole)s **7** and the monoselenium analogues, which contain a tetravalent sulfur atom. They are characterized by much high electron affinities and long absorption maxima compared with those of the related Kekulé-type isomer **8**. The CV study also shows their high electron affinities comparable to that of *p*-benzoquinone. Their fluorescence spectra were measured. Their electronic properties and reactivities are explained by the MNDO-PM3 calculations. In the X-ray crystal structure analysis of the dibromo-derivative, the molecular structure demonstrates the hypervalency on the sulfur atoms and the 14π-electron ring moiety. The crystal structure shows a set of two ribbon columns linked by short S•••N and N•••N contacts. These columns interact with each other through short Br•••N contacts. Donor-π-acceptor molecules were also synthesized by introduction of electron-donating groups into the nonclassical skeleton. Their amphoteric redox properties were investigated in the CV study. The electron-donating

ability of the dimethylaminobenzene derivative is similar to that of TTF, indicating that it is a promising electron donor for organic conductors.

At the end of the thesis, my research work is summarized and gives some suggestions as the conclusion of this thesis.

References and Notes

(1) (a) J. R. Ferraro and J. M. Williams, *Introduction to Synthetic Electrical Conductors*, Academic Press, San Diego, **1987**, p. 8. (b) J. M. Williams, J. R. Ferraro, R. J. Thorn, K. D. Carlson, U. Geiser, H. H. Wang, A. M. Kini, and M.-H. Whangbo, *Organic Superconductors*, Prentice Hall, Englewood Cliffs, New Jersey, **1992**. (c) M. R. Bryce, *Chem. Soc. Rev.*, **1991**, *20*, 355.

(2) (a) J. B. Torrance, *Acc. Chem. Res.*, **1979**, *12*, 79. (b) G. Saito and J. P. Ferraris, *Bull. Chem. Soc. Jpn.*, **1980**, *53*, 2141.

(3) (a) F. Wudl, *Acc. Chem. Res.*, **1984**, *17*, 227. (b) J. M. Williams, M. A. Beno, H. H. Wang, P. C. W. Leung, T. J. Emge, U. Geiser, and K. D. Carlson, *Acc. Chem. Res.*, **1985**, *18*, 261.

(4) (a) Y. Yamashita, T. Suzuki, T. Mukai, and G. Saito, *J. Chem. Soc., Chem. Commun.*, **1985**, 1044; T. Suzuki, H. Fujii, Y. Yamashita, C. Kabuto, S. Tanaka, M. Harasawa, T. Mukai, and T. Miyashi, *J. Am. Chem. Soc.*, **1992**, *114*, 3034. (b) T. Suzuki, C. Kabuto, Y. Yamashita, G. Saito, T. Mukai, and T. Miyashi, *Chem. Lett.*, **1987**, 2285.

(5) Measured at a Pt electrode in acetonitrile with 0.1 mol dm^{-3} Et_4NClO_4, scan rate 100 mV s^{-1}.

(6) Y. Yamashita, T. Suzuki, G. Saito, and T. Mukai, *Chem. Lett.*, **1985**, 1759.

(7) A. Ugawa, K. Iwasaki, A. Kawamoto, K. Yakushi, Y. Yamashita, and T. Suzuki, *Phys. Rev. B*, **1991**, *43*, 14718; K. Iwasaki, A. Ugawa, A. Kawamoto, Y. Yamashita, K. Yakushi, T. Suzuki, and T. Miyashi, *Bull. Chem. Soc. Jpn.*, **1992**, *65*, 3350.

(8) T. Suzuki, C. Kabuto, Y. Yamashita, T. Mukai, T. Miyashi, and G. Saito, *Bull. Chem. Soc. Jpn.*, **1988**, *61*, 483.

(9) C. Kabuto, Y. Fukazawa, T. Suzuki, Y. Yamashita, T. Miyashi, and T. Mukai, *Tetrahedron Lett.*, **1986**, *27*, 925.

(10) C. Kabuto, T. Suzuki, Y. Yamashita, and T. Mukai, *Chem. Lett.*, **1986**, 1433.

(11) T. Suzuki, C. Kabuto, Y. Yamashita, T. Mukai, and T. Miyashi, *J. Chem. Soc., Chem. Commun.*, **1988**, 895; T. Suzuki, C. Kabuto, Y. Yamashita, and T. Mukai, *Bull. Chem. Soc. Jpn.*, **1987**, *60*, 2111.

(12) T. Suzuki, T. Fukushima, Y. Yamashita, and T. Miyashi, *J. Am. Chem. Soc.*, **1994**, *116*, 2793.

(13) T. Suzuki, Y. Yamashita, C. Kabuto, and T. Miyashi, *J. Chem. Soc., Chem. Commun.*, **1989**, 1102.

(14) Y. Yamashita, Y. Kobayashi, and T. Miyashi, *Angew. Chem., Int. Ed. Engl.*, **1989**, *28*, 1052.

(15) (a) Y. Yamashita, S. Tanaka, K. Imaeda, H. Inokuchi, and M. Sano, *Chem. Lett.*, **1992**, 419; Y. Yamashita and S. Tanaka, *Chem. Lett.*, **1993**, 73. (b) Y. Yamashita, S. Tanaka, and M. Tomura, *Phosphorus, Sulfur Silicon Relat. Elem.*, **1992**, *67*, 327.

(16) Measured at a Pt electrode in benzonitrile with 0.1 mol dm^{-3} *n*-Bu_4NClO_4, scan rate 100 mV s^{-1}.

(17) Y. Yamashita, S. Tanaka, K. Imaeda, H. Inokuchi, and M. Sano, *J. Org. Chem.*, **1992**, *57*, 5517; Y. Yamashita, S. Tanaka, K. Imaeda, and H. Inokuchi, *Chem. Lett.*, **1991**, 1213.

(18) Y. Yamashita, J. Eguchi, T. Suzuki, C. Kabuto, T. Miyashi, and S. Tanaka, *Angew. Chem., Int. Ed. Engl.*, **1990**, *29*, 643.

(19) M. Tomura, S. Tanaka, and Y. Yamashita, *Heterocycles*, **1993**, *35*, 69; A. E. Underhill, I. Hawkins, S. Edge, S. B. Wilkes, K. S. Varma, A. Kobayashi, and H. Kobayashi, *Synth. Met.*, **1993**, *55-57*, 1914.

(20) T. Suzuki, T. Okubo, A. Okada, Y. Yamashita, and T. Miyashi, *Heterocycles*, **1993**, *35*, 395.

(21) K. Akiba, K. Ishikawa, and N. Inamoto, *Bull. Chem. Soc. Jpn.*, **1978**, *51*, 2674.

Chapter 2 Electron Donor Molecules containing Electron-accepting Units: 7-(1,3-Dithiol-2-ylidene)-4-methyl-4,7-dihydro[1,2,5]thiadiazolo[3,4-b]pyridines

Introduction

Molecules containing fused thiadiazole rings are of interest as components of organic conductors.[1-3] The most interesting feature is that the heteroatoms of the thiadiazole rings make intermolecular interactions strong.[3-5] The crystal structure of 4,7-dimethyl-4,7-dihydro[1,2,5]thiadiazolo[3,4-*b*]pyrazine **1** was reported to form a sheet-like network by short S•••N contacts as shown in Figure 1.[5] The contact distance of 3.05 Å is significantly shorter than the sum of their van der Waals radii (3.35 Å). The molecules on a coplanar sheet are also linked by the hydrogen bonds between the olefinic H atoms and the N atoms of the thiadiazole rings (2.50 Å). These strong S•••N interactions are attributable to an electrostatic interaction because of the polarized structure. The sulfur atom has a large coefficient in its HOMO according to the MNDO calculations. Compound **1** is a strong electron donor due to the 12π-electron ring system and afforded electrical conducting charge-transfer (CT) complexes with several types of electron acceptors.[5] 4,9-Dimethyl-4,9-dihydro[1,2,5]thiadiazolo[3,4-*b*]quinoxaline **2a** and the selenadiazole analogue **2b** also afforded moderately conducting CT complexes with iodine.[6] On the other hand, 4-(1,3-dithiol-2-ylidene)-1-methyl-1,4-dihydropyridine **3** has not been prepared except for the dibenzo-derivative **4**[7] because of an instability of the ring system. I have now replaced one amine group of compound **1** with a 1,3-dithiol-2-ylidene unit to give a derivative of **3**, 7-(1,3-dithiol-2-ylidene)-4-methyl-4,7-dihydro[1,2,5]thiadiazolo[3,4-*b*]pyridine **5a**, which is expected to have a good electron-donating ability and intramolecular CT interactions based on a donor-π-acceptor

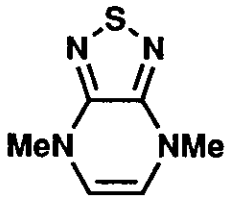

1

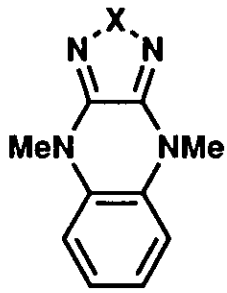

2a X = S
2b X = Se

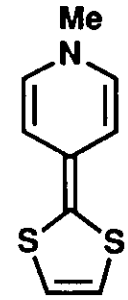

3

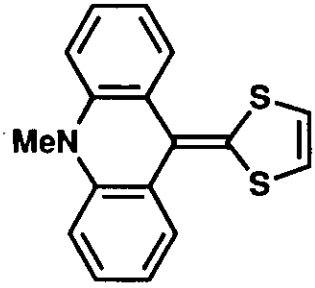

4

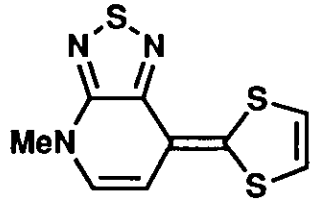

5a

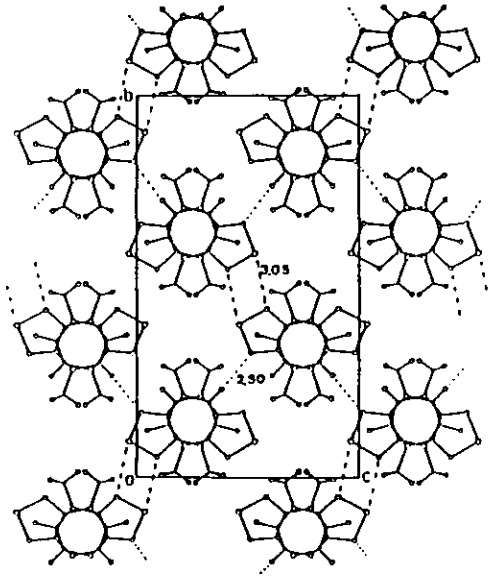

Figure 1. Sheet-like network of **1**. Broken lines; S•••N interactions and hydrogen bonds. (*Angew. Chem., Int. Ed. Engl.*, **1990**, *29*, 643.)

system. The crystal structure is also of interest in order to investigate intermolecular interactions caused by heteroatom contacts. In this chapter, I report the preparation, properties, and structure of **5a** and its derivatives.

Results and Discussion

Preparation and Properties

Compound **5a** and its derivatives **5b-d** were synthesized as summarized in Scheme 1. 4-Methyl-4,7-dihydro[1,2,5]thiadiazolo[3,4-*b*]pyridin-7-one **7** was obtained by methylation of chloropyridine **6**[8] with methyl trifluoromethanesulfonate followed by

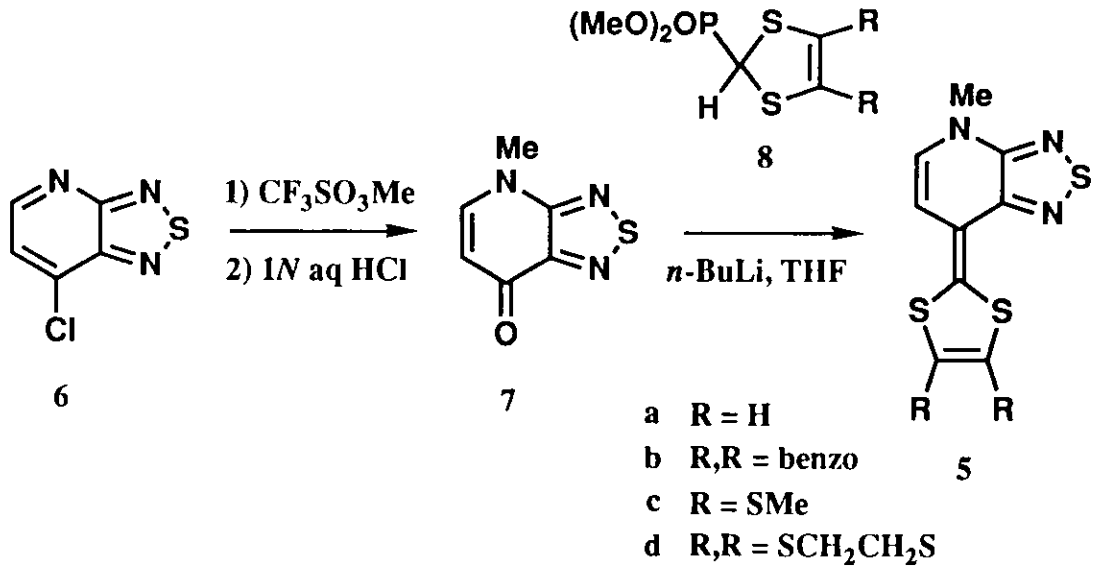

Scheme 1

hydrolysis with hydrochloric acid. The C=O stretching frequency was observed at 1631 cm^{-1} in the IR spectrum, and the ^{1}H and ^{13}C NMR spectra indicated the *N*-methylpyridone skeleton. Compounds **5a-d** were prepared in 27-55% yields by a Wittig-

Horner reaction of pyridone **7** with carbanions derived from phosphonate esters **8a-d**[7] in tetrahydrofuran (THF). These structures were determined by elemental analyses and their molecular ion peaks in the mass spectra, and they were supported by the ^{1}H and ^{13}C NMR spectra. The donor **5a** (mp 163-164 °C) was sublimed at 120 °C and 1 Torr to give a single crystal as red needles. The absorption maxima of **5a-d** were observed around 510 and 490 nm in dichloromethane as displayed in Figure 2 (real line), and the values are listed in Table 1. Since the concentration dependence of the absorbance is small, they are regarded as the intramolecular CT bands due to the donor-π-acceptor system. The spectrum in cyclohexane (broken line in Figure 2) exhibits sharp absorption bands, whose maxima are blue-shifted from those in dichloromethane (Table 1). According to the result of solvent effects, the polarized molecules **5** seem to be considerably solvated in polar solvents.

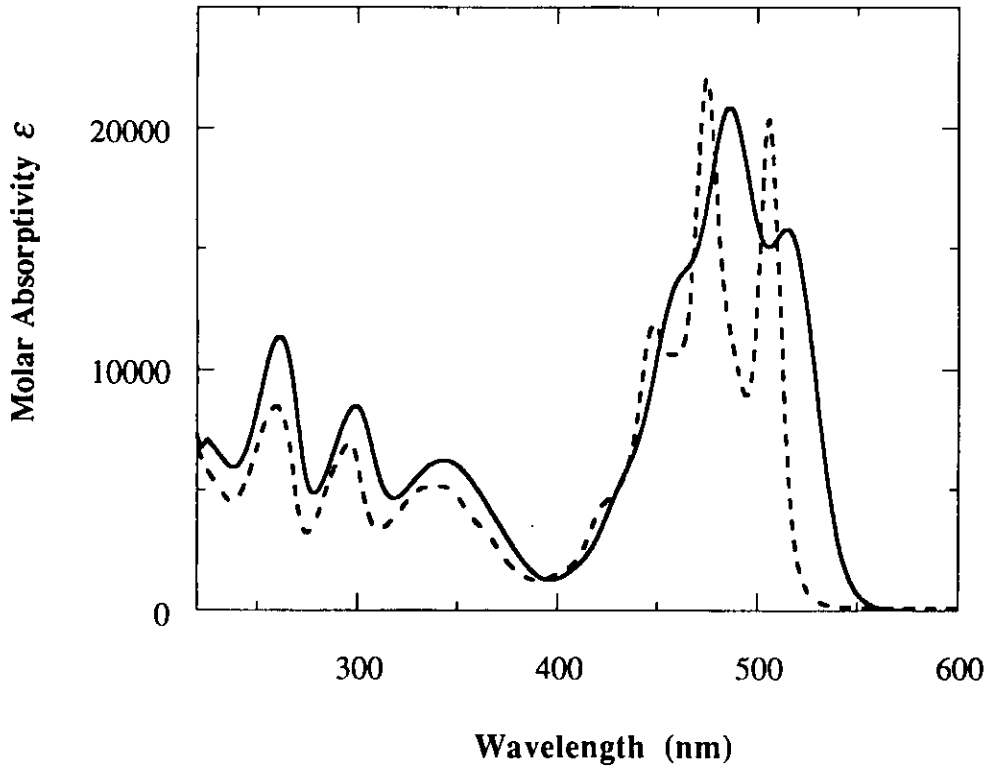

Figure 2. Absorption spectra of **5a** in dichloromethane (——) and cyclohexane (- - - -).

Table 1. Absorption maxima[a] of donors **5**.

Donor	λ_{max} / nm (log ε)		
5a	515 (4.20)	487 (4.32)	464 (4.15) sh
5a[b]	506 (4.31)	475 (4.34)	449 (4.07)
5b	509 (4.16)	482 (4.30)	461 (4.17) sh
5c	518 (4.25)	490 (4.34)	468 (4.17) sh
5d	521 (4.22)	493 (4.29)	469 (4.10) sh

[a] In CH_2Cl_2. [b] In cyclohexane.

The cyclic voltammograms (CV) of **5a-d** show two reversible one-electron redox waves (Figure 3). The half-wave oxidation potentials in benzonitrile are given in Table 2. The substitution effect in the 1,3-dithiole moiety for the electron-donating ability shows a tendency similar to that of tetrathiafulvalene (TTF). These values are lower than those of the corresponding TTF derivatives, indicating that **5a** is a stronger electron donor than TTF. The differences (ΔE) between the first and second oxidation potentials are similar to that of TTF.

Table 2. Oxidation potentials[a] of donors **5**.

Donor	E_1 / V	E_2 / V	ΔE
5a	+0.22	+0.66	0.44
5b	+0.33	+0.76	0.43
5c	+0.28	+0.66	0.38
5d	+0.27	+0.68	0.41
TTF	+0.32	+0.76	0.44

[a] 0.1 mol dm^{-3} n-Bu_4NPF_6 in PhCN, Pt electrode, scan rate 100 mV s^{-1}, V vs. standard calomel electrode (SCE).

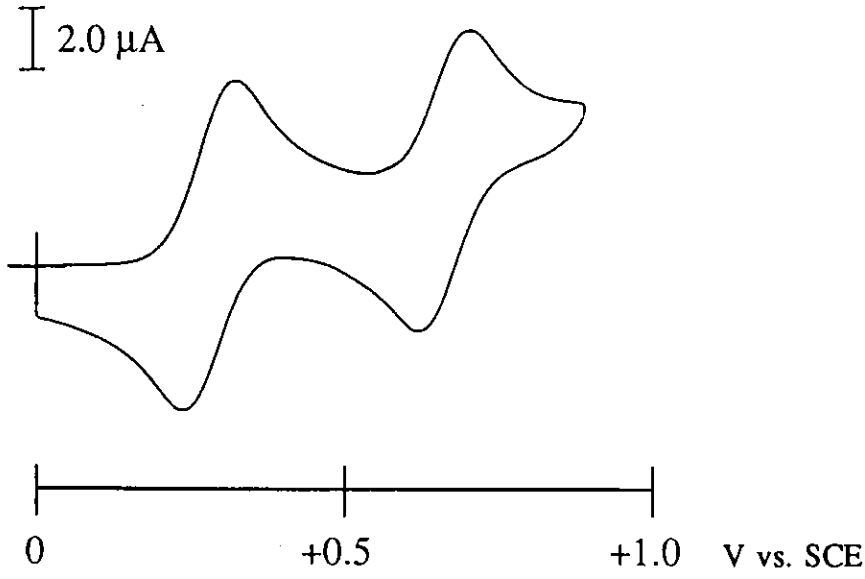

Figure 3. CV of **5c** in benzonitrile.

X-Ray Crystal Structure Analysis

In order to investigate the intermolecular interactions in crystal, an X-ray structure analysis of **5a** was carried out. The crystal data and the final atomic coordinates are presented in the subsequent experimental section. There exist two crystallographically independent molecules (molecule 1 and molecule 2) in the crystal, and Figure 4 provides the molecular structure of molecule 1 with bond lengths. The molecules are planar, and the intramolecular distances between the S atom of the dithiole and the N atom of the thiadiazole (2.86 Å for molecule 1 and 2.89 Å for molecule 2) are shorter than the sum of their van der Waals distances (3.35 Å) as found in the related molecules.[1,2] The S-N bond lengths (1.641-1.655 Å) are shorter than those of **1** (1.662 and 1.671 Å),[5] indicating some delocalization of the π-electrons. Both molecule 1 and molecule 2 are uniformly stacked with intermolecular distances of 3.46 and 3.57 Å, respectively.

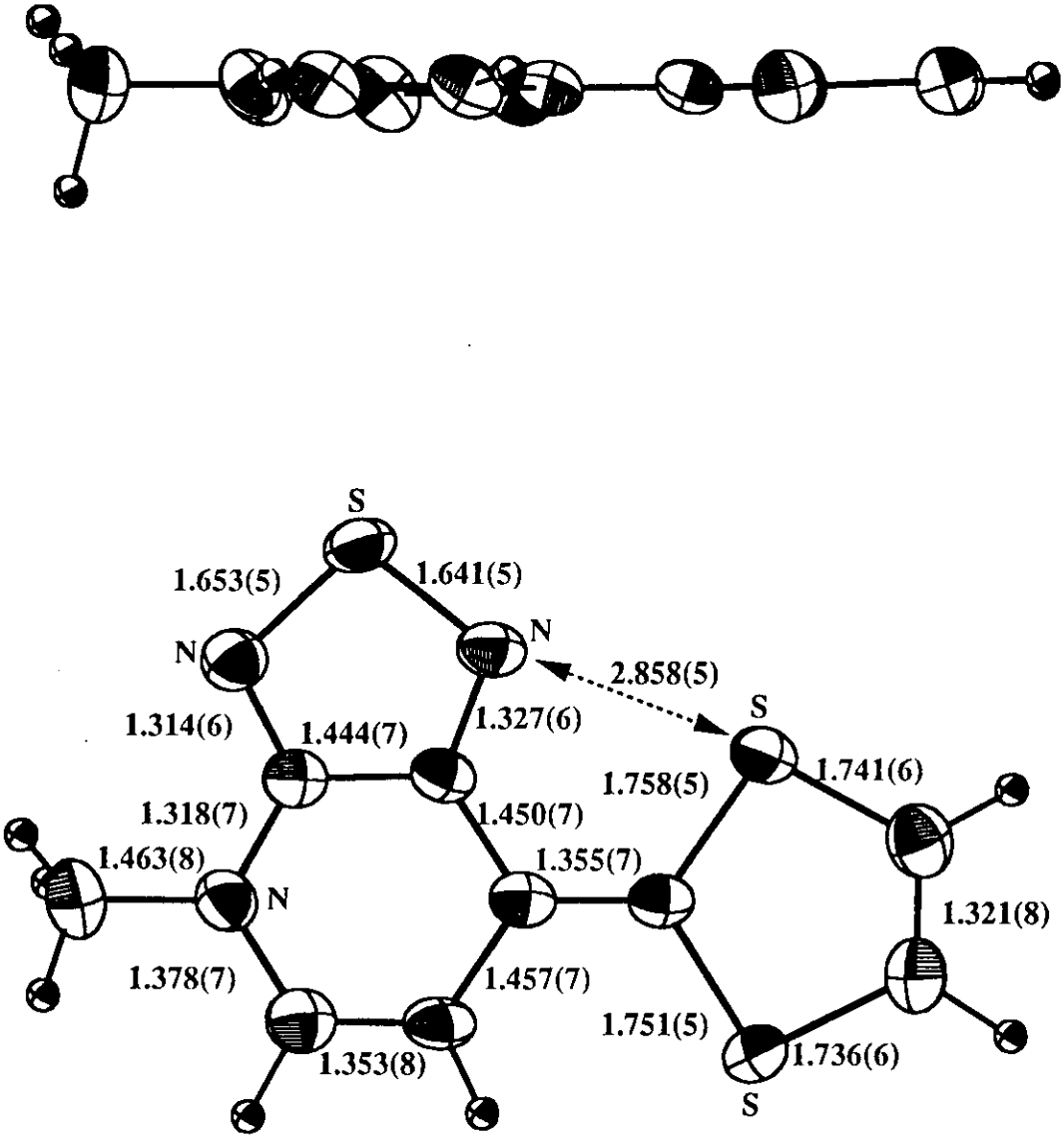

Figure 4. Views of the molecular structure of **5a** (molecule 1) with bond lengths (Å) (ORTEP).

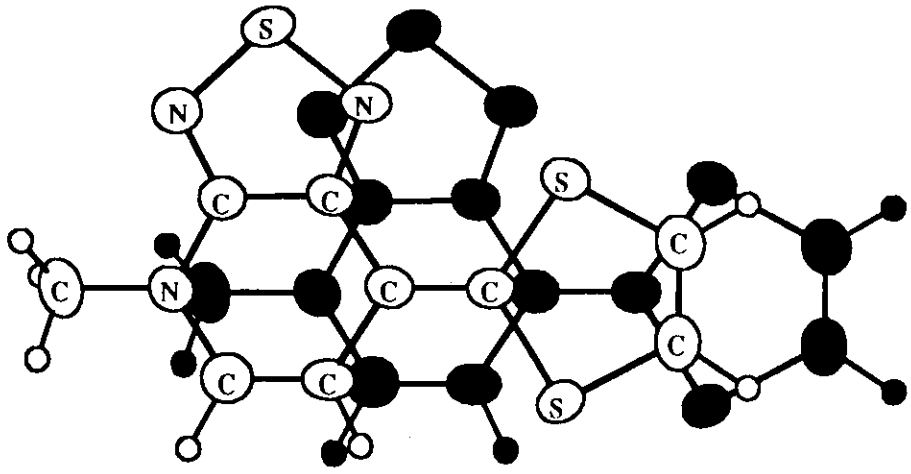

Figure 5. Overlap mode of **5a** (molecule 1).

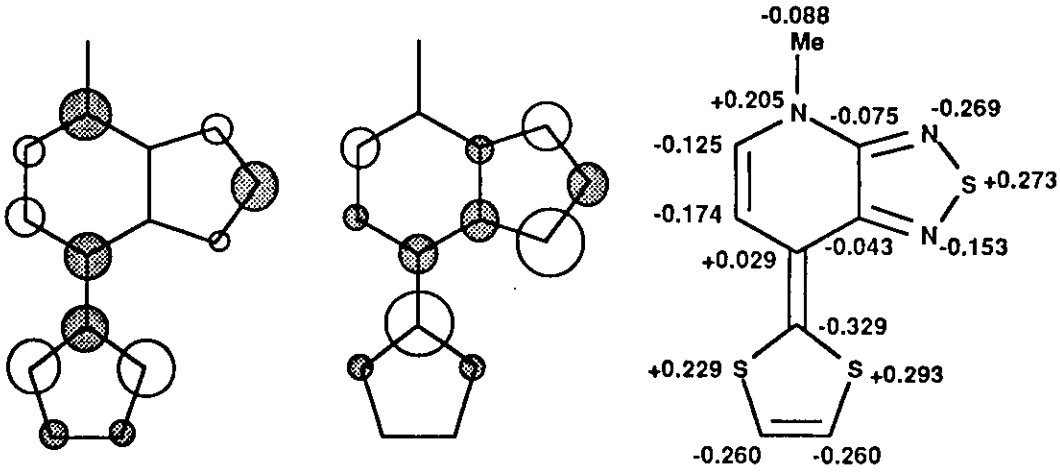

Figure 6. HOMO, LUMO, and net atomic charges of **5a** calculated by the MNDO-PM3 method.

(*a*)

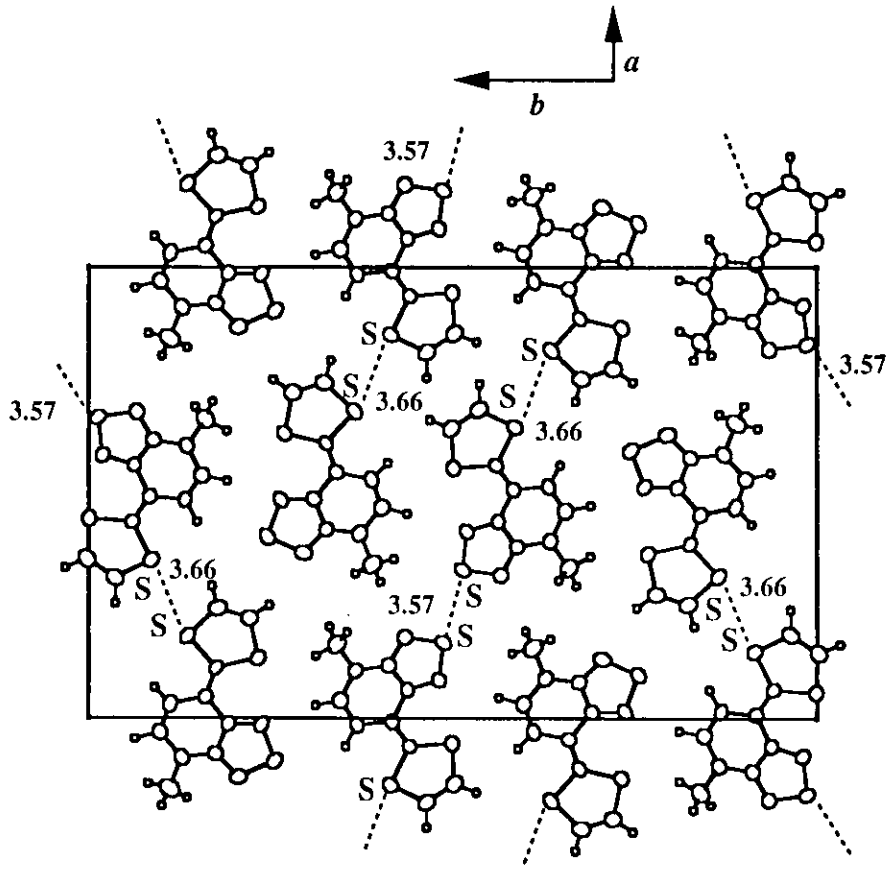

(*b*)

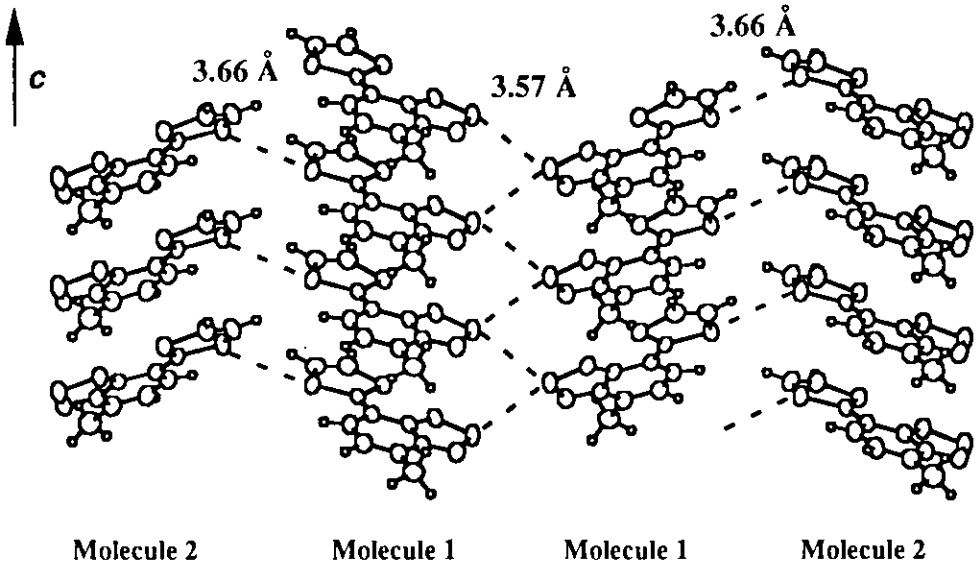

Figure 7. Crystal structure of **5a**. (*a*) Intermolecular interactions. (*b*) Columnar structure.

The overlap mode of molecule 1, which is similar to that of molecule 2, is shown in Figure 5. This mode is in accord with that of an effective interaction between the HOMO and LUMO shown in Figure 6.[9]

The crystal structure is constructed of a set of four columns along the *c* axis as shown in Figure 7. These columns interact with each other by short S•••S contacts. The contact distance between the dithioles is 3.66 Å, and that between the thiadiazole rings in molecule 1 is 3.57 Å. These values are shorter than the sum of the van der Waals radii (3.70 Å). The fact that the intermolecular distance of molecule 1 is shorter than that of molecule 2 is ascribable to the unique zigzag S•••S contacts. Although the net atomic charges of **5a** calculated by the MNDO-PM3 method (Figure 6) show that the molecule is highly polarized, the S•••N contacts arising from the electrostatic effect are not observed. As mentioned above, an exchange of the functional groups has resulted in the large modification of the crystal structure.

Properties of CT Complexes and Cation Radical Salts

The donors **5a-d** formed conducting CT complexes with tetracyanoquinodimethane (TCNQ) and the properties are summarized in Table 3. The donor **5a** gave a 1 : 1 CT complex, which shows a high electrical conductivity (1 S cm^{-1}) as a compressed pellet. According to the C≡N stretching frequency, the degree of CT in the complex is 0.67.[10] The donor **5d** gave the ClO_4 salt of the cation radical as a single crystal by an electrochemical oxidation in THF. The molar ratio is 2 : 1 based on elemental analyses. The salt showed semiconductive behavior (E_a = 0.15 eV) as displayed in Figure 8, and its electrical conductivity was 4.4 x 10^{-2} S cm^{-1} (sample 1) or 3.7 x 10^{-2} S cm^{-1} (sample 2) at room temperature. Furthermore, compound **5d** reacted with *n*-Bu_4NI_3 in THF to give the I_3 salt (1 : 1), whose conductivity was 1 x 10^{-6} S cm^{-1}. The $AuBr_2$ salt, which was

obtained by an electrochemical oxidation in chlorobenzene, also exhibited low conducting behavior (σ_{rt} = 3.3 x 10^{-7} S cm^{-1}, E_a = 0.55 eV).

Table 3. Properties of CT complexes of donors **5** with TCNQ.

Donor	D : A[a]	σ / S cm^{-1} [b]	ν_{CN} / cm^{-1}
5a	1 : 1	1	2196
5b	2 : 1	3 x 10^{-6}	2198
5c	2 : 1	2 x 10^{-3}	2201
5d	4 : 3	0.2	2195

[a] Determined on the basis of elemental analyses; D = donor; A = acceptor. [b] Determined by a two-probe technique on compressed pellets at room temperature.

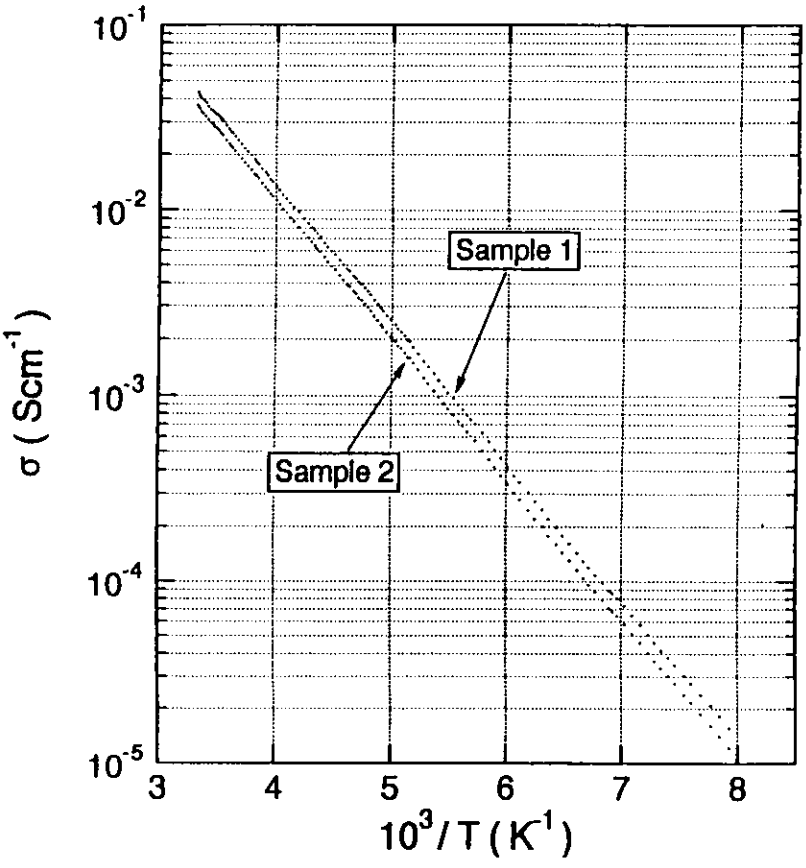

Figure 8. Temperature dependence of the electrical conductivity of $(\mathbf{5d})_2 \cdot (ClO_4)$.

Modification of Heterocycles

In order to investigate intramolecular interactions and heteroatom contacts, I also designed molecules **9**, **10**, and **11**. Molecule **9** is expected to be a stronger electron donor than **5a** because of the strong pyridylidene character. A Wittig-Horner reaction of

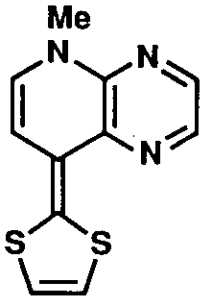

9

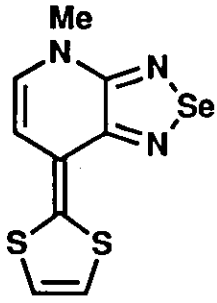

10

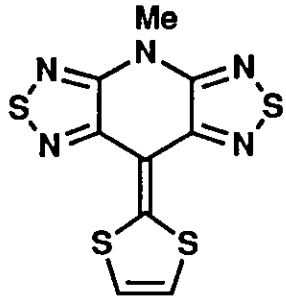

11

the corresponding pyridone with a carbanion derived from phosphonate ester **8b** was carried out by a similar procedure as **5**, resulting in a trace amount of the benzo-derivative of **9**. The result seems to be concerned with the high electron affinity of the starting pyrazinopyridone derivative. On the other hand, modification of the short zigzag S•••S contacts is of interest. A Wittig-Horner reaction for the selenadiazole analogue **10** was not attempted in this research work because of the failure to obtain the corresponding pyridone derivative. Since crystal structures of molecule **11** are expected to give two-dimensionally expanded molecular networks in neutral and cation radical states, the molecule is also of interest as a donor for organic conductors.

Summary

Novel electron donors **5** were synthesized using a Wittig-Horner reaction. These compounds were characterized by intramolecular CT bands around 510 and 490 nm due to the donor-π-acceptor unit and stronger electron-donating abilities than TTF derivertives in the CV study. The X-ray crystal structure analysis of **5a** revealed that the molecule is planar and has an intramolecular short S•••N contact. The molecular overlap is in accord with that of an effective interaction between the HOMO and LUMO. The crystal structure, which is composed of a set of four columns interacted with each other through short S•••S contacts, is fairly different from that of compound **1**. Compounds **5** formed conducting CT complexes with TCNQ. The complex of **5a** showed a high electrical conductivity (1 S cm^{-1}) as a compressed pellet, and the degree of CT was evaluated as 0.67 according to the C≡N stretching frequency. The cation radical salts of **5d** were prepared by an electrochemical oxidation, and its ClO_4 salt showed semiconducting behavior with σ_{rt} = 4.4 x 10^{-2} S cm^{-1} and E_a = 0.15 eV.

Experimental

General. Melting points were measured on BÜCHI B-535 (< 200 °C) or YANACO MP-500D melting point apparatus and are uncorrected. IR spectra were determined on a PERKIN-ELMER FTIR 1600 spectrometer. ^1H and ^{13}C NMR spectra were obtained using a JEOL JNM-GX400 (400 MHz) spectrometer. Chemical shifts are reported in ppm from tetramethylsilane as an internal standard and are given in δ units. Mass spectra (EI) were obtained with a SHIMADZU GCMS-QP1000EX mass spectrometer operating at 70 eV by a direct inlet system. UV / Vis absorption spectra were determined on a SHIMADZU UV-3101PC spectrometer. Elemental analyses were performed on YANACO MT-3 CHN CORDER. Purification of chromatography was

performed using MERCK aluminium oxide 90 (activity I, neutral). All solvents were dried and purified by the usual methods.

4-Methyl-4,7-dihydro[1,2,5]thiadiazolo[3,4-*b*]pyridin-7-one (7). To a solution of pyridine **6**[8] (1.03 g, 6.0 mmol) in dichloromethane (10 ml) was added dropwise methyl trifluoromethanesulfonate (0.90 ml, 8.0 mmol) in an ice bath under argon. The reaction mixture was stirred for 7 h at room temperature. After removal of the solvent under argon flow, ether (30 ml) was added. The precipitate was filtered, washed with ether, and dried *in vacuo*. The obtained salt was added into 1*N* hydrochloric acid (10 ml), and the solution was stirred at 100 °C for 5 h. After cooling, dichloromethane (30 ml) was added, and the aqueous layer was neutralized with NaOH solution and $NaHCO_3$ solution. The organic layer was separated, and the aqueous layer was extracted with dichloromethane (20 ml x 2). The combined organic solution was dried over Na_2SO_4 and concentrated. The residue was sublimed at 140 °C and 1 Torr to give pyridone **7** (0.90 g, 89%) as pale yellow needles. mp 162-163 °C (from acetone); IR (KBr) 3064, 1631 (C=O), 1609, 1530, 1410, 1268, 886, 826, 542 cm^{-1}; ^1H NMR ($CDCl_3$) δ 3.94 (s, 3 H, CH_3), 6.27 (d, J = 7.9 Hz, 1 H), 7.60 (d, J = 7.9 Hz, 1 H); ^{13}C NMR ($CDCl_3$) δ 38.9, 111.3, 143.3, 146.4, 155.2, 173.2; MS *m/z* (relative intensity) 167 (M^+, 100), 139 (47), 126 (24). Anal. Calcd. for $C_6H_5N_3OS$: C, 43.10; H, 3.01; N, 25.14. Found: C, 43.23; H, 3.11; N, 25.37.

7-(1,3-Dithiol-2-ylidene)-4-methyl-4,7-dihydro[1,2,5]thiadiazolo-[3,4-*b*]pyridine (5) (General Procedure). To the carbanion prepared from **8a** (280 mg, 1.3 mmol) and *n*-BuLi in *n*-hexane (1.6 M, 0.78 ml, 1.25 mmol) in dry THF (20 ml) was added pyridone **7** (167 mg, 1.0 mmol) at -78 °C under argon. The reaction mixture was stirred for 30 min at -78 °C. After the cooling bath was removed, the mixture was further stirred for 3 h, and it was poured into aqueous NaCl solution (30 ml). Dichloromethane (70 ml) was added and the organic layer was separated. The aqueous layer was extracted with dichloromethane (30 ml x 2). The combined organic solution was dried over Na_2SO_4 and concentrated. The residue was chromatographed on a short

column (aluminium oxide, CH_2Cl_2) to give **5a** (80 mg, 32%) as red needles. Compounds **5b-d** were also obtained by similar procedures using the corresponding phosphonate esters **8b-d**.

5a: red needles; decomp 163-164 °C (from ethanol); IR (KBr) 3077, 1625, 1536, 1507, 1471, 1410, 785, 720, 642, 523 cm^{-1}; ^1H NMR (DMSO-d_6, 70 °C) δ 3.32 (s, 3 H, CH_3), 5.34 (d, J = 7.8 Hz, 1 H), 6.40 (d, J = 7.8 Hz, 1 H), 6.93 (d, J = 6.4 Hz, 1 H), 6.97 (d, J = 6.4 Hz, 1 H); ^{13}C NMR (DMSO-d_6) δ 37.3, 103.8, 112.2, 119.2, 122.0, 128.0, 128.8, 147.1, 154.2; UV (CH_2Cl_2) λ_{max} 515 nm (log ε 4.20), 487 (4.32), 464 sh (4.15), 343 (3.79), 299 (3.93), 262 (4.05); MS *m/z* (relative intensity) 253 (M^+, 88), 238 (100), 180 (18). Anal. Calcd. for $C_9H_7N_3S_3$: C, 42.66; H, 2.78; N, 16.59. Found: C, 42.89; H, 3.02; N, 16.47.

5b: 44% yield; orange crystals; decomp 230-231 °C (from chloroform); IR (KBr) 1626, 1537, 1520, 1472, 1417, 1321, 1208, 788, 760, 738, 723, 528 cm^{-1}; ^1H NMR (DMSO-d_6) δ 3.36 (s, 3 H, CH_3), 5.43 (d, J = 7.9 Hz, 1 H), 6.56 (d, J = 7.9 Hz, 1 H), 7.26-7.29 (m, 2 H), 7.60-7.65 (m, 2 H); UV (CH_2Cl_2) λ_{max} 509 nm (log ε 4.16), 482 (4.30), 461 sh (4.17), 333 (3.89), 299 (3.97), 261 (4.16), 226 (4.24); MS *m/z* (relative intensity) 303 (M^+, 100), 288 (87). Anal. Calcd. for $C_{13}H_9N_3S_3$: C, 51.45; H, 2.99; N, 13.85. Found: C, 51.75; H, 3.09; N, 13.56.

5c: 55% yield; red prisms; decomp 157-158 °C (from ethyl acetate); IR (KBr) 2914, 1623, 1535, 1495, 1467, 1415, 1280, 792, 469 cm^{-1}; ^1H NMR (DMSO-d_6) δ 2.47 (s, 3 H, SCH_3), 2.48 (s, 3 H, SCH_3), 5.31 (d, J = 7.9 Hz, 1 H), 6.53 (d, J = 7.9 Hz, 1 H); ^{13}C NMR (DMSO-d_6) δ 18.3, 18.4, 37.3, 102.5, 113.8, 121.3, 125.6, 127.4, 129.1, 146.6, 154.1; UV (CH_2Cl_2) λ_{max} 518 nm (log ε 4.25), 490 (4.34), 468 sh (4.17), 339 (3.85), 261 (4.24), 225 (4.13); MS *m/z* (relative intensity) 345 (M^+, 100), 330 (29), 297 (27), 195 (81), 180 (50), 151 (27). Anal. Calcd. for $C_{11}H_{11}N_3S_5$: C, 38.23; H, 3.21; N, 12.16. Found: C, 38.26; H, 3.20; N, 12.19.

5d: 27% yield; red crystals; decomp 218-219 °C (from toluene); IR (KBr) 1626, 1532, 1508, 1468, 1413, 1358, 1319, 1280, 1208, 1008, 809, 786, 759, 729, 528, 472

cm^{-1}; ^1H NMR (DMSO-d_6) δ 3.35 (s, 3 H, CH_3), 3.44 (s, 4 H, SCH_2CH_2S), 5.32 (d, J = 7.8 Hz, 1 H), 6.54 (d, J = 7.8 Hz, 1 H); ^{13}C NMR (DMSO-d_6) δ 28.7, 28.9, 37.3, 102.8, 110.7, 113.5, 113.9, 118.8, 129.2, 146.6, 154.0; UV (CH_2Cl_2) λ_{max} 521 nm (log ε 4.22), 493 (4.29), 469 sh (4.10), 339 (3.85), 262 (4.21), 227 (4.17); MS m/z (relative intensity) 343 (M^+, 95), 315 (66), 239 (20), 227 (22), 195 (84), 180 (48), 151 (100). Anal. Calcd. for $C_{11}H_9N_3S_5$: C, 38.45; H, 2.64; N, 12.23. Found: C, 38.60; H, 2.80; N, 11.98.

Preparation of CT Complexes of 5 with TCNQ. To a solution of the donor **5a** (25.3 mg, 0.1 mmol) in hot acetonitrile (5 ml) was added a solution of TCNQ (20.4 mg, 0.1 mmol) in hot acetonitrile (5 ml). After standing for 2 h, the resulting precipitate was collected, washed with acetonitrile, and dried to give black crystals (34.8 mg, 76%). **5b**-TCNQ complex was similarly obtained. Complexes **5c**-TCNQ and **5d**-TCNQ were prepared in refluxing chlorobenzene.

5a-TCNQ (1 : 1) salt: black crystals; decomp 222-223 °C; IR (KBr) 2196 cm^{-1} (C≡N); σ_{rt} = 1 S cm^{-1} (pellet). Anal. Calcd. for $C_{21}H_{11}N_7S_3$: C, 55.12; H, 2.42; N, 21.43. Found: C, 55.32; H, 2.71; N, 21.46.

5b-TCNQ (2 : 1) salt: 64% yield; black needles; decomp 233-235 °C; IR (KBr) 2198 cm^{-1} (C≡N); σ_{rt} = 3 x 10^{-6} S cm^{-1} (pellet). Anal. Calcd. for $C_{25}H_{13}N_7S_3$: C, 56.27; H, 2.73; N, 17.27. Found: C, 56.26; H, 3.00; N, 17.31.

5c-TCNQ (2 : 1) salt: 75% yield; black crystals; decomp 193-195 °C; IR (KBr) 2201 cm^{-1} (C≡N); σ_{rt} = 2 x 10^{-3} S cm^{-1} (pellet). Anal. Calcd. for $C_{23}H_{15}N_7S_5$: C, 45.61; H, 2.93; N, 15.65. Found: C, 45.62; H, 3.18; N, 15.70.

5d-TCNQ (4 : 3) salt: 87% yield; black crystals; decomp 222-223 °C; IR (KBr) 2195 cm^{-1} (C≡N); σ_{rt} = 0.2 S cm^{-1} (pellet). Anal. Calcd. for $C_{80}H_{48}N_{24}S_{20}$: C, 48.36; H, 2.44; N, 16.92. Found: C, 48.39; H, 2.63; N, 16.62.

Cation Radical Salts of 5d. A solution of **5d** (17 mg, 0.05 mmol) in dry THF (50 ml) containing 0.1 mol dm^{-3} n-Bu_4NClO_4 (1.71 g) was electrolyzed by applying constant current of 2 μA under argon for 2 weeks to afford (**5d**)$_2$•(ClO_4) as black needles

(4 mg). A reaction of **5d** and *n*-Bu_4NI_3 in THF gave (**5d**)•(I_3). The $AuBr_2$ salt was obtained by an electrochemical oxidation in chlorobenzene (50 ml) containing **5d** (5 mg) and *n*-Bu_4NAuBr_2 (0.10 g) under argon.

(**5d**)$_2$•(ClO_4): decomp 265-266 °C; σ_{rt} = 4.4 x 10^{-2} (sample 1), 3.7 x 10^{-2} S cm^{-1} (sample 2) (by a two-probe technique on single crystal), E_a = 0.15 eV. Anal. Calcd. for $C_{22}H_{18}ClN_6O_4S_{10}$: C, 33.59; H, 2.31; N, 10.69. Found: C, 33.33; H, 2.38; N, 10.57.

(**5d**)•(I_3): deep purple crystals; decomp > 237 °C; σ_{rt} = 1 x 10^{-6} S cm^{-1} (pellet). Anal. Calcd. for $C_{11}H_9I_3N_3S_5$: C, 18.24; H, 1.25; N, 5.80. Found: C, 18.36; H, 1.28; N, 5.86.

(**5d**)•($AuBr_2$)$_x$: purple plates; decomp 202-204 °C; σ_{rt} = 3.3 x 10^{-7} S cm^{-1} (by a two-probe technique on single crystal), E_a = 0.55 eV.

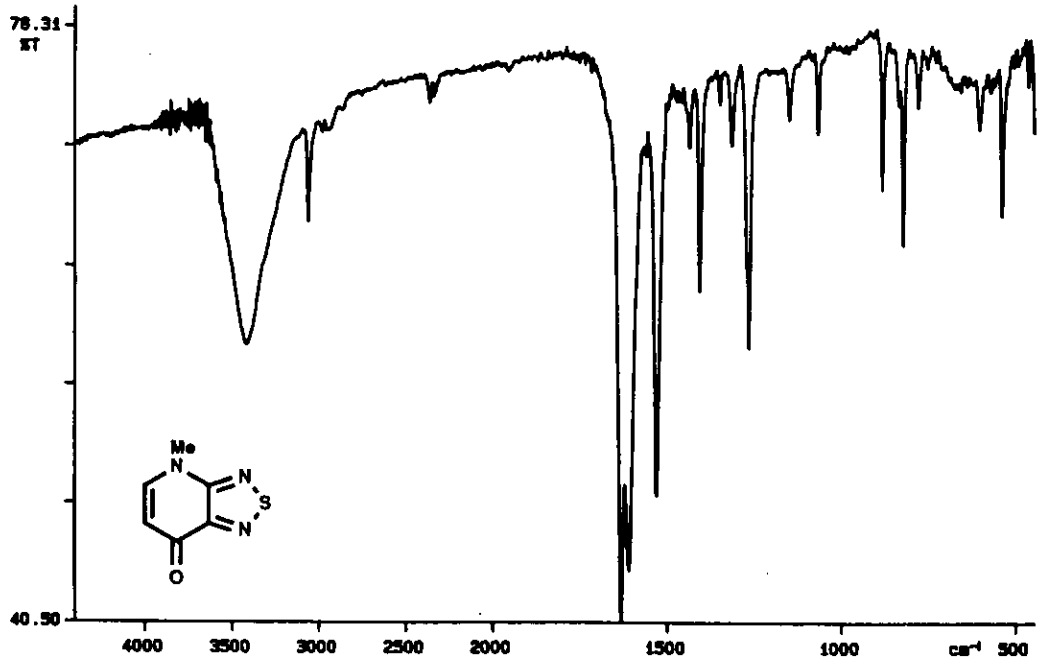

Figure 9. IR spectrum of **7**.

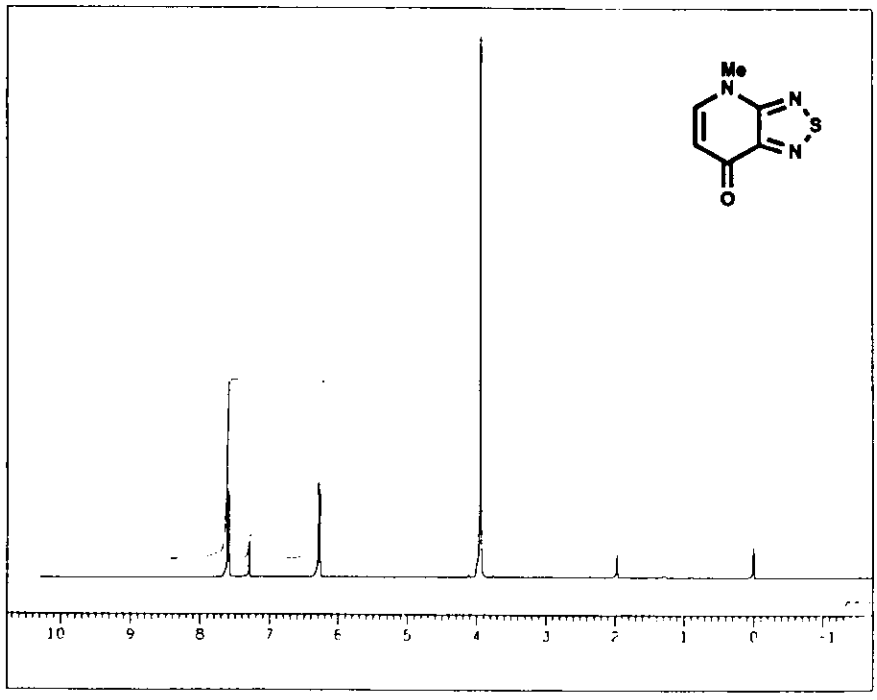

Figure 10. ^{1}H NMR spectrum of **7** in $CDCl_3$.

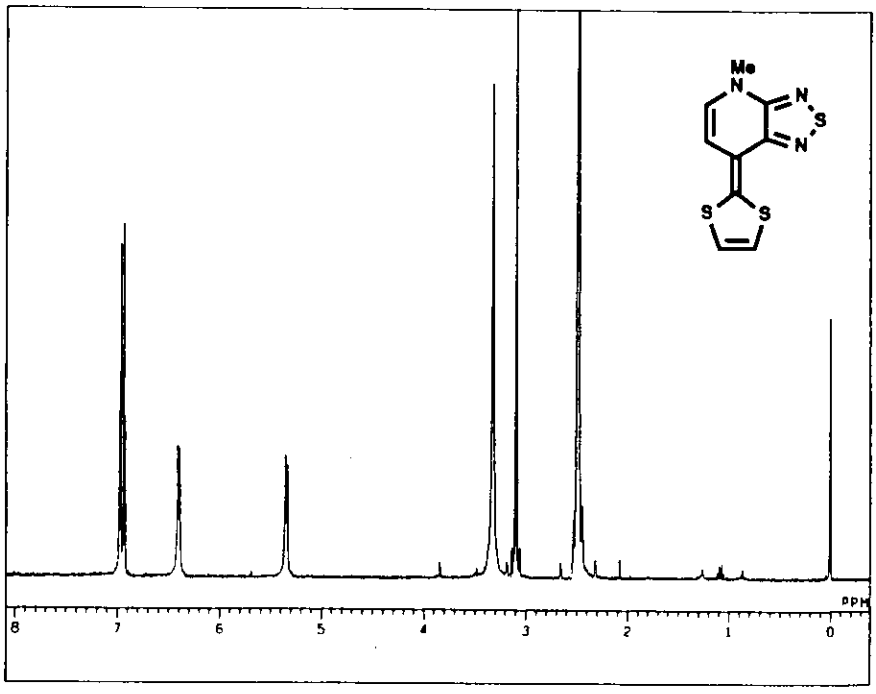

Figure 11. ^{1}H NMR spectrum of **5a** at 70 °C in DMSO-d_6.

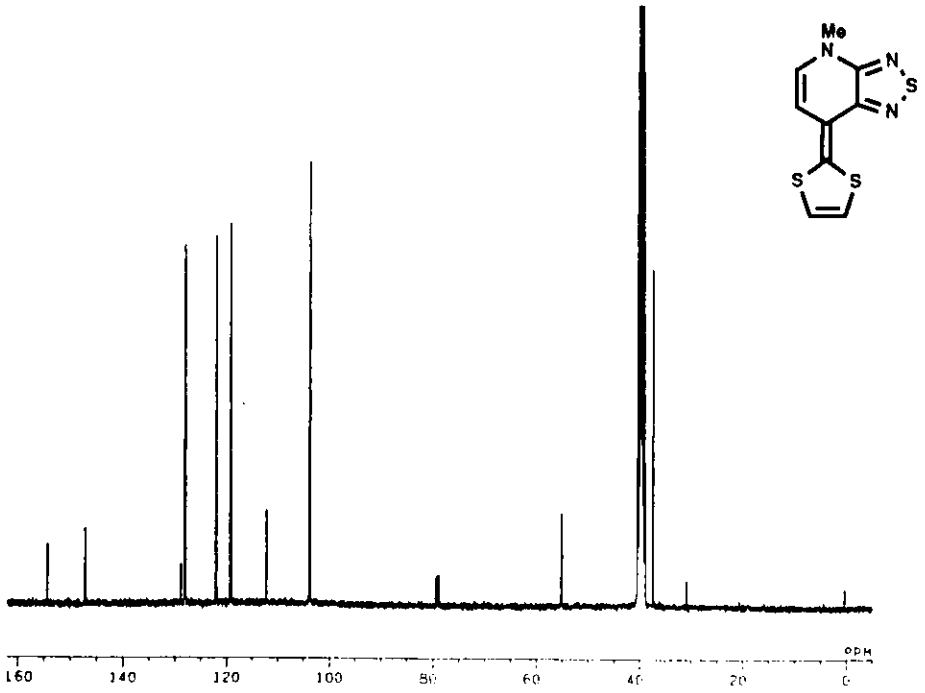

Figure 12. ^{13}C NMR spectrum of **5a** in DMSO-d_6.

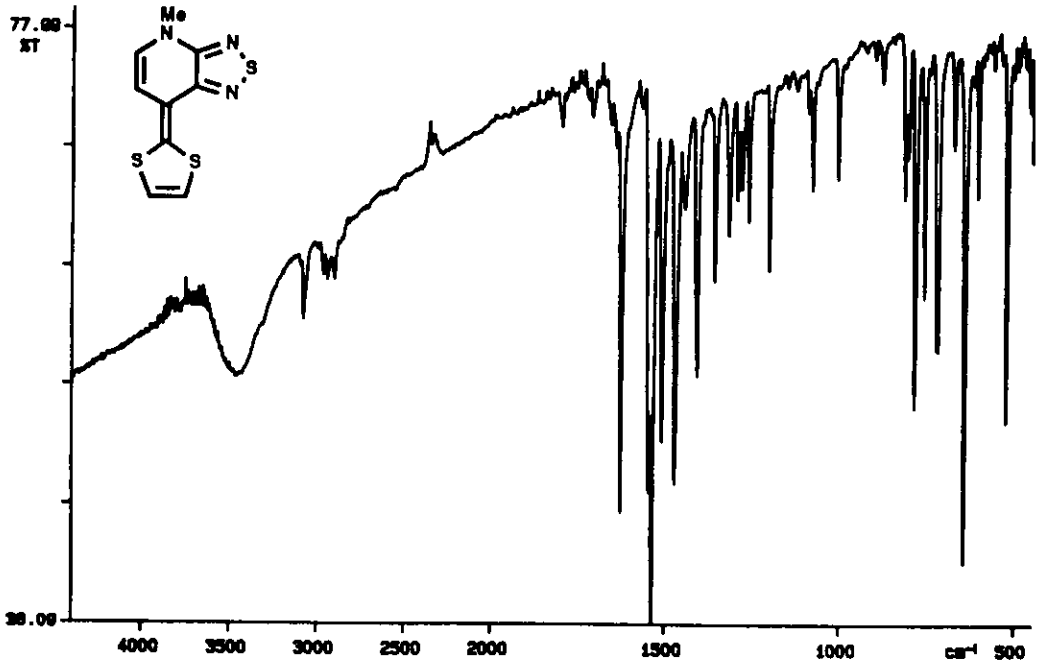

Figure 13. IR spectrum of **5a**.

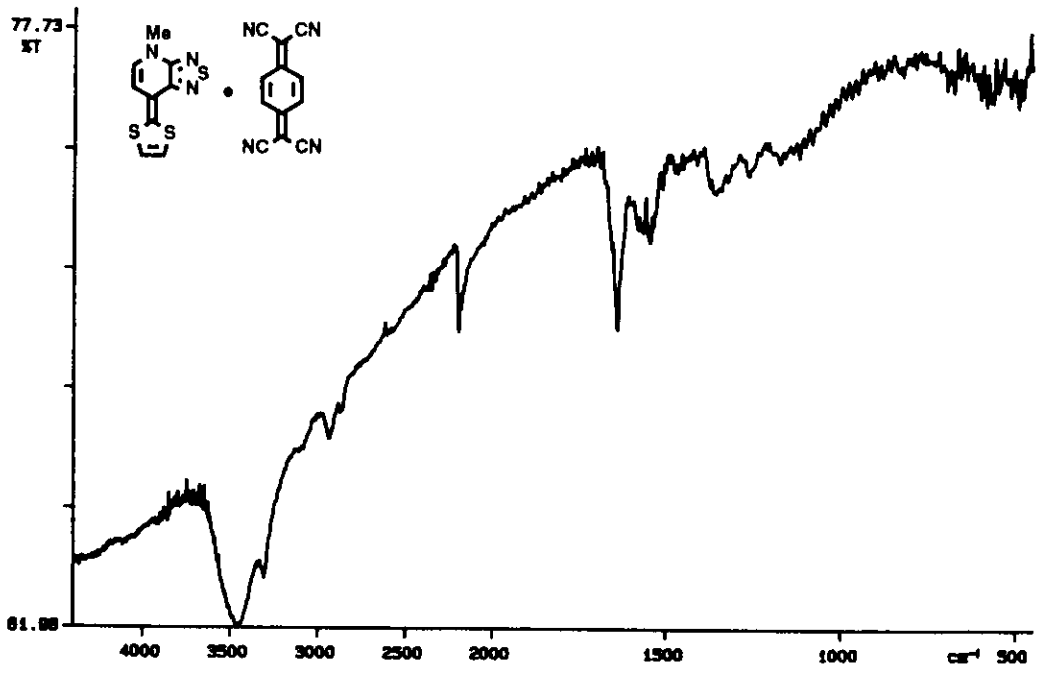

Figure 14. IR spectrum of **5a**-TCNQ complex.

X-Ray Crystal Structure Analysis. A needle-like crystal with dimensions of 0.05 x 0.05 x 0.25 mm^3 along the *a*, *b*, and *c* axes was prepared by sublimation (120 °C, 1 Torr) for the X-ray study. Crystal data are as follows: $C_9H_7N_3S_3$, M = 253.39, orthorhombic, space group $P2_12_12_1$, a = 17.8055(14), b = 28.8428(24), c = 3.9462(1) Å, V = 2026.6(2) $Å^3$, Z = 8, D_c = 1.66 g cm^{-3}, $F(000)$ = 1040, $\mu(Cu_{K\alpha})$ = 63.32 cm^{-1}, S = 1.27. The diffraction data were collected at 296 K by an ENRAF-NONIUS CAD4 diffractometer (40 kV, 32 mA) with graphite-monochromated Cu K_α radiation (λ = 1.5418 Å). Cell parameters were determined by least-squares procedures on 25 reflections (44° < 2θ < 50°). A total of 1872 unique data (2θ < 140°) was measured using the ω - 2θ scan method, and 1866 independent reflections ($|F_o| > 3\sigma|F_o|$) were used for the analysis. No absorption correction was applied. The structure was solved by the

direct method with the program MULTAN 78.[11] The positions of the hydrogen atoms were obtained from difference Fourier maps. The atomic parameters were refined by a block-diagonal least-squares procedure; $w^{-1} = \sigma(F_o)^2 + (0.015\sigma|F_o|)^2$. Anisotropic temperature factors were used for refining the non-hydrogen atoms, and isotropic temperature factors were adopted for the hydrogen atoms. The final R and R_w values are 0.0449 and 0.0433. The maximum residual electron density was 0.37 e Å^{-3}. The atomic scattering factors were taken from International Tables for X-Ray Crystallography.[12] The calculations were performed on a HITAC M-680H computer in Computer Center of Institute for Molecular Science using the programs UNICS III[13] and ORTEP[14]. Lists of the final atomic coordinates with equivalent isotropic thermal parameters (Table 4), bond lengths (Table 5), and bond angles (Table 6) are as follows.

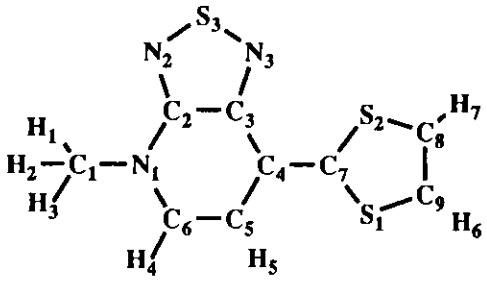

Molecule 1

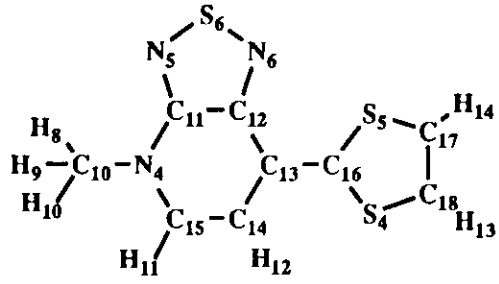

Molecule 2

Table 4. Final atomic coordinates and equivalent isotropic thermal parameters[a] (Å2).

Atom	x	y	z	B_{eq}
S1	0.1479 (1)	0.0855 (0)	1.0026 (5)	3.2
S2	0.0563 (1)	0.0009 (0)	1.0010 (5)	3.1
S3	-0.1691 (1)	0.0132 (0)	0.5211 (5)	3.5
S4	0.3168 (1)	0.1354 (0)	1.3886 (5)	3.6
S5	0.3663 (1)	0.2320 (0)	1.3710 (5)	3.2

Atom	x	y	z	B_{eq}
S6	0.5961 (1)	0.2553 (0)	0.9301 (5)	3.9
N1	-0.1058 (2)	0.1342 (1)	0.3532 (14)	3.1
N2	-0.1808 (2)	0.0660 (1)	0.3669 (14)	3.3
N3	-0.0847 (2)	0.0191 (1)	0.6824 (14)	3.1
N4	0.5883 (2)	0.1278 (1)	0.7993 (14)	3.5
N5	0.6316 (3)	0.2054 (2)	0.8001 (14)	3.7
N6	0.5151 (2)	0.2369 (1)	1.0806 (14)	3.3
C1	-0.1648 (3)	0.1597 (2)	0.1749 (19)	4.0
C2	-0.1183 (3)	0.0883 (2)	0.4361 (15)	2.8
C3	-0.0626 (3)	0.0623 (2)	0.6218 (16)	2.7
C4	0.0082 (3)	0.0832 (2)	0.7193 (16)	2.7
C5	0.0151 (3)	0.1316 (2)	0.6202 (17)	3.0
C6	-0.0391 (3)	0.1546 (2)	0.4486 (17)	3.4
C7	0.0629 (3)	0.0596 (2)	0.8842 (16)	2.6
C8	0.1454 (3)	-0.0021 (2)	1.1819 (18)	3.7
C9	0.1864 (3)	0.0360 (2)	1.1826 (17)	3.5
C10	0.6568 (3)	0.1110 (2)	0.6357 (21)	4.8
C11	0.5799 (3)	0.1740 (2)	0.8722 (17)	3.0
C12	0.5134 (3)	0.1914 (2)	1.0329 (16)	2.8
C13	0.4529 (3)	0.1602 (2)	1.1287 (17)	2.9
C14	0.4694 (3)	0.1116 (2)	1.0556 (18)	3.5
C15	0.5314 (3)	0.0978 (2)	0.9015 (18)	3.7
C16	0.3881 (3)	0.1744 (2)	1.2770 (16)	2.7
C17	0.2764 (3)	0.2205 (2)	1.5208 (20)	3.8
C18	0.2544 (3)	0.1769 (2)	1.5331 (20)	3.9
H1	-0.139 (3)	0.189 (2)	0.066 (15)	4.5
H2	-0.204 (4)	0.169 (2)	0.367 (21)	8.5

Atom	x	y	z	B_{eq}
H3	-0.192 (3)	0.145 (2)	-0.027 (18)	6.7
H4	-0.028 (3)	0.189 (2)	0.369 (17)	5.6
H5	0.063 (3)	0.148 (1)	0.647 (14)	3.6
H6	0.243 (3)	0.036 (1)	1.294 (15)	3.5
H7	0.164 (3)	-0.032 (2)	1.295 (17)	4.2
H8	0.645 (3)	0.081 (2)	0.517 (18)	7.1
H9	0.694 (3)	0.100 (2)	0.803 (18)	6.7
H10	0.677 (4)	0.134 (2)	0.461 (22)	10.4
H11	0.545 (3)	0.063 (2)	0.882 (19)	7.5
H12	0.432 (3)	0.090 (2)	1.098 (17)	6.3
H13	0.205 (3)	0.168 (2)	1.616 (18)	6.4
H14	0.247 (3)	0.247 (2)	1.597 (19)	6.6

[a] $B_{eq} = (4/3)\Sigma_i\Sigma_j\beta_{ij}\boldsymbol{a}_i \cdot \boldsymbol{a}_j$.

Table 5. Bond lengths (Å).

Molecule 1	Distance	Molecule 2	Distance
S1 - C7	1.751 (5)	S4 - C16	1.753 (5)
S1 - C9	1.736 (6)	S4 - C18	1.730 (6)
S2 - C7	1.758 (5)	S5 - C16	1.747 (5)
S2 - C8	1.741 (6)	S5 - C17	1.737 (6)
S3 - N2	1.653 (5)	S6 - N5	1.655 (5)
S3 - N3	1.641 (5)	S6 - N6	1.648 (5)
N1 - C1	1.463 (8)	N4 - C10	1.463 (8)
N1 - C2	1.381 (7)	N4 - C11	1.373 (7)
N1 - C6	1.378 (7)	N4 - C15	1.393 (7)
N2 - C2	1.314 (6)	N5 - C11	1.322 (7)

Molecule 1	Distance	Molecule 2	Distance
N3 - C3	1.327 (6)	N6 - C12	1.327 (6)
C1 - H1	1.044 (49)	C10 - H8	0.994 (58)
C1 - H2	1.067 (73)	C10 - H9	0.993 (64)
C1 - H3	1.020 (66)	C10 - H10	1.028 (74)
C2 - C3	1.444 (7)	C11 - C12	1.434 (7)
C3 - C4	1.450 (7)	C12 - C13	1.453 (7)
C4 - C5	1.457 (7)	C13 - C14	1.461 (7)
C4 - C7	1.355 (7)	C13 - C16	1.357 (7)
C5 - C6	1.353 (8)	C14 - C15	1.322 (8)
C5 - H5	0.976 (45)	C14 - H12	0.927 (54)
C6 - H4	1.064 (52)	C15 - H11	1.025 (56)
C8 - C9	1.321 (8)	C17 - C18	1.319 (8)
C8 - H7	1.029 (51)	C17 - H14	0.979 (54)
C9 - H6	1.097 (50)	C18 - H13	0.969 (57)

Table 6. Bond angles (degree).

Molecule 1	Angle	Molecule 2	Angle
C7 - S1 - C9	95.7 (3)	C16 - S4 - C18	96.0 (3)
C7 - S2 - C8	95.5 (3)	C16 - S5 - C17	95.4 (3)
N2 - S3 - N3	99.4 (2)	N5 - S6 - N6	99.5 (2)
C1 - N1 - C2	118.7 (4)	C10 - N4 - C11	120.4 (5)
C1 - N1 - C6	122.3 (4)	C10 - N4 - C15	121.8 (4)
C2 - N1 - C6	119.0 (5)	C11 - N4 - C15	117.7 (5)
S3 - N2 - C2	105.5 (4)	S6 - N5 - C11	105.2 (4)
S3 - N3 - C3	107.4 (4)	S6 - N6 - C12	106.8 (4)
N1 - C1 - H1	106.9 (28)	N4 - C10 - H8	108.5 (32)

Molecule 1			Angle	Molecule 2			Angle
N1	- C1	- H2	105.0 (39)	N4	- C10	- H9	112.0 (38)
N1	- C1	- H3	120.9 (30)	N4	- C10	- H10	111.5 (37)
H1	- C1	- H2	111.3 (43)	H8	- C10	- H9	100.7 (48)
H1	- C1	- H3	101.9 (46)	H8	- C10	- H10	108.4 (57)
H2	- C1	- H3	110.7 (51)	H9	- C10	- H10	115.0 (52)
N1	- C2	- N2	123.8 (5)	N4	- C11	- N5	122.9 (5)
N1	- C2	- C3	120.5 (4)	N4	- C11	- C12	121.4 (5)
N2	- C2	- C3	115.7 (5)	N5	- C11	- C12	115.7 (5)
N3	- C3	- C2	112.1 (4)	N6	- C12	- C11	112.9 (4)
N3	- C3	- C4	126.9 (5)	N6	- C12	- C13	126.3 (5)
C2	- C3	- C4	121.1 (4)	C11	- C12	- C13	120.8 (4)
C3	- C4	- C5	113.7 (5)	C12	- C13	- C14	113.2 (5)
C3	- C4	- C7	123.0 (5)	C12	- C13	- C16	123.8 (5)
C5	- C4	- C7	123.3 (5)	C14	- C13	- C16	123.0 (5)
C4	- C5	- C6	122.9 (5)	C13	- C14	- C15	123.2 (5)
C4	- C5	- H5	120.0 (27)	C13	- C14	- H12	117.8 (34)
C6	- C5	- H5	116.5 (28)	C15	- C14	- H12	118.7 (35)
N1	- C6	- C5	122.9 (5)	N4	- C15	- C14	123.6 (5)
N1	- C6	- H4	119.0 (30)	N4	- C15	- H11	113.8 (34)
C5	- C6	- H4	118.0 (30)	C14	- C15	- H11	121.9 (35)
S1	- C7	- S2	113.5 (3)	S4	- C16	- S5	113.4 (3)
S1	- C7	- C4	122.4 (4)	S4	- C16	- C13	122.0 (4)
S2	- C7	- C4	124.1 (4)	S5	- C16	- C13	124.6 (4)
S2	- C8	- C9	117.5 (5)	S5	- C17	- C18	118.0 (4)
S2	- C8	- H7	121.4 (28)	S5	- C17	- H14	115.9 (31)
C9	- C8	- H7	121.0 (28)	C18	- C17	- H14	126.0 (32)
S1	- C9	- C8	117.8 (5)	S4	- C18	- C17	117.2 (4)

Molecule 1			Angle	Molecule 2			Angle
S1	- C9	- H6	121.4 (23)	S4	- C18	- H13	121.2 (31)
C8	- C9	- H6	120.9 (23)	C17	- C18	- H13	121.7 (33)

Electrochemical Measurements. Cyclic voltammetry was performed on a TOHO TECHNICAL RESEARCH Polarization Unit PS-07 potentiostat / galvanostat. The electrochemical measurements were carried out in distilled benzonitrile containing 0.1 mol dm^{-3} tetrabutylammonium hexafluorophosphate using Pt working and counter electrodes and a standard calomel electrode (SCE). The concentration of each sample was *ca.* 1 mmol dm^{-3}. The solution was degassed by argon bubbling. The scan rate was 100 mV s^{-1}. All values are given in V vs. SCE.

References and Notes

(1) Y. Yamashita and S. Tanaka, *Chem. Lett.*, **1993**, 73; Y. Yamashita, S. Tanaka, K. Imaeda, H. Inokuchi, and M. Sano, *Chem. Lett.*, **1992**, 419.

(2) Y. Yamashita, S. Tanaka, K. Imaeda, H. Inokuchi, and M. Sano, *J. Org. Chem.*, **1992**, *57*, 5517; K. Imaeda, Y. Yamashita, Y. Li, T. Mori, H. Inokuchi, and M. Sano, *J. Mater. Chem.*, **1992**, *2*, 115; Y. Yamashita, S. Tanaka, K. Imaeda, and H. Inokuchi, *Chem. Lett.*, **1991**, 1213.

(3) T. Suzuki, C. Kabuto, Y. Yamashita, T. Mukai, T. Miyashi, and G. Saito, *Bull. Chem. Soc. Jpn.*, **1988**, *61*, 483; T. Suzuki, Y. Yamashita, C. Kabuto, and T. Miyashi, *J. Chem. Soc., Chem. Commun.*, **1989**, 1102.

(4) C. Kabuto, T. Suzuki, Y. Yamashita, and T. Mukai, *Chem. Lett.*, **1986**, 1433; Y. Yamashita, K. Saito, T. Suzuki, C. Kabuto, T. Mukai, and T. Miyashi, *Angew. Chem.*,

Int. Ed. Engl., **1988**, *27*, 434; M. Tomura, S. Tanaka, and Y. Yamashita, *Heterocycles*, **1993**, *35*, 69.

(5) Y. Yamashita, J. Eguchi, T. Suzuki, C. Kabuto, T. Miyashi, and S. Tanaka, *Angew. Chem., Int. Ed. Engl.*, **1990**, *29*, 643. Oxidation potentials of **1**: E_1 = +0.15 V, E_2 = +0.95 V (irreversible) vs. SCE; measured at a Pt electrode in acetonitrile with 0.1 mol dm^{-3} Et_4NClO_4, scan rate 100 mV s^{-1}.

(6) Y. Yamashita, K. Saito, T. Mukai, and T. Miyashi, *Tetrahedron Lett.*, **1989**, *30*, 7071.

(7) K. Akiba, K. Ishikawa, and N. Inamoto, *Bull. Chem. Soc. Jpn.*, **1978**, *51*, 2674. 9-Methyl-10-(1,3-benzodithiol-2-ylidene)-9,10-dihydro-9-azaanthracene: UV (CH_2Cl_2) λ_{max} 395 nm (log ε 4.30).

(8) G. H. Harts, K. B. de Roos, and C. A. Salemink, *Recl. Trav. Chim. Pays-Bas*, **1970**, *89*, 5.

(9) Calculated by the MNDO-PM3 method, MOPAC program, J. J. P. Stewart, *J. Comput. Chem.*, **1989**, *10*, 209, 221.

(10) J. S. Chappell, A. N. Bloch, W. A. Bryden, M. Maxfield, T. O. Poehler, and D. O. Cowan, *J. Am. Chem. Soc.*, **1981**, *103*, 2442.

(11) P. Main, S. E. Hull, L. Lessinger, G. Germain, J.-P. Declercq, and M. M. Woolfson, *MULTAN 78, A System of Computer Programs for the Automatic Solution of Crystal Structures from X-Ray Diffraction Data*, University of York, England and Louvain-la-Nerve, Belgium, **1978**.

(12) *International Tables for X-Ray Crystallography, Vol. 4*, Kynoch Press, Birmingham, **1974**.

(13) T. Sakurai and K. Kobayashi, *UNICS III, Rikagaku Kenkyusho Hokoku*, **1979**, *55*, 69.

(14) C. K. Johnson, *ORTEP Report ORNL-3794*, Oak Ridge National Laboratory, Tennessee, **1965**.

Chapter 3 Nonplanar Electron Donor: 4,9-Bis(1,3-benzodithiol-2-ylidene)-4,9-dihydronaphtho[2,3-c][1,2,5]thiadiazole

Introduction

Much attention has been focused on the development of new electron donors and acceptors affording organic conductors.[1] One of the molecular design strategies is to prepare planar molecules forming stable ion radical states.[1] However, it seems possible to use nonplanar molecules as components of organic conductors if good intermolecular interactions are achieved.[2] In this connection, 4,9-bis(1,3-benzodithiol-2-ylidene)-4,9-dihydronaphtho[2,3-*c*][1,2,5]thiadiazole **1**, which is nonplanar because of the steric hindrance caused by the *peri*-hydrogen atoms, is interesting since it has extended π-conjugation leading to a decrease in on-site Coulombic repulsion.[3] In practice, a cation radical salt of **1** showed a high electrical conductivity (σ_{rt} = 8.3 S cm^{-1} for the 1 : 1 PF_6 salt). Furthermore, compound **1** exhibited an electrical conductivity of 2.3 x 10^{-7} S cm^{-1} as a single component. In this chapter, I report the X-ray crystal analysis of **1** in order to investigate the molecular structure and the molecular packing.

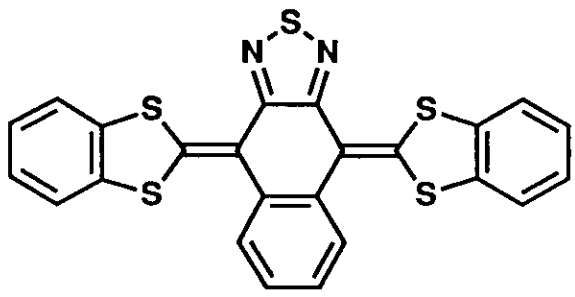

1

X-Ray Crystal Structure Analysis

A single crystal was obtained by recrystallization from chloroform for the X-ray study. The crystal data and the final atomic coordinates are shown in the experimental section. The molecule has a *Cs* symmetry and is butterfly-shaped because of the steric interaction between the S atoms of the dithioles and the *peri*-hydrogen atoms as shown in Figure 1. The distance between the S atom and the H atom is 2.49 Å, and that between the S atom and the C atom is 3.04 Å (Figure 1*a*). They are both shorter than the sum of their van der Waals radii (S•••H: 3.00 Å, S•••C: 3.50 Å). The angle formed by the central six-membered ring and the 1,3-dithiole ring is 158.1° (Figure 1*b*). The central six-membered ring is folded with the angle of 155.7° (Figure 1*c*), and the delocalization in the ring moiety is strongly disturbed judging from the bond lengths and angles. The intramolecular distance between the S atom of the dithiole and the N atom of the thiadiazole (2.78 Å) is shorter than the sum of their van der Waals distances (3.35 Å) (Figure 1*a*).

(*a*)

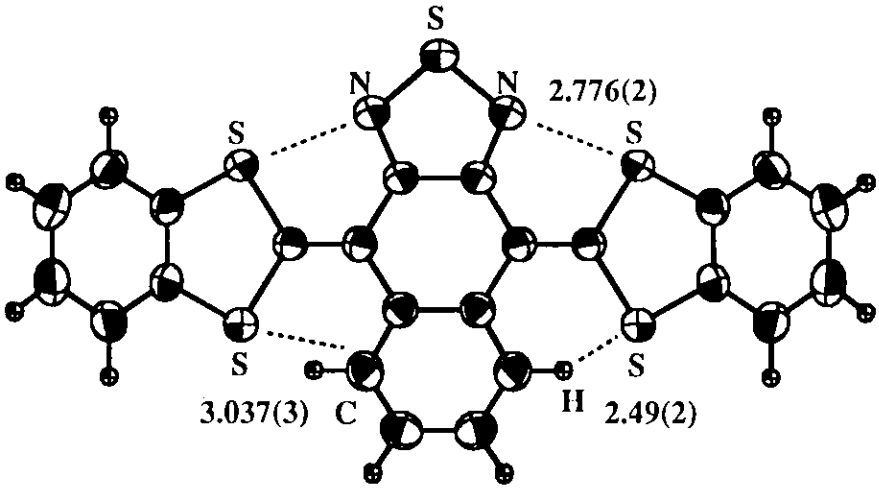

(*b*)

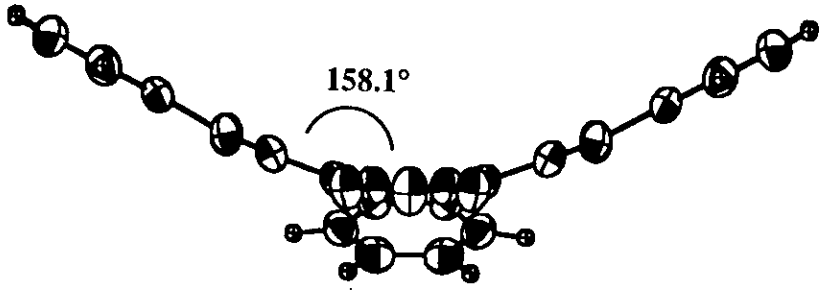

(*c*)

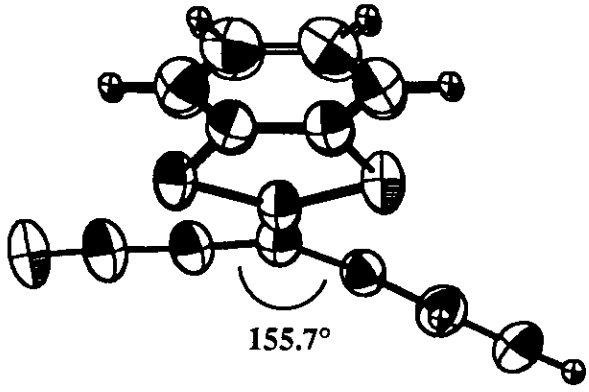

Figure 1. Molecular structure of **1**. (*a*) Heteroatom contacts; S•••H (neutral: 2.49 Å; salt: 2.23 and 2.27 Å), S•••C (neutral: 3.037 Å; salt: 2.998 and 2.999 Å), S•••N (neutral: 2.776 Å; salt: 2.652 and 2.667 Å). (*b*) Side view (neutral: 158.1°; salt: 159.1° and 159.6°). (*c*) Side view (neutral: 155.7°; salt: 159.9°).

(*a*)

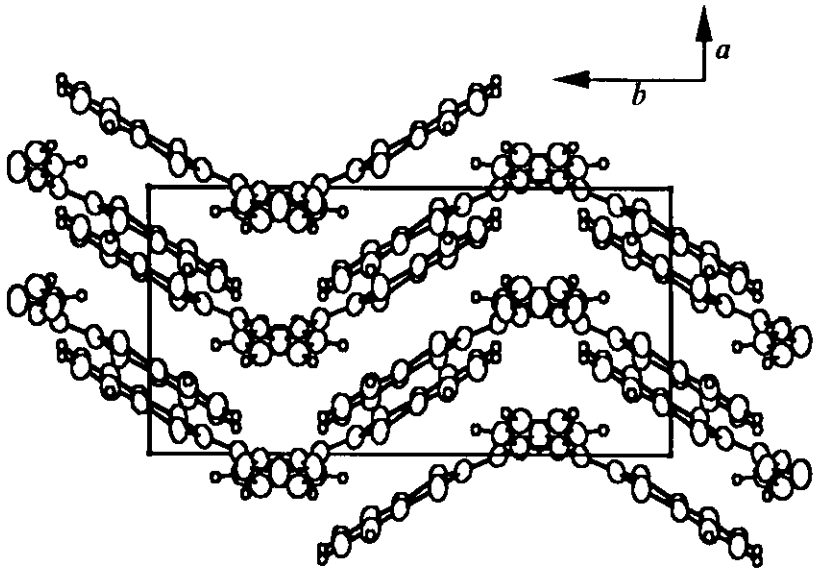

(*b*)

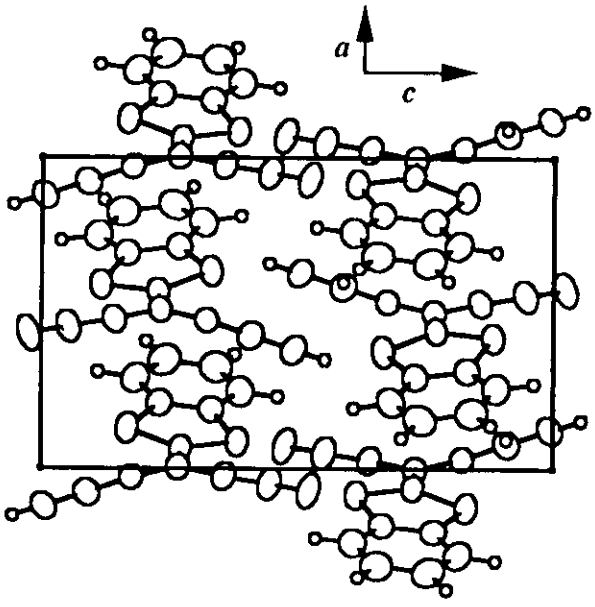

Figure 2. Crystal structure of **1**. (*a*) View along the *c* axis. (*b*) View along the *b* axis. Intermolecular distances between the central six-membered rings: 3.88-4.19 Å, between the 1,3-dithiole rings: 3.36-3.98 Å, and between the thiadiazole ring and the fused benzene ring: 3.33-3.90 Å.

Interestingly, the molecules are stacked alternately along the *a* axis as shown in Figure 2. The intermolecular distances between the central six-membered rings are 3.88-4.19 Å. The distances between the 1,3-dithiole rings are 3.36-3.98 Å, and those between the thiadiazole ring and the fused benzene ring are 3.33-3.90 Å. These values demonstrate that it is possible to interact with each other in the column. The overlap mode is good as shown in Figure 3, and the molecular shape seems to make the uniform columnar packing as a kind of template.

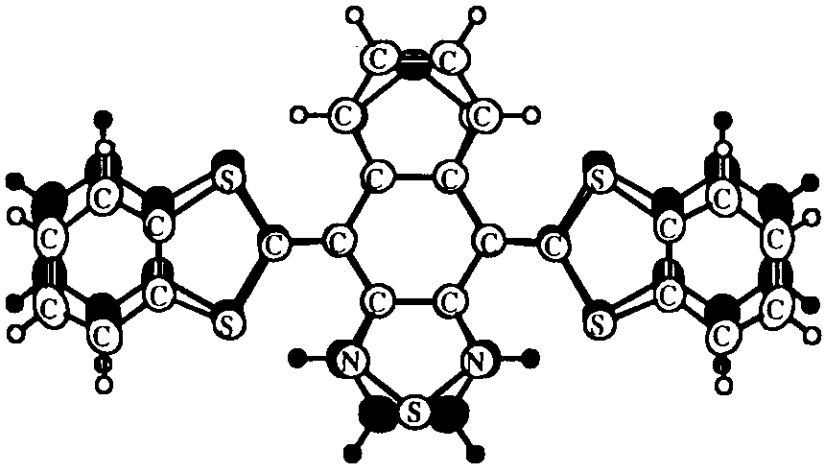

Figure 3. Overlap mode of **1** .

According to the X-ray crystal structure analysis of the PF_6 salt, the angles formed by the central six-membered ring and the 1,3-dithiole rings are 159.1° and 159.6°. The central six-membered ring is folded with the angle of 159.9°. The distances between the S atoms of the dithioles and the *peri*-hydrogen atoms are 2.23 and 2.27 Å, and those between the S atoms and the C atoms are 3.00 Å. Thus, the molecular structure of the PF_6 salt is similar to that of the neutral molecule, indicating a small conformational change

between the neutral and the cation radical states. Since the intramolecular S•••N contact distances, which are 2.65 and 2.67 Å, are a little shorter than that in the neutral state, it is considerable that the attractive interaction suppresses the conformational change. The molecules uniformly make columnar stacks (Figure 4), where the distances between the central six-membered ring and the thiadiazole ring are 3.60-3.65 Å. Another interesting feature is the overlap between the fused benzene rings leading to an intercolumnar interaction with an intermolecular distance of 3.59 Å.

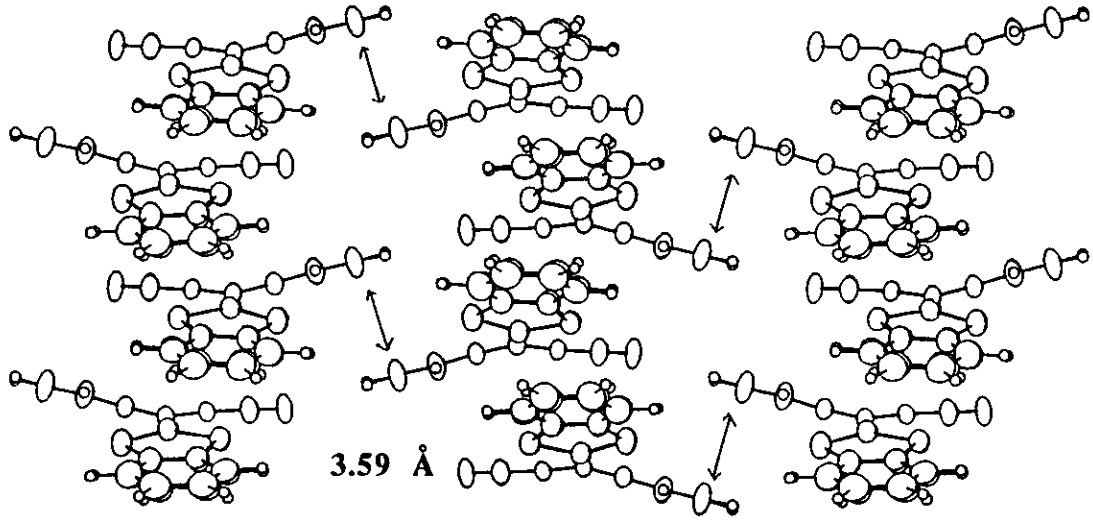

Figure 4. Crystal structure of the PF_6 salt. Only molecules of **1** are shown for clarity.

Figure 5 shows the HOMO, LUMO, and atomic charges calculated by using the final atomic coordinates of the X-ray crystal structure analysis.[4] The central six-membered ring and the dithioles have larger atomic orbital coefficients in the HOMO and

LUMO, indicating that the good overlap between these rings is required for an electrical conductivity. The S atoms of the dithioles have significantly positive charges (+0.300) and the N atoms have significantly negative charges (-0.192). Therefore, the intramolecular S•••N interactions are explained by a strong electrostatic effect.

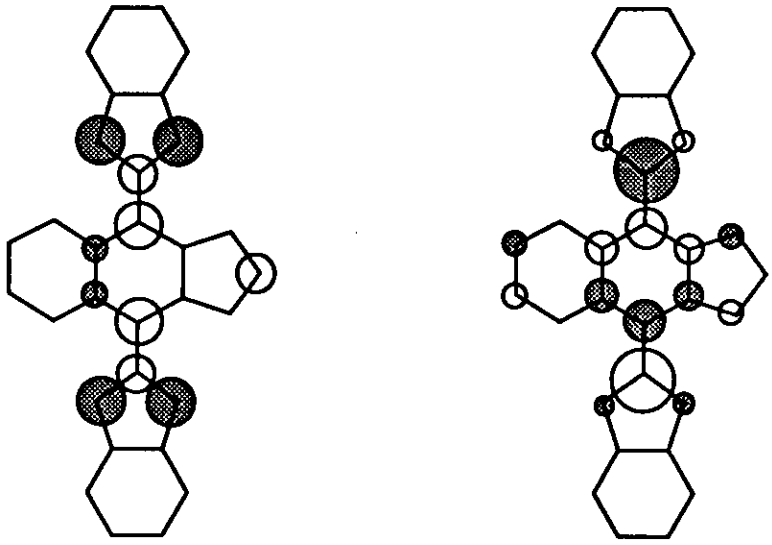

HOMO LUMO

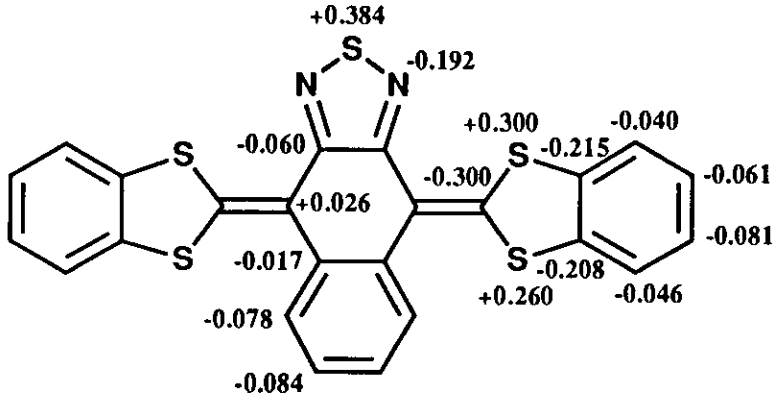

Atomic charges

Figure 5. HOMO, LUMO, and net atomic charges of **1** calculated by the MNDO-PM3 method.

Summary

The X-ray crystal structure analysis of nonplanar molecule **1** showed a unique butterfly-shaped structure. The angle formed by the central six-membered ring and the 1,3-dithiole ring is 158.1°, and the central six-membered ring is folded with the angle of 155.7°. The intramolecular short S•••N contacts were observed, and the distance (2.78 Å) is significantly shorter than the sum of their van der Waals radii (3.35 Å). The molecules are uniformly stacked to make columnar packing. The good electrical conductivity as a single component is ascribable to the effective intermolecular overlap. The conformational change between the neutral and the cation radical states is small because of the attractive intramolecular S•••N contacts arising from a strong electrostatic effect.

Experimental

X-Ray Crystal Structure Analysis of 1. A needle-like crystal with dimensions of 0.08 x 0.10 x 0.35 mm^3 along the a, b, and c axes was prepared by recrystallization from chloroform for the X-ray study. Crystal data are as follows: $C_{24}H_{12}N_2S_5$, M = 488.70, orthorhombic, space group $Pnma$, a = 8.1358(5), b = 18.7956(29), c = 13.5395(14) Å, V = 2070.4(4) $Å^3$, Z = 4, D_c = 1.57 g cm^{-3}, $F(000)$ = 1000, $\mu(Cu_{K\alpha})$ = 52.15 cm^{-1}, S = 1.37. The diffraction data were collected at 296 K by an ENRAF-NONIUS CAD4 diffractometer (40 kV, 32 mA) with graphite-monochromated Cu K_α radiation (λ = 1.5418 Å). Cell parameters were determined by least-squares procedures on 25 reflections (44° < 2θ < 50°). A total of 1783 unique data (2θ < 140°) was measured using the ω - 2θ scan method, and 1720 independent reflections ($|F_o| > 3\sigma|F_o|$) were used for the analysis. No absorption correction was applied. The structure was solved by the direct method with the program MULTAN 78.[5]

The positions of the hydrogen atoms were located by difference Fourier maps. The atomic parameters were refined by a block-diagonal least-squares procedure; $w^{-1} = \sigma(F_o)^2 + (0.015\sigma|F_o|)^2$. Anisotropic temperature factors were used for refining the non-hydrogen atoms, and isotropic temperature factors were adopted for the hydrogen atoms. The final R and R_w values are 0.0387 and 0.0411. The maximum residual electron density was 0.30 e Å^{-3}. The atomic scattering factors were taken from International Tables for X-Ray Crystallography.[6] The calculations were performed on a HITAC M-680H computer in Computer Center of Institute for Molecular Science using the programs UNICS III[7] and ORTEP[8]. Lists of the final atomic coordinates with equivalent isotropic thermal parameters (Table 1), bond lengths (Table 2), and bond angles (Table 3) are as follows.

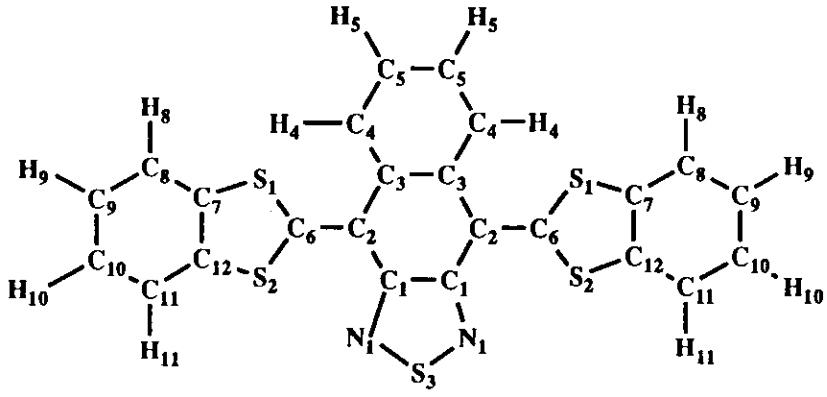

Table 1. Final atomic coordinates and equivalent isotropic thermal parameters[a] (Å^2).

Atom	X	Y	Z	B_{eq}
S1	0.3707 (1)	0.0554 (0)	0.6683 (0)	3.8
S2	0.4144 (1)	0.0558 (0)	0.8836 (0)	3.5
S3	0.5719 (1)	0.2500 (0)	1.0240 (1)	4.6
N1	0.5494 (3)	0.1835 (1)	0.9468 (1)	4.2
C1	0.5251 (3)	0.2118 (1)	0.8578 (2)	3.5
C2	0.4946 (3)	0.1718 (1)	0.7682 (2)	3.3

Atom	X	Y	Z	B_{eq}
C3	0.5291 (3)	0.2120 (1)	0.6767 (2)	3.3
C4	0.5779 (3)	0.1774 (1)	0.5903 (2)	3.9
C5	0.6232 (3)	0.2135 (1)	0.5063 (2)	4.2
C6	0.4362 (3)	0.1034 (1)	0.7723 (1)	3.3
C7	0.2906 (3)	-0.0174 (1)	0.7311 (2)	3.4
C8	0.2115 (3)	-0.0741 (1)	0.6841 (2)	4.2
C9	0.1552 (4)	-0.1298 (1)	0.7406 (2)	4.8
C10	0.1770 (4)	-0.1299 (1)	0.8420 (2)	4.8
C11	0.2545 (3)	-0.0741 (1)	0.8891 (2)	4.2
C12	0.3114 (3)	-0.0172 (1)	0.8329 (2)	3.5
H4	0.592 (3)	0.128 (1)	0.590 (2)	5.0
H5	0.654 (3)	0.186 (1)	0.446 (2)	5.0
H8	0.192 (3)	-0.074 (1)	0.611 (1)	3.6
H9	0.097 (3)	-0.166 (1)	0.705 (2)	6.2
H10	0.138 (3)	-0.166 (1)	0.879 (2)	5.7
H11	0.270 (3)	-0.074 (1)	0.962 (2)	4.8

[a] $B_{eq} = (4/3)\Sigma_i\Sigma_j\beta_{ij}\boldsymbol{a}_i \cdot \boldsymbol{a}_j$.

Table 2. Bond lengths (Å).

Atom	Atom	Distance	Atom	Atom	Distance
S1	-C6	1.756 (2)	S1	-C7	1.737 (2)
S2	-C6	1.761 (2)	S2	-C12	1.748 (2)
S3	-N1	1.639 (2)	N1	-C1	1.331 (3)
C1	-C1	1.435 (3)	C1	-C2	1.450 (3)
C2	-C3	1.478 (3)	C2	-C6	1.372 (3)
C3	-C3	1.429 (3)	C3	-C4	1.396 (3)

Atom	Atom	Distance	Atom	Atom	Distance
C4	-C5	1.375 (3)	C4	-H4	0.944 (24)
C5	-C5	1.374 (4)	C5	-H5	1.004 (23)
C7	-C8	1.398 (3)	C7	-C12	1.388 (3)
C8	-C9	1.377 (4)	C8	-H8	1.007 (20)
C9	-C10	1.384 (4)	C9	-H9	0.966 (26)
C10	-C11	1.382 (4)	C10	-H10	0.902 (40)
C11	-C12	1.392 (3)	C11	-H11	1.000 (22)

Table 3. Bond angles (degree).

Atom	Atom	Atom	Angle	Atom	Atom	Atom	Angle
N1	-C1	-C1	113.5 (2)	N1	-C1	-C2	125.1 (2)
C1	-C1	-C2	121.3 (2)	C3	-C2	-C6	125.5 (2)
C3	-C2	-C1	113.8 (2)	C6	-C2	-C1	120.8 (2)
C2	-C3	-C4	121.2 (2)	C2	-C3	-C3	120.8 (2)
C4	-C3	-C3	117.8 (2)	C3	-C4	-C5	122.7 (2)
C3	-C4	-H4	119.7 (1)	C5	-C4	-H4	117.2 (14)
C4	-C5	-C5	119.5 (2)	C4	-C5	-H5	119.0 (13)
C5	-C5	-H5	121.5 (13)	S1	-C6	-S2	113.2 (1)
S1	-C6	-C2	123.6 (2)	S2	-C6	-C2	123.1 (2)
S1	-C7	-C8	123.3 (2)	S1	-C7	-C12	116.0 (2)
C8	-C7	-C12	120.7 (2)	C7	-C8	-C9	118.7 (2)
C7	-C8	-H8	121.2 (12)	C9	-C8	-H8	120.1 (12)
C8	-C9	-C10	120.7 (3)	C8	-C9	-H9	115.2 (15)
C10	-C9	-H9	124.0 (15)	C9	-C10	-C11	121.1 (3)
C9	-C10	-H10	120.4 (16)	C11	-C10	-H10	118.5 (16)
C10	-C11	-C12	118.8 (2)	C10	-C11	-H11	120.8 (13)

Atom	Atom	Atom	Angle	Atom	Atom	Atom	Angle
C12	-C11	-H11	120.4 (13)	S2	-C12	-C7	116.8 (1)
S2	-C12	-C11	123.2 (2)	C7	-C12	-C11	120.0 (2)

References

(1) (a) M. R. Bryce, *Chem. Soc. Rev.*, **1991**, *20*, 355. (b) F. Ogura, T. Otsubo, and Y. Aso, *Sulfur Rep.*, **1992**, *11*, 439.

(2) (a) M. Adam, V. Enkelmann, H.-J. Rader, J. Röhrich, and K. Müllen, *Angew. Chem., Int. Ed. Engl.*, **1992**, *31*, 309. (b) A. Ohta, T. Kobayashi, and H. Kato, *J. Chem. Soc., Chem. Commun.*, **1993**, 431.

(3) (a) Y. Yamashita, Y. Kobayashi, and T. Miyashi, *Angew. Chem., Int. Ed. Engl.*, **1989**, *28*, 1052. (b) M. R. Bryce, M. A. Coffin, M. B. Hursthouse, A. I. Karaulov, K. Müllen, and H. Scheich, *Tetrahedron Lett.*, **1991**, *32*, 6029; M. R. Bryce, A. J. Moore, M. Hasan, G. J. Ashwell, A. T. Fraser, W. Clegg, M. B. Hursthouse, and A. I. Karaulov, *Angew. Chem., Int. Ed. Engl.*, **1990**, *29*, 1450.

(4) Calculated by the MNDO-PM3 method, MOPAC program, J. J. P. Stewart, *J. Comput. Chem.*, **1989**, *10*, 209, 221.

(5) P. Main, S. E. Hull, L. Lessinger, G. Germain, J.-P. Declercq, and M. M. Woolfson, *MULTAN 78, A System of Computer Programs for the Automatic Solution of Crystal Structures from X-Ray Diffraction Data*, University of York, England and Louvain-la-Nerve, Belgium, **1978**.

(6) *International Tables for X-Ray Crystallography, Vol. 4*, Kynoch Press, Birmingham, **1974**.

(7) T. Sakurai and K. Kobayashi, *UNICS III, Rikagaku Kenkyusho Hokoku*, **1979**, *55*, 69.

(8) C. K. Johnson, *ORTEP Report ORNL-3794*, Oak Ridge National Laboratory, Tennessee, **1965**.

Chapter 4 Molecule containing both π-Donor and π-Acceptor Units: 4H,8H-8-(1,3-Dithiol-2-ylidene)benzo[1,2-c:4,5-c´]bis([1,2,5]thiadiazol)-4-one

Introduction

Although many organic conductors are known, they are composed of multi-components such as charge-transfer (CT) complexes. Usual organic compounds are insulators as single components. However, molecules containing both donor and acceptor units are expected to exhibit unusual electrical properties owing to intramolecular CT interactions. 4*H*,8*H*-4,8-Bis(1,3-dithiol-2-ylidene)benzo[1,2-*c*:4,5-*c*´]bis([1,2,5]thiadiazole) (BTQBT **1**) is one of the most conductive materials as a single component.[1] The electrical conductivity at room temperature is 3.7 x 10^{-6} S cm^{-1} (E_a = 0.24 eV) for a crystal obtained by sublimation at 370 °C and 50 Torr.[2] The crystal showed small anisotropy in conductivity ($\sigma_{//} / \sigma_{\perp} \approx 2$) and a Hall effect, which is unusual as observation in organic semiconductors. According to the Hall effect study, the sign of carriers was determined to be positive and the Hall mobility was found to be *ca.* 4 cm^2 s^{-1} V^{-1} at room temperature. This conducting behavior is attributed to strong intermolecular interactions in the crystal.

The X-ray crystal structure analysis of BTQBT reveals that the molecules form a sheet-like network by intermolecular short S•••S contacts as shown in Figure 1.[1] The S•••S contact distance of 3.26 Å is much shorter than the sum of the van der Waals radii (3.70 Å). The molecules uniformly make stacks with an intermolecular distance of 3.46 Å. The overlap mode is in accord with that of the most effective interaction between the HOMO and LUMO, suggesting that an intermolecular CT interaction exists.

One of the 1,3-dithiole groups of BTQBT is replaced with a carbonyl group to give 4*H*,8*H*-8-(1,3-dithiol-2-ylidene)benzo[1,2-*c*:4,5-*c*´]bis([1,2,5]thiadiazol)-4-one

(*a*)

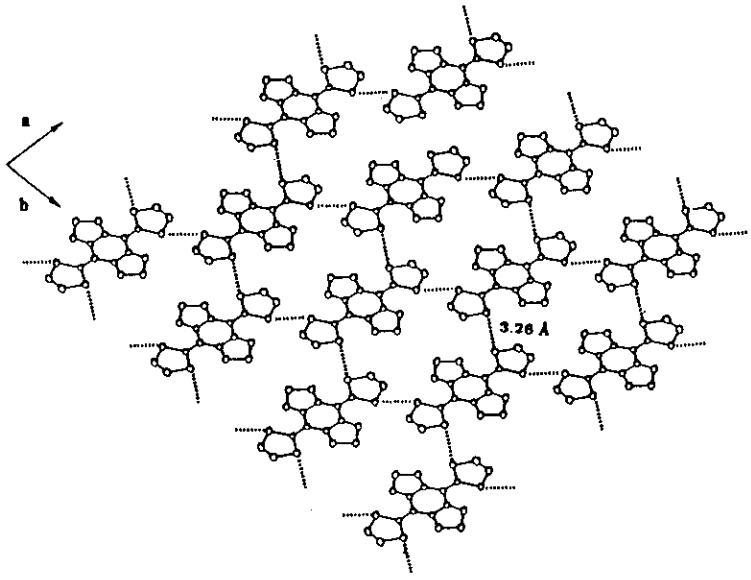

(*b*)

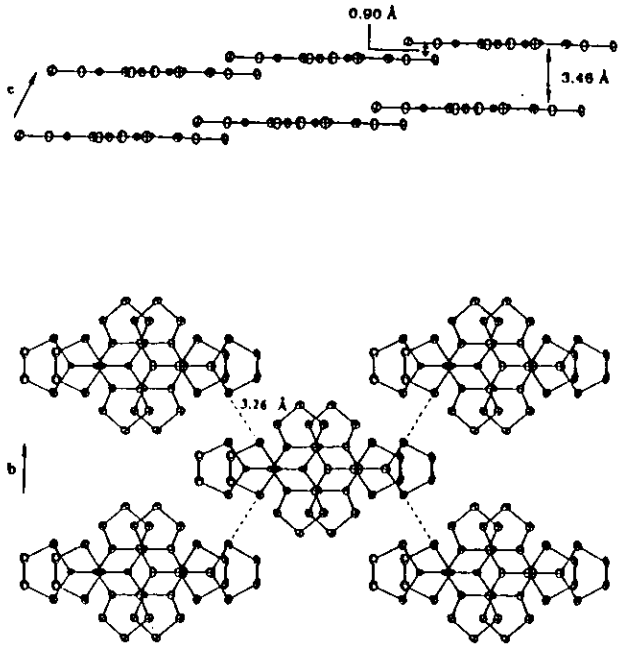

Figure 1. Views of the crystal structure of **1**. (*a*) Sheet-like network. Broken lines; short S•••S contacts. (*b*) Overlap mode. (*J. Org. Chem.*, **1992**, *57*, 5517.)

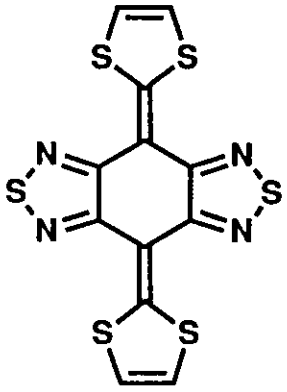

1

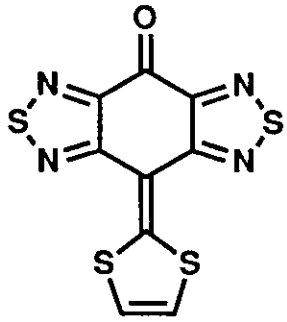

2

(BTQT **2**), which is considered to be more polarized than BTQBT **1**. BTQT **2** is expected to exhibit unusual electrical properties due to intramolecular CT interactions because of a molecule containing both donor and acceptor units.[3] In this chapter, I report the X-ray crystal structure analysis and electrical behavior of BTQT **2**.

Results and Discussion

X-Ray Crystal Structure Analysis

BTQT **2** was prepared by a Wittig-Horner reaction of quinone **3**[4] with an equivalent of a carbanion derived from phosphonate ester **4**[5] in a similar procedure as

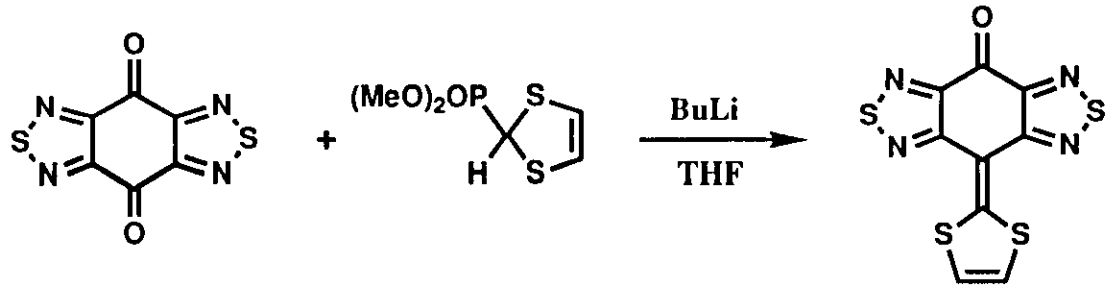

3 4 2

Scheme 1

BTQBT **1** (Scheme 1).[1] The longest absorption maximum was observed at 620 nm (sh) in a KBr disk, and it is red-shifted in comparison with that of BTQBT **1** [542 nm (sh)]. The C=O stretching frequency (1645 cm^{-1}) was observed lower than that of quinone **3** (1700 cm^{-1}). These facts indicate the highly polarized molecular structure of BTQT **2**.

In order to determine the molecular structure of BTQT **2** as well as to study intermolecular interactions, a single crystal was prepared by sublimation for the X-ray crystal structure analysis. The crystal data and the final atomic coordinates are shown in the experimental part. In this crystal there exist two crystallographically independent molecules (molecule 1 and molecule 2). Figure 2 gives the molecular structure of molecule 1. The molecules are planar, and the intramolecular distances between the S atoms of the dithioles and the N atoms of the thiadiazoles (2.80 and 2.82 Å for molecule 1, 2.77 and 2.83 Å for molecule 2) are shorter than the sum of their van der Waals distances (3.35 Å). Similar short S•••N contacts are observed in BTQBT **1** (2.78 Å) (Figure 3) and the related molecules[6]. The central six-membered ring of molecule 1 is distorted with large bond alternation, suggesting that molecule 1 has an increased quinoid character. The C=O (1.235 Å) and central C=C (1.395 Å) bond lengths of molecule 2 are longer than those of molecule 1 (C=O: 1.218 Å, C=C: 1.375 Å). The difference may be attributed to the modification in intermolecular interactions, since the O atom of molecule 2 is in an intermolecular S•••O contact. These molecular structures seem to be affected by intermolecular heteroatom contacts. Molecules 1 and 2 are both uniformly stacked with intermolecular distances of 3.36 and 3.40 Å, respectively (Figure 4). The overlap mode of molecule 1 is shown in Figure 5, and those of molecule 2 and BTQBT are similar. This overlap is in accord with an effective interaction between the HOMO and LUMO shown in Figure 6,[7] suggesting that an intermolecular CT interaction is possible in the crystal.

Three-dimensional intermolecular heteroatom contacts between molecules 1 and 2 were also observed as shown in Figure 7. Thus, the S•••S contact distance between the thiadiazole ring and the 1,3-dithiole ring is 3.42 Å, and the distance between the S atom of the 1,3-dithiole and the N atom of the thiadiazole is 3.14 Å. The S atom of the thiadiazole

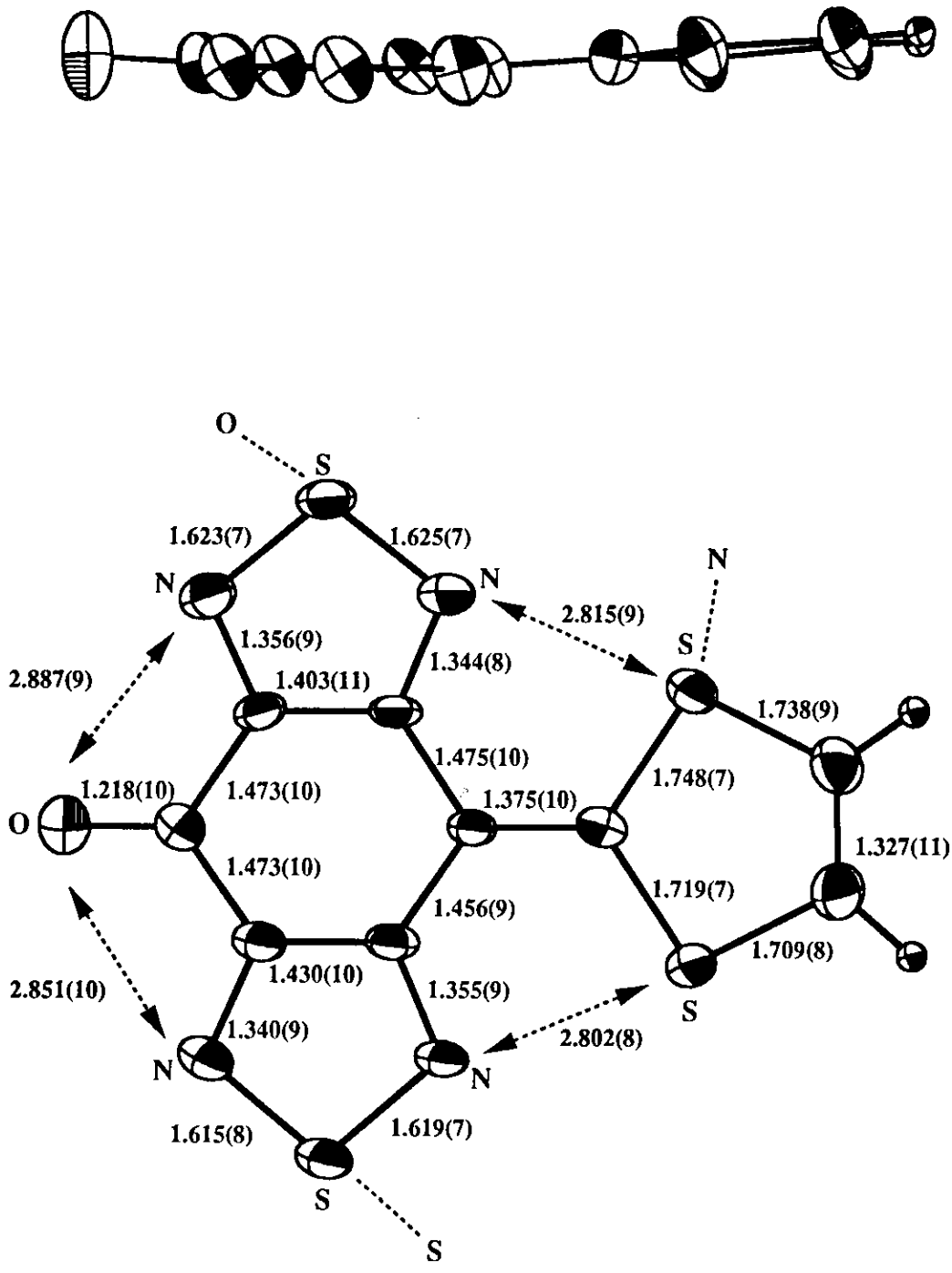

Figure 2. Molecular structure of BTQT **2** (molecule 1) with bond lengths (Å) (ORTEP).

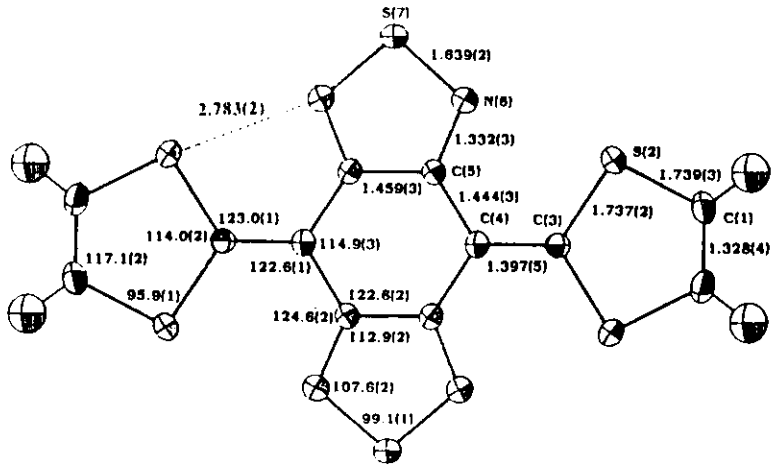

Figure 3. Molecular structure of BTQBT **1** with bond lengths (Å) (ORTEP). (*J. Org. Chem.*, **1992**, *57*, 5517.)

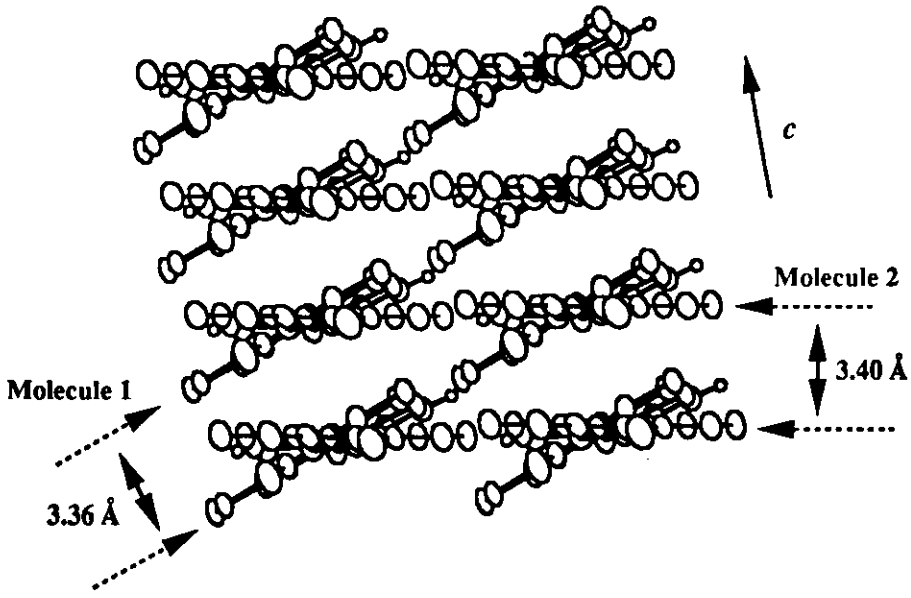

Figure 4. View of the columnar stacking of BTQT **2**.

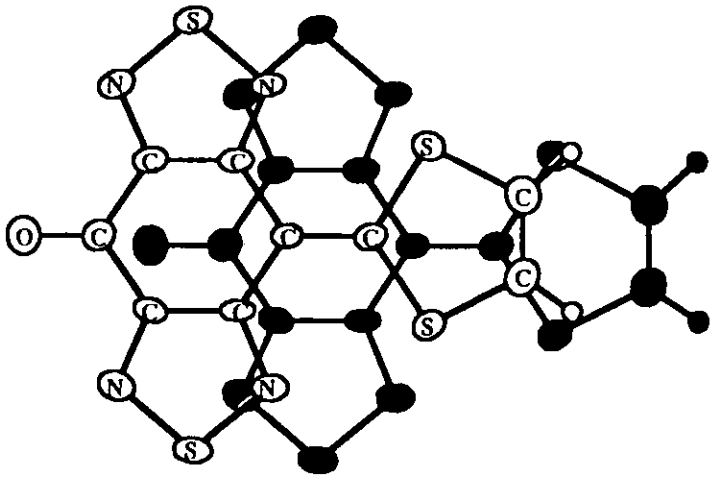

Figure 5. Overlap mode of BTQT **2** (molecule 1).

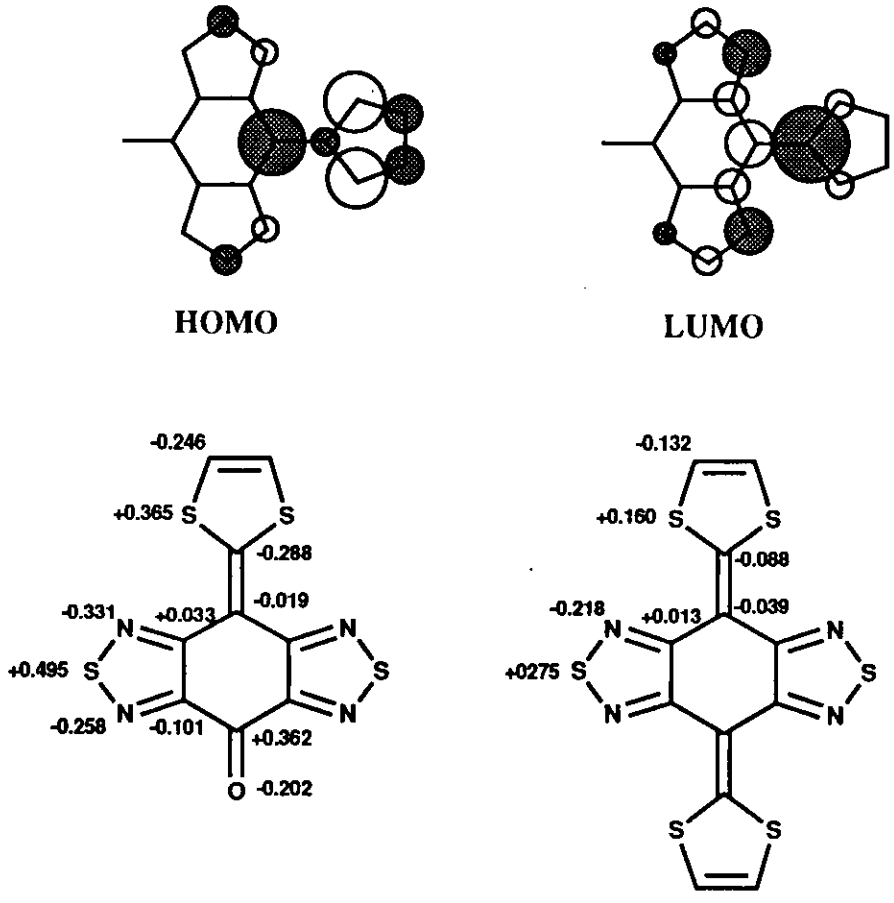

Figure 6. HOMO, LUMO, and net atomic charges of BTQT **2**.

(*a*)

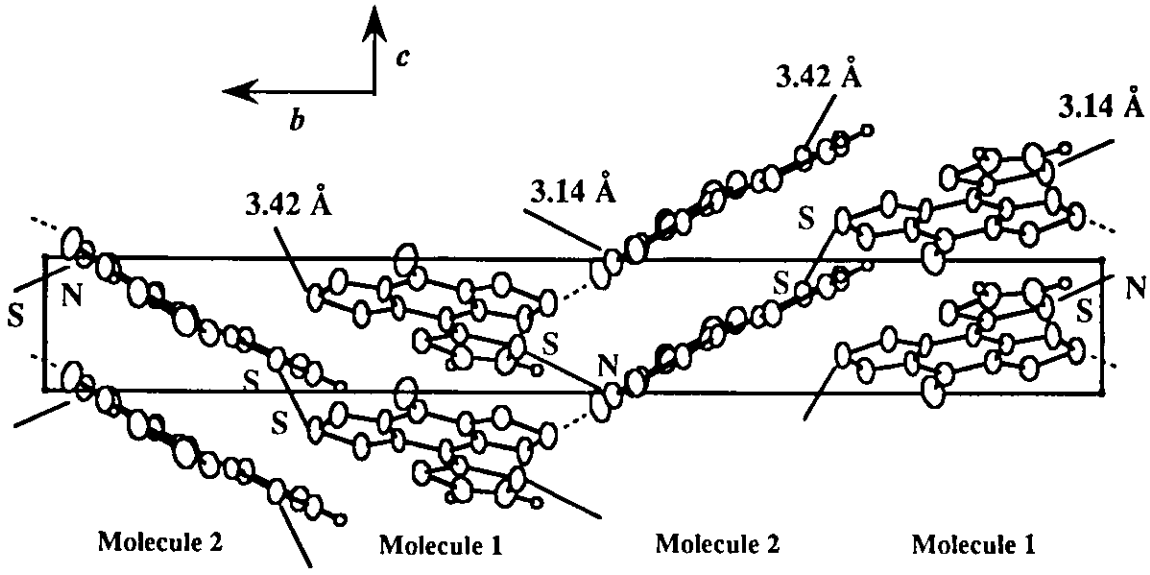

(*b*)

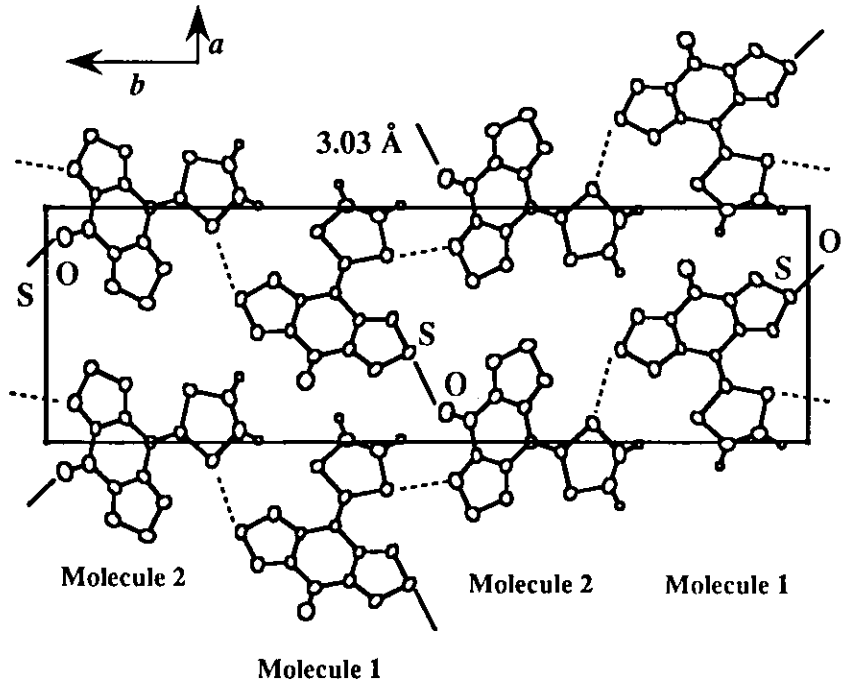

Figure 7. Three-dimensional heteroatom contacts. (*a*) View along the *a* axis. (*b*) View along the *c* axis.

in molecule 1 is also in contact with the O atom in molecule 2 (3.03 Å). These heteroatom contacts are in sharp contrast with those in the BTQBT crystal, where the heteroatoms of the thiadiazole rings are not involved in the intermolecular interactions (Figure 1*a*).[1] The net atomic charges of BTQT calculated by the MNDO method[8] show that the molecule is highly polarized (Figure 6), with the N atoms and the O atom negatively charged and the S atoms positively charged. Therefore, the S•••N and S•••O contacts are ascribable to electrostatic interactions, and the fact that the S•••S contact distance is longer than 3.26 Å of BTQBT **1** may be concerned with Coulombic repulsion.

Electrical Property of BTQT

BTQT **2** showed unusual behavior on measurement of the resistivity of single crystals prepared by sublimation. The correlation of the current (I) with voltage (E) fails to obey Ohm's law as shown in Figure 8. The electric field was applied between gold electrodes at a distance of *ca.* 0.5 mm. The current increases approximately in proportion to E^3. This behavior was independent of the polarity of the applied field and was reproducible for several runs in several crystals with different dimensions. In view of the fact that the E^3 behavior extends to low applied voltage and is not strongly dependent on crystal thickness, space-charge-limited behavior is unlikely. It is a considerable view that the nonlinear correlation observed in the BTQT crystal may be caused by increases of carrier number (n) and carrier mobility (μ) resulting from a subtle change of the intermolecular overlap of the highly polarized BTQT molecule induced by the electric field. In order to investigate this point, the temperature dependence of resistivity under different applied electric fields (state I: 5 V and state II: 100 V) was studied. The resistivity at room temperature was *ca.* 10^8 Ω cm for state I and 3 x 10^5 Ω cm for state II. The activation energy was also determined to be 0.30 and 0.22 eV, respectively. Since the carrier number n depends on the Boltzmann factor $\exp(-E_g / 2kT)$, the ratio of n at room

temperature between state I and state II can be calculated to be *ca.* 1 / 20. This value is not large enough to explain the *ca.* 300 times lower resistivity for state II. The non-ohmic behavior is unprecedented as organic crystals.

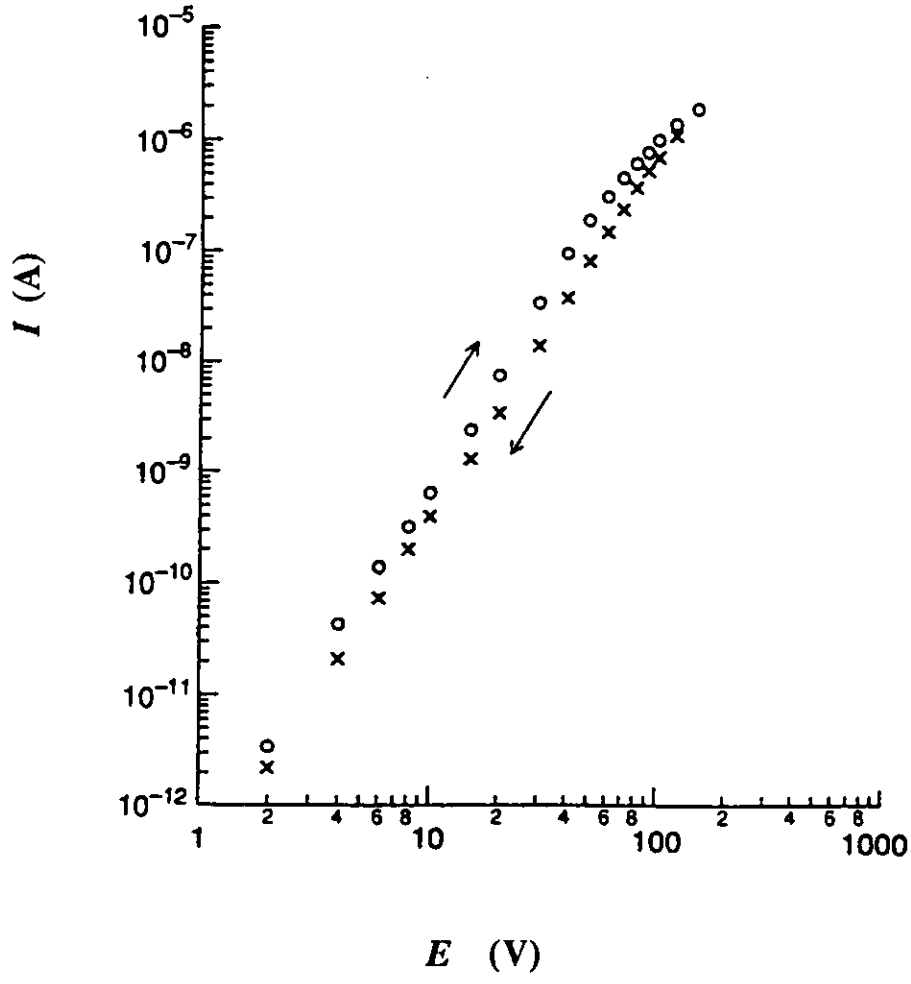

Figure 8. Relationship between current (*I*) and voltage (*E*) for a single crystal of BTQT **2** at room temperature.

Summary

BTQT **2** was investigated with its crystal structure and electrical conducting behavior. The planar structure and intramolecular short S•••N contacts were observed in the X-ray crystal structure analysis. The molecular overlap is close to that of BTQBT **1**. The overlap mode is caused by the most effective interaction between the HOMO and LUMO, suggesting an intermolecular CT interaction. On the other hand, the molecular packing is in sharp contrast with that of BTQBT, which makes a sheet-like network with short S•••S contacts. BTQT molecules are three-dimensionally connected with each other through short S•••S, S•••N, and S•••O contacts. These S•••N and S•••O contacts are ascribable to electrostatic interactions due to the highly polarized molecular structure. The electrical conducting behavior fails to obey Ohm's law. The current increased approximately in proportion to the third power of voltage. This result suggested that a highly polarized molecule exhibits unique electrical behavior susceptible to an applied electric field. The non-ohmic behavior observed here is unprecedented as organic crystals.

Experimental

X-Ray Crystal Structure Analysis of BTQT 2. A needle-like crystal with dimensions of 0.08 x 0.20 x 0.40 mm^3 along the a, b, and c axes was prepared by sublimation (350 °C) for the X-ray study. Crystal data are as follows: $C_9H_2N_4OS_4$, M = 310.41, monoclinic, space group $P2_1$, a = 9.311(2), b = 30.089(4), c = 3.868(1) Å, β = 101.09(1)°, V = 1063.5(3) $Å^3$, Z = 4, D_c = 1.94 g cm^{-3}, $F(000)$ = 624, $\mu(Cu_{K\alpha})$ = 80.58 cm^{-1}, S = 2.46. The diffraction data were collected at 296 K by an ENRAF-NONIUS CAD4 diffractometer (40 kV, 32 mA) with graphite-monochromated Cu K_α radiation (λ = 1.5418 Å). Cell parameters were determined by least-squares procedures on 25 reflections (44° < 2θ < 50°). A total of 1971 unique data (2θ < 140°) was measured

using the ω - 2θ scan method, and 1961 independent reflections ($|F_o| > 3\sigma|F_o|$) were used for the analysis. No absorption correction was applied. The structure was solved by the direct method with the program SHELX 86.[8] The positions of the hydrogen atoms were located by a difference Fourier map and the program HYCO 80. The atomic parameters were refined by a block-diagonal least-squares procedure; $w^{-1} = \sigma(F_o)^2 + (0.015\sigma|F_o|)^2$. Anisotropic temperature factors were used for refining the non-hydrogen atoms, and isotropic temperature factors were adopted for the hydrogen atoms. The final R and R_w values are 0.0461 and 0.0568. The maximum residual electron density was 0.56 e Å^{-3}. The atomic scattering factors were taken from International Tables for X-Ray Crystallography.[9] The calculations were performed on a HITAC M-680H computer in Computer Center of Institute for Molecular Science using the programs UNICS III[10] and ORTEP[11]. Lists of the final atomic coordinates with equivalent isotropic thermal parameters (Table 1), bond lengths (Table 2), and bond angles (Table 3) are as follows.

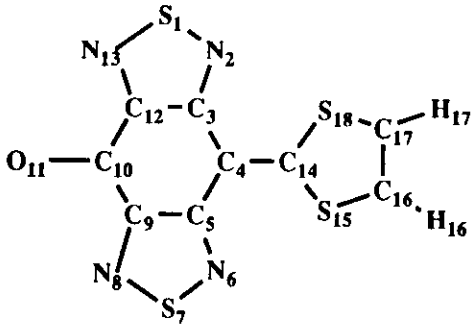

Molecule 1

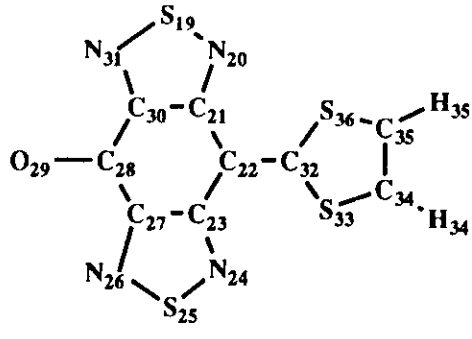

Molecule 2

Table 1. Final atomic coordinates and equivalent isotropic thermal parameters[a] (Å^2).

Atom	x	y	z	B_{eq}
S1	-0.3805 (2)	0.0238 (1)	1.3244 (5)	2.8
N2	-0.5230 (6)	0.0460 (2)	1.4403 (18)	2.8

Atom	x	y	z	B_{eq}
C3	-0.5190 (7)	0.0898 (2)	1.3758 (18)	2.1
C4	-0.6323 (7)	0.1208 (2)	1.4477 (19)	2.2
C5	-0.6011 (7)	0.1665 (2)	1.3641 (18)	2.1
N6	-0.6870 (7)	0.2014 (2)	1.4138 (18)	2.9
S7	-0.6076 (2)	0.2448 (1)	0.2905 (5)	2.9
N8	-0.4659 (7)	0.2233 (2)	1.1723 (18)	2.9
C9	-0.4755 (7)	0.1795 (2)	1.2274 (19)	2.4
C10	-0.3648 (7)	0.1483 (2)	1.1457 (19)	2.6
O11	-0.2624 (6)	0.1595 (2)	1.0120 (18)	4.2
C12	-0.3961 (7)	0.1024 (2)	1.2401 (20)	2.5
N13	-0.3082 (6)	0.0681 (2)	1.1902 (16)	2.7
C14	-0.7588 (7)	0.1082 (2)	1.5536 (17)	2.2
S15	-0.8951 (2)	0.1444 (1)	1.6103 (5)	2.6
C16	-1.0091 (8)	0.1057 (3)	1.7355 (21)	3.0
C17	-0.9634 (8)	0.0638 (3)	1.7599 (23)	3.4
S18	-0.7940 (2)	0.0531 (1)	1.6537 (5)	2.7
S19	0.4103 (2)	0.3678 (1)	0.4685 (6)	3.6
N20	0.2628 (6)	0.3452 (2)	0.5537 (17)	3.0
C21	0.1493 (7)	0.3718 (2)	0.4158 (20)	2.6
C22	-0.0001 (7)	0.3630 (2)	0.4368 (18)	2.2
C23	-0.1032 (7)	0.3961 (2)	0.2812 (19)	2.4
N24	-0.2463 (6)	0.3957 (2)	0.2756 (17)	2.7
S25	-0.3149 (2)	0.4402 (1)	0.0732 (6)	3.1
N26	-0.1687 (7)	0.4621 (2)	-0.0211 (18)	3.2
C27	-0.0593 (7)	0.4350 (2)	0.1063 (19)	2.5
C28	0.0935 (9)	0.4433 (2)	0.0679 (22)	3.2
O29	0.1286 (7)	0.4748 (2)	-0.1024 (18)	4.2

Atom	x	y	z	B_{eq}
C30	0.1966 (8)	0.4102 (2)	0.2474 (21)	2.8
N31	0.3404 (7)	0.4122 (2)	0.2571 (20)	3.5
C32	-0.0429 (7)	0.3237 (2)	0.5796 (18)	2.3
S33	-0.2230 (2)	0.3111 (1)	0.6038 (5)	2.7
C34	-0.1889 (8)	0.2600 (2)	0.8054 (21)	3.1
C35	-0.0503 (9)	0.2467 (3)	0.8653 (22)	3.3
S36	0.0791 (2)	0.2817 (1)	0.7521 (5)	2.8
H16	1.103 (10)	0.116 (3)	1.792 (25)	5.6
H17	1.012 (9)	0.034 (3)	1.829 (22)	4.7
H34	0.278 (9)	0.247 (3)	0.880 (21)	4.0
H35	-0.010 (11)	0.221 (3)	0.963 (25)	5.0

[a] $B_{eq} = (4/3)\Sigma_i\Sigma_j\beta_{ij}\boldsymbol{a}_i \cdot \boldsymbol{a}_j$.

Table 2. Bond lengths (Å).

Molecule 1		Distance	Molecule 2		Distance
S1	-N2	1.625 (7)	S19	-N20	1.624 (7)
S1	-N13	1.623 (7)	S19	-N31	1.634 (7)
N2	-C3	1.344 (8)	N20	-C21	1.351 (9)
C3	-C4	1.475 (10)	C21	-C22	1.435 (10)
C3	-C12	1.403 (11)	C21	-C30	1.439 (11)
C4	-C5	1.456 (9)	C22	-C23	1.433 (9)
C4	-C14	1.375 (10)	C22	-C32	1.395 (10)
C5	-N6	1.355 (9)	C23	-N24	1.330 (10)
C5	-C9	1.430 (10)	C23	-C27	1.450 (10)
N6	-S7	1.619 (7)	N24	-S25	1.617 (6)
S7	-N8	1.615 (8)	S25	-N26	1.618 (7)

Molecule 1		Distance	Molecule 2		Distance
N8	-C9	1.340 (9)	N26	-C27	1.323 (9)
C9	-C10	1.473 (10)	C27	-C28	1.482 (12)
C10	-O11	1.218 (10)	C28	-O29	1.235 (11)
C10	-C12	1.473 (10)	C28	-C30	1.461 (10)
C12	-N13	1.356 (9)	C30	-N31	1.335 (10)
C14	-S15	1.719 (7)	C32	-S33	1.741 (8)
C14	-S18	1.748 (7)	C32	-S36	1.743 (7)
S15	-C16	1.709 (8)	S33	-C34	1.726 (8)
C16	-C17	1.327 (11)	C34	-C35	1.330 (12)
C17	-S18	1.738 (9)	C35	-S36	1.722 (9)

Table 3. Bond angles (degree).

Molecule 1			Angle	Molecule 2			Angle
N2	-S1	-N13	99.5 (3)	N20	-S19	-N31	99.9 (4)
S1	-N2	-C3	107.3 (5)	S19	-N20	-C21	107.5 (5)
N2	-C3	-C4	122.6 (6)	N20	-C21	-C22	124.2 (7)
N2	-C3	-C12	112.9 (6)	N20	-C21	-C30	111.7 (6)
C4	-C3	-C12	124.5 (6)	C22	-C21	-C30	124.1 (6)
C3	-C4	-C5	112.0 (6)	C21	-C22	-C23	115.3 (6)
C3	-C4	-C14	124.7 (6)	C21	-C22	-C32	122.3 (6)
C5	-C4	-C14	123.1 (6)	C23	-C22	-C32	122.4 (6)
C4	-C5	-N6	123.4 (6)	C22	-C23	-N24	126.1 (7)
C4	-C5	-C9	123.6 (6)	C22	-C23	-C27	122.0 (6)
N6	-C5	-C9	113.0 (6)	N24	-C23	-C27	111.9 (6)
C5	-N6	-S7	105.5 (5)	C23	-N24	-S25	107.6 (5)
N6	-S7	-N8	101.8 (4)	N24	-S25	-N26	100.0 (4)

Molecule 1			Angle	Molecule 2			Angle
S7	-N8	-C9	105.4 (5)	S25	-N26	-C27	106.8 (5)
C5	-C9	-N8	114.3 (6)	C23	-C27	-N26	113.8 (7)
C5	-C9	-C10	124.3 (6)	C23	-C27	-C28	123.1 (6)
N8	-C9	-C10	121.3 (7)	N26	-C27	-C28	123.1 (7)
C9	-C10	-O11	123.8 (7)	C27	-C28	-O29	122.9 (7)
C9	-C10	-C12	111.3 (6)	C27	-C28	-C30	113.2 (7)
O11	-C10	-C12	124.9 (7)	O29	-C28	-C30	123.9 (8)
C3	-C12	-C10	124.2 (6)	C21	-C30	-C28	122.1 (7)
C3	-C12	-N13	114.1 (6)	C21	-C30	-N31	114.9 (6)
C10	-C12	-N13	121.7 (7)	C28	-C30	-N31	123.2 (7)
S1	-N13	-C12	106.2 (5)	S19	-N31	-C30	106.2 (6)
C4	-C14	-S15	124.2 (5)	C22	-C32	-S33	123.9 (5)
C4	-C14	-S18	122.4 (5)	C22	-C32	-S36	123.4 (5)
S15	-C14	-S18	113.4 (4)	S33	-C32	-S36	112.7 (4)
C14	-S15	-C16	96.9 (4)	C32	-S33	-C34	97.1 (4)
S15	-C16	-C17	117.3 (6)	S33	-C34	-C35	115.8 (6)
S15	-C16	-H16	118.6 (60)	S33	-C34	-H34	113.1 (48)
C17	-C16	-H16	124.1 (61)	C35	-C34	-H34	130.8 (48)
C16	-C17	-S18	116.9 (6)	C34	-C35	-S36	118.4 (6)
C16	-C17	-H17	132.1 (51)	C34	-C35	-H35	130.1 (68)
S18	-C17	-H17	111.0 (51)	S36	-C35	-H35	111.5 (68)
C14	-S18	-C17	95.5 (4)	C32	-S36	-C35	96.0 (4)

References

(1) (a) Y. Yamashita, S. Tanaka, K. Imaeda, H. Inokuchi, and M. Sano, *J. Org. Chem.*, **1992**, *57*, 5517. (b) Y. Yamashita, S. Tanaka, K. Imaeda, and H. Inokuchi, *Chem. Lett.*, **1991**, 1213.

(2) K. Imaeda, Y. Yamashita, Y. Li, T. Mori, H. Inokuchi, and M. Sano, *J. Mater. Chem.*, **1992**, *2*, 115.

(3) (a) R. M. Metzger and C. A. Panetta, *New J. Chem.*, **1991**, *15*, 209. (b) S. L. Buchwalter, R. Iyengar, A. Viehbeck, and T. R. O'Toole, *J. Am. Chem. Soc.*, **1991**, *113*, 376.

(4) R. Neidlein, D. Tran-Viet, A. Gieren, M. Kokkinidis, R. Wilckens, H. Geserich, and W. Ruppel, *Chem. Ber.*, **1982**, *115*, 2898.

(5) K. Akiba, K. Ishikawa, and N. Inamoto, *Bull. Chem. Soc. Jpn.*, **1978**, *51*, 2674.

(6) Y. Yamashita, S. Tanaka, K. Imaeda, H. Inokuchi, and M. Sano, *Chem. Lett.*, **1992**, 419.

(7) Calculated by the MNDO method, MOPAC program, J. J. P. Stewart, *QCPE Bull.*, **1983**, *3*, 419.

(8) G. M. Sheldrick, *SHELX 86, Program for Crystal Structure Determination*, University of Cambridge, England, **1986**.

(9) *International Tables for X-Ray Crystallography, Vol. 4*, Kynoch Press, Birmingham, **1974**.

(10) T. Sakurai and K. Kobayashi, *UNICS III, Rikagaku Kenkyusho Hokoku*, **1979**, *55*, 69.

(11) C. K. Johnson, *ORTEP Report ORNL-3794*, Oak Ridge National Laboratory, Tennessee, **1965**.

Chapter 5 Nonclassical π-Electron Ring Systems: Benzo[1,2-c:4,5-c´]bis([1,2,5]thiadiazole)s and the Monoselenium Analogues

Introduction

Heterocycles containing hypervalent sulfur atoms have attracted considerable attention due to their unique electronic structures and reactivities.[1] 1,2,5-Thiadiazole rings containing a tetravalent sulfur atom are more stable than the related thiophene rings as found in stable bis([1,2,5]thiadiazolo)[3,4-*b*:3´,4´-*e*]pyrazine **1**[2] and [1,2,5]thiadiazolo-[3,4-*c*][1,2,5]thiadiazole **2**[3]. The pyrazine derivative **1** has a strong electron-accepting ability[2] and forms a ribbon-like network by short intermolecular contacts between the hypervalent S atoms and the N atoms as shown in Figure 1. In this context, benzo[1,2-*c*:4,5-*c*´]bis([1,2,5]thiadiazole) **3a** is expected to have a high electron affinity and to form a unique molecular network. This compound resembles the framework of bis([1,2,5]thiadiazolo)tetracyanoquinodimethane (BTDA **4**), which is an electron acceptor in organic metals and forms a sheet-like network through short S•••N≡C contacts as displayed in Figure 1 of Chapter 1 (p. 3).[4] However, **5**, which was prepared from **4**, is its only reported derivative.[5] H_2BTDA **5a** was demonstrated to dissociate into the dianion **7** ($BTDA^{2-}$) in a polar solvent (Scheme 1), and the pK_{a2} value was determined to be -0.2 from measurement in water by an absorptiometric method, indicating a unique property of the benzobis(thiadiazole) molecule and the stability of the dianion **7**. I have now synthesized the benzobis(thiadiazole) derivatives **3b** and **3c** and the analogous selenadiazoles **6b** and **6c**.[6] In this chapter, I report their preparation and characterization, and the crystal structure of **3b**. Moreover, novel heterocycles containing both donor and acceptor units were synthesized by introduction of electron-donating groups into the electron-accepting benzobis(thiadiazole) skeleton, and their amphoteric properties are also

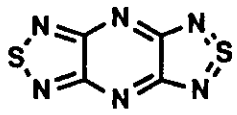

1

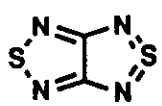

2

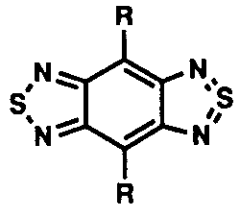

3a R = H
3b R = Br
3c R = Ph

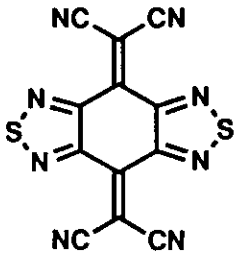

4

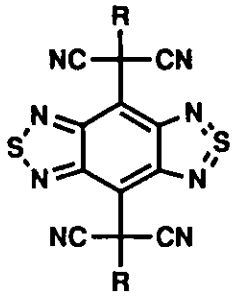

5a R = H
5b R = $C(CH_3)_2CN$

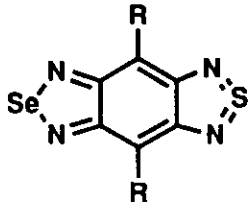

6a R = H
6b R = Br
6c R = Ph

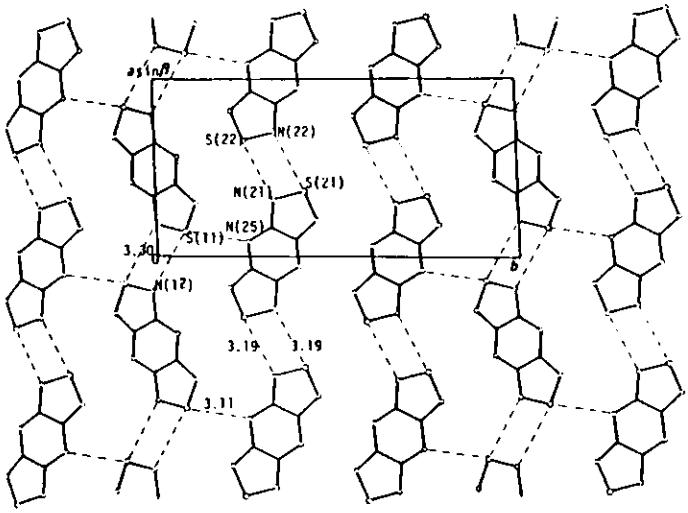

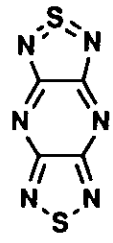

Figure 1. Ribbon-like network of **1**. Broken lines reveal short S•••N contacts (3.11 Å , 3.19 Å, and 3.30 Å). (*Angew. Chem., Int. Ed. Engl.*, **1988**, *27*, 434.)

characterized by an electrochemical study.

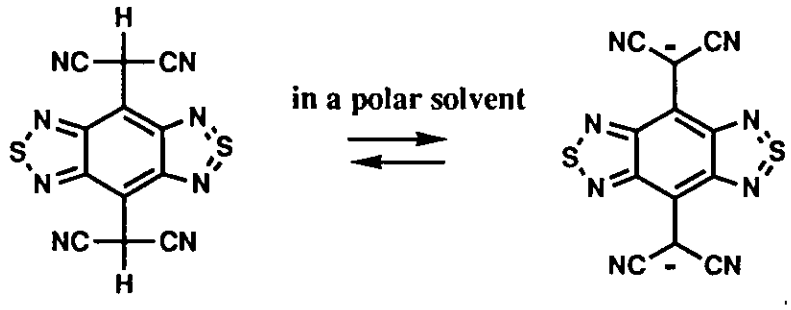

5a H_2BTDA **7 $BTDA^{2-}$**

Scheme 1

Results and Discussion

Preparation and Properties of Nonclassical Benzobis(thiadiazole)s

Heterocycles **3b,c** and **6b,c** were synthesized as summarized in Scheme 2. Reduction of dinitrobenzothiadiazole **8a**[7] with iron dust in acetic acid gave diamine **9a**.[8] Heterocycle **3b** was prepared in 74% yield by reaction of diamine **9a** with thionyl chloride in pyridine at room temperature. The analogous heterocycle **6b** was obtained in 40% yield from diamine **9a** and selenium dioxide. The palladium-catalyzed coupling [$PdCl_2(PPh_3)_2$] of bromide **8a** with tributylphenyltin **10a**[9] in tetrahydrofuran (THF) afforded **8b**, which was reduced with iron dust to give diamine **9b**. Heterocycle **3c** was prepared in 95% yield by reaction of diamine **9b** with *N*-thionylaniline and trimethylsilyl chloride in pyridine at 80 °C. The selenium compound **6c** was obtained in 82% yield from diamine **9b** and selenium dioxide. These heterocycles were purified by sublimation under reduced pressure and isolated as deep red crystals for **3b** (decomp > 280 °C), purple

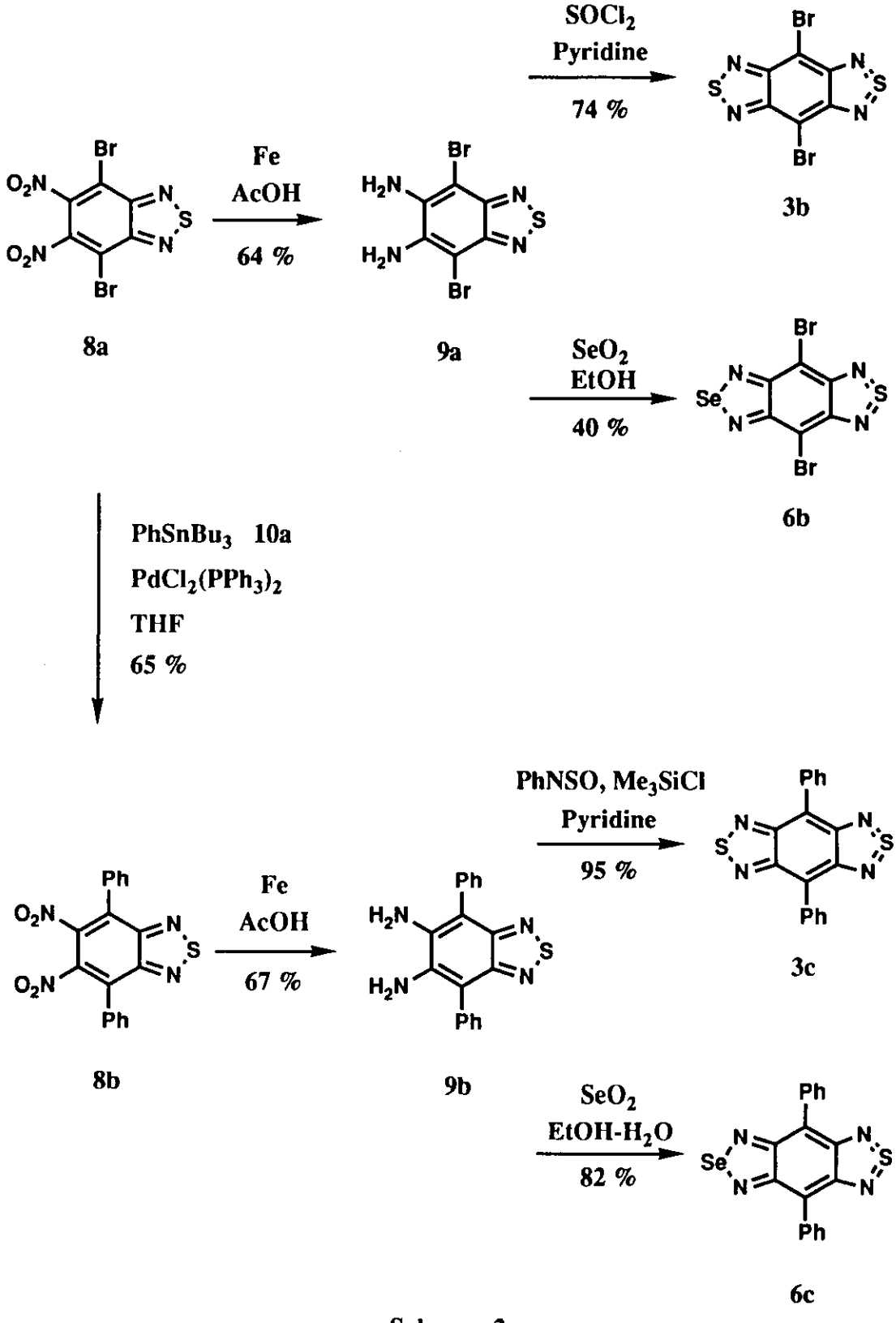
SOCl2
Pyridine
74 %
Br
3b
Fe
AcOH
64 %
8a
9a
SeO2
EtOH
40 %
6b
PhSnBu3 10a
PdCl2(PPh3)2
THF
65 %
PhNSO, Me3SiCl
Pyridine
95 %
Ph
3c
Fe
AcOH
67 %
8b
9b
SeO2
EtOH-H2O
82 %
6c

Scheme 2

prisms for **3c** (decomp 310-311 °C), purple crystals for **6b** (decomp > 280 °C), and blue crystals for **6c** (decomp 367-371 °C). These structures were determined by elemental analyses and their molecular ion peaks in the mass spectra. Other spectra also supported the benzobis(thiadiazole) skeleton. The absorption maxima of **3b,c** and **6b,c** are listed in Table 1.

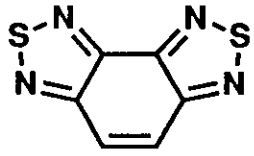

11

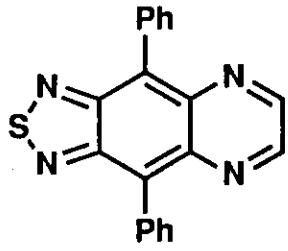

12

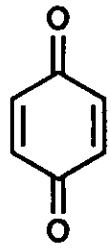

13

Table 1. Absorption maxima[a] of heterocycles **3**, **6**, **11**, and **12**.

Heterocycle	λ_{max} / nm (log ε)
3b	524 (3.64)
3c	558 (3.99)
6b	609[b]
6c	625 (4.01)
11	283 (4.57)
12	471 (3.99)

[a] In CH_2Cl_2. [b] Molar absorptivity was not obtained because of its low solubility.

These values are much red-shifted compared with that of benzobis(thiadiazole) **11**[10], whose thiadiazole ring can be represented by a standard Kekulé structure. Moreover, the value of **3c** is longer than that of thiadiazoloquinoxaline **12**, which was obtained from **9b** and 1,4-dioxane-2,3-diol. As the result, the nonclassical heterocycles **3** and **6** are

characterized by the red-shifted absorption maxima. The red shifts of **6b,c** from **3b,c** are regarded as a polar effect caused by the selenium atom. Introduction of substituents in the 4- and 8-positions in **3** and **6** seems favorable to underscore this effect, since these positions have larger atomic orbital coefficients in the HOMO and LUMO as shown in Figure 2.[11]

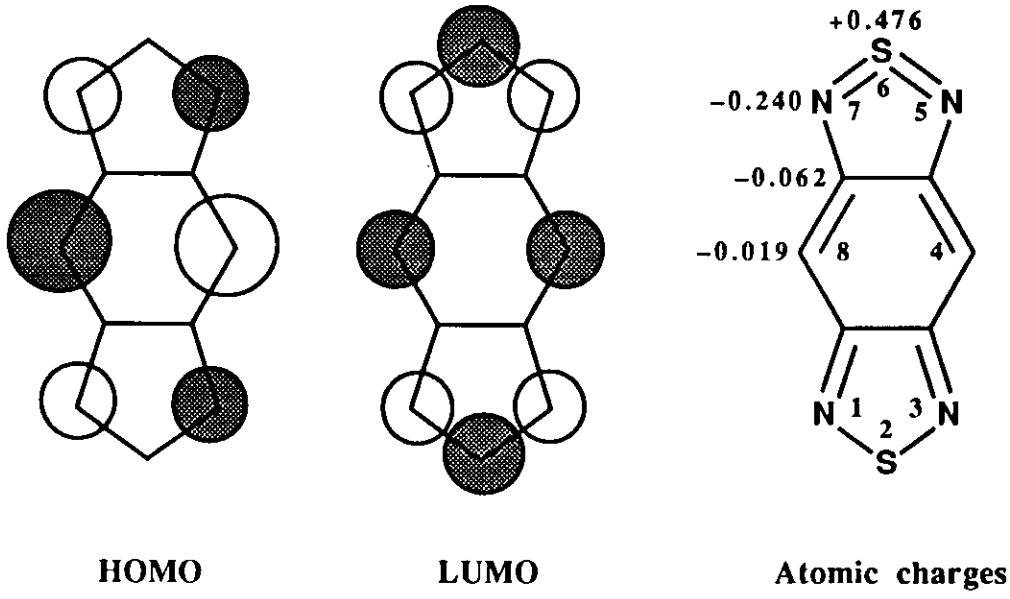

HOMO **LUMO** **Atomic charges**

Figure 2. HOMO, LUMO, and net atomic charges of **3a** calculated by the MNDO-PM3 method.

The cyclic voltammograms (CV) of **3b,c** and **6c** in dichloromethane showed two reversible one-electron redox waves. The half-wave reduction potentials are given in Table 2. The first reduction potentials of these heterocycles are comparable to that of *p*-benzoquinone **13** (E = -0.46 V). The electron-withdrawing bromo groups at 4- and 8-positions further increase the reduction potentials. The fact that the Kekulé-type isomer **11** is a weaker acceptor (Table 2) shows that the high electron affinity of **3** and **6** is attributable to the 14π-electron ring system containing a tetravalent sulfur atom, which

generates a more stable Kekulé-type thiadiazole ring upon accepting an electron. In addition, compound **3c** is a stronger electron acceptor than thiadiazoloquinoxaline **12**.

Table 2. Reduction potentials[a] of heterocycles **3**, **6**, **11**, and **12**.

Heterocycle	E_1 / V	E_2 / V	ΔE
3b	-0.35	-1.10	0.75
3c	-0.61	-1.30	0.69
6b	-0.26[b]		
6c	-0.53	-1.21	0.68
11	-1.45		
12	-0.82	-1.46[c]	(0.64)

[a] 0.1 mol dm^{-3} n-Bu_4NClO_4 in CH_2Cl_2, Pt electrode, scan rate 100 mV s^{-1}, V vs. standard calomel electrode (SCE). [b] Measured using a larger Pt electrode because of its low solubility. [c] Irreversible wave. Calculated as E_p - 0.03 V.

X-Ray Crystal Structure Analysis

In order to investigate molecular structures and molecular packing in crystals of the nonclassical benzobis(thiadiazole)s, an X-ray crystal structure analysis of **3b** was carried out. The single crystal was obtained by recrystallization from benzonitrile. The crystal data and the final atomic coordinates are presented in the subsequent experimental part. In the crystal, the molecule is planar and has a C_i symmetry (Figure 3). The S-N bond lengths (1.601 Å and 1.603 Å) are shorter than those of **11** (1.615 Å and 1.620 Å),[12] and the N-C bond lengths (1.354 Å and 1.357 Å) are longer than those of **11** (1.325 Å and 1.337 Å). The bond lengths of the thiadiazole rings are similar to those of the pyrazine derivative **1** (S-N bond lengths: 1.597 Å and 1.609 Å, N-C bond lengths: 1.347 Å and 1.370 Å).[2] These results strongly indicate the hypervalency on the sulfur atoms of **3b** and

1. Furthermore, the C1-C3 bond length (1.457 Å) is longer than those of C1-C2 bond (1.399 Å) and C2-C3 bond (1.391 Å), suggesting that heterocycle **3b** has a delocalized 14π-electron ring system. On the other hand, since the delocalization in the central benzene ring of **11** is strongly disturbed as judged by the bond lengths, it is considerable that the two thiadiazole rings have a stable 6π-electron character like **11A**.[12] Thus, the difference in the molecular structures between **3** and **11** results in drastic changes in their electron properties.

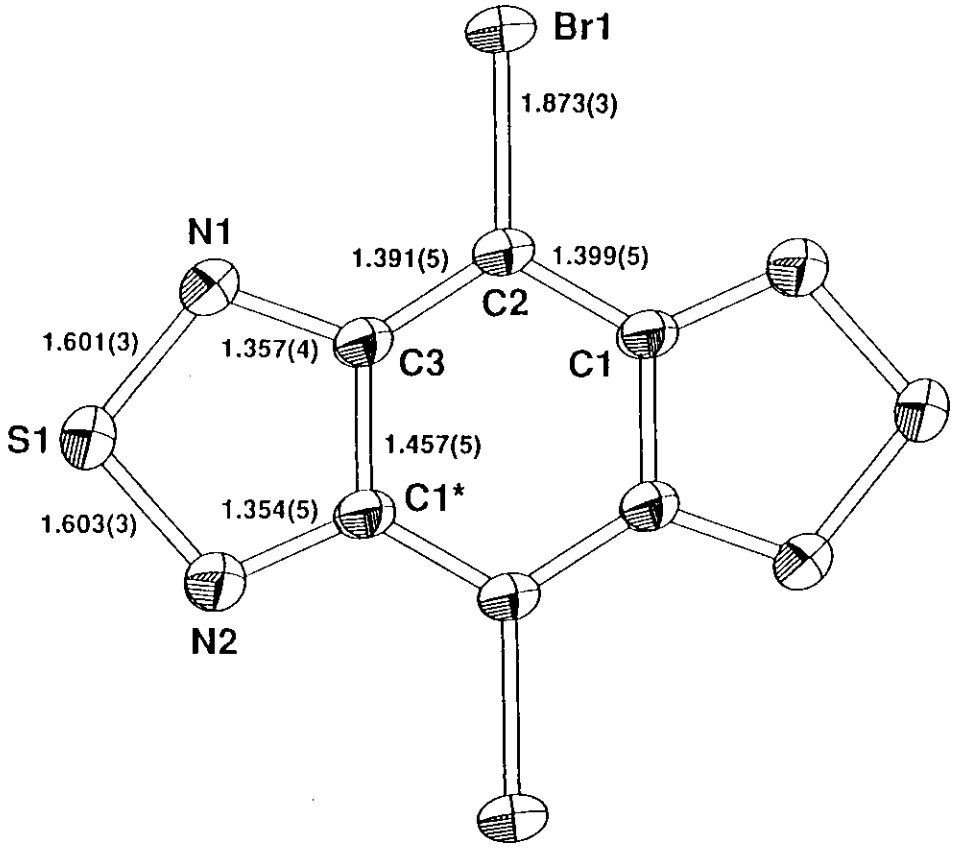

Figure 3. Molecular structure of **3b** with bond lengths (Å) (ORTEP).

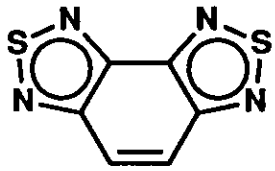

11A

Although the molecule is uniformly stacked along the *c* axis, the overlap mode shown in Figure 4*a* indicates less effective interactions between the HOMO and LUMO (Figure 2). The crystal structure is composed of a set of two ribbon columns, which extend in the [011] and [01-1] directions and are characterized by short intermolecular S•••N and N•••N contacts (Figure 4*b*). These columns interact with each other through short Br•••N contacts to form a three-dimensional network. The distances of the relevant contacts, S•••N (3.06 Å), N•••N (2.91 Å), and Br•••N (3.10 Å), are significantly shorter than the sum of their van der Waals radii (3.35, 3.10, and 3.40 Å). According to the net atomic charges of **3a** calculated by the MNDO-PM3 method, the hypervalent S atoms have significant positive charge and the N atoms significant negative charge (Figure 2). Thus, the S•••N interactions are attributed to an electrostatic effect, which seems to induce dense packing in the crystal (D_c = 2.58 g cm^{-3}).

(*a*)

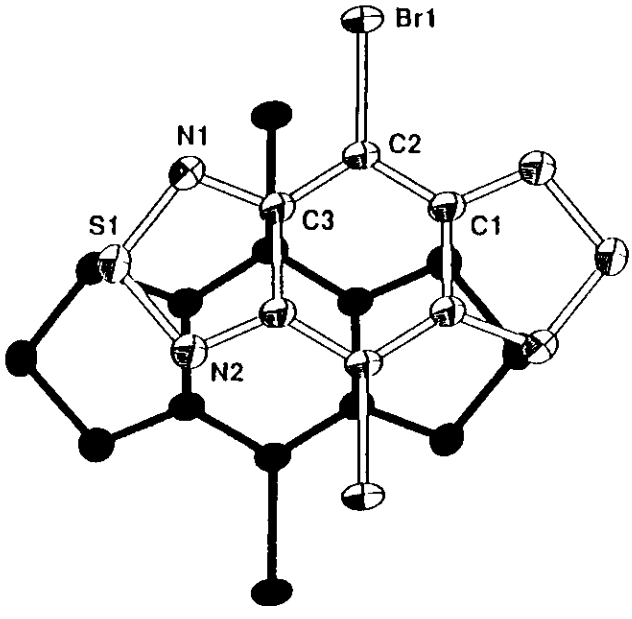

(*b*)

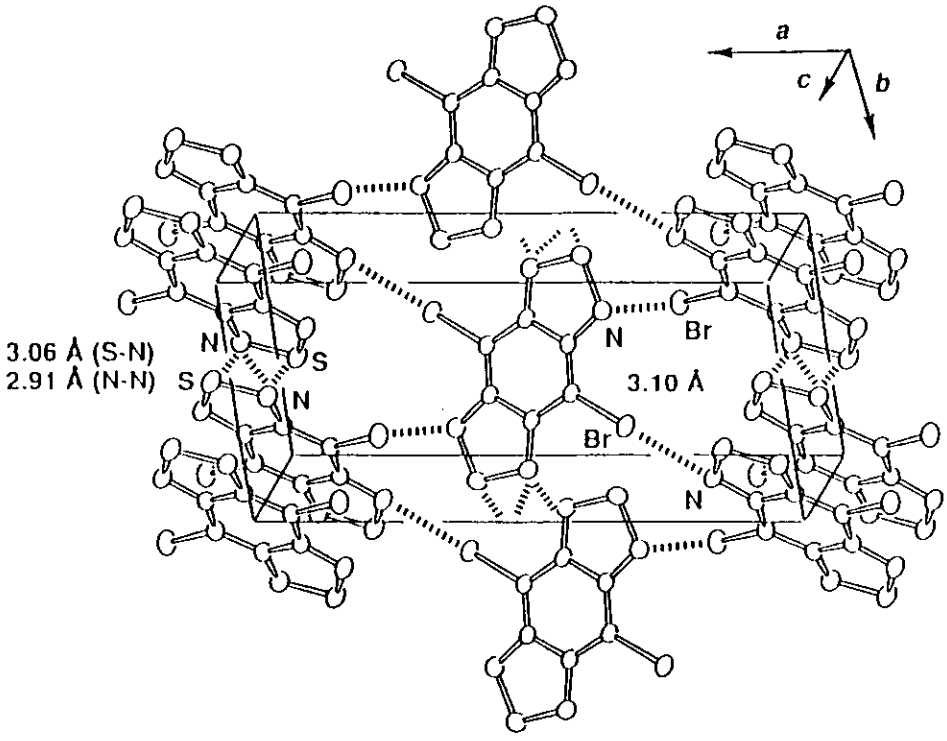

Figure 4. Crystal structure of **3b**. (*a*) Overlap mode. (*b*) Ribbon-like network.

Molecular Orbital Calculations

MNDO-PM3 calculations[11] for **3a** and **6a** also show that the energy levels of the HOMOs are higher than that of **11**, and that the energy levels of the LUMOs are lower than that of **11** as shown in Figure 5. These results are supported by the longer

absorption maxima and the higher electron affinities of **3** and **6**. Thus, the electronic properties of the heterocycles containing the hypervalent sulfur atoms are fairly different from those of the Kekulé-type isomer. On the other hand, substitution of a sulfur atom by a selenium atom little affects the HOMO and LUMO of the 14π-electron ring system.

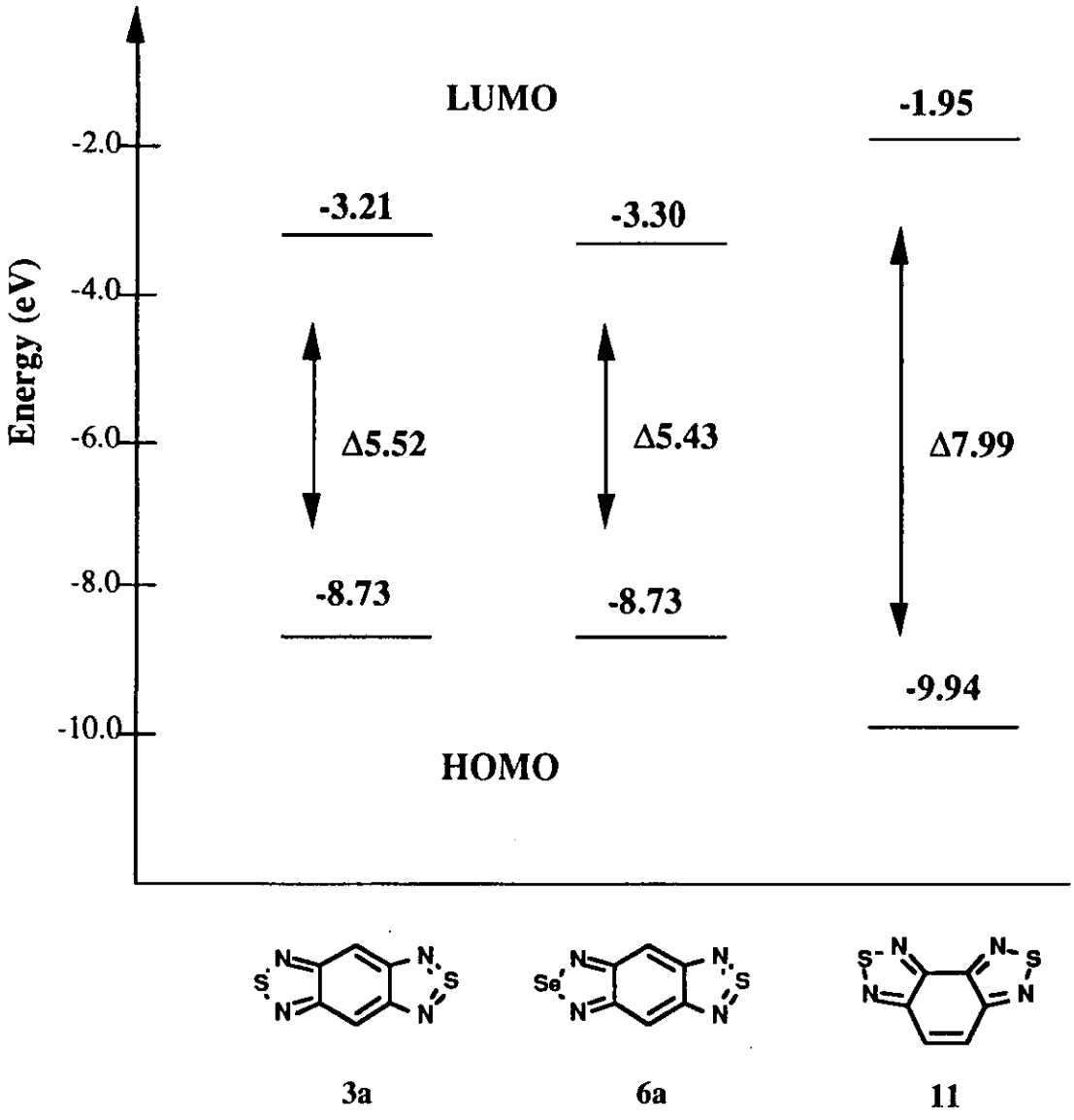

Figure 5. Energy diagram of the HOMOs and LUMOs in heterocycles **3a**, **6a**, and **11**.

According to the net atomic charges displayed in Figure 6, the sulfur atom of **6a** is charged more positively than those of **3a**, indicating that the contribution of the structure containing a tetravalent selenium atom is small. The fact that the S•••N contact distance (3.06 Å) in the crystal of **3b** is shorter than that of **11** (3.13 Å)[12] may be concerned with the difference in the charge densities of the S and N atoms.

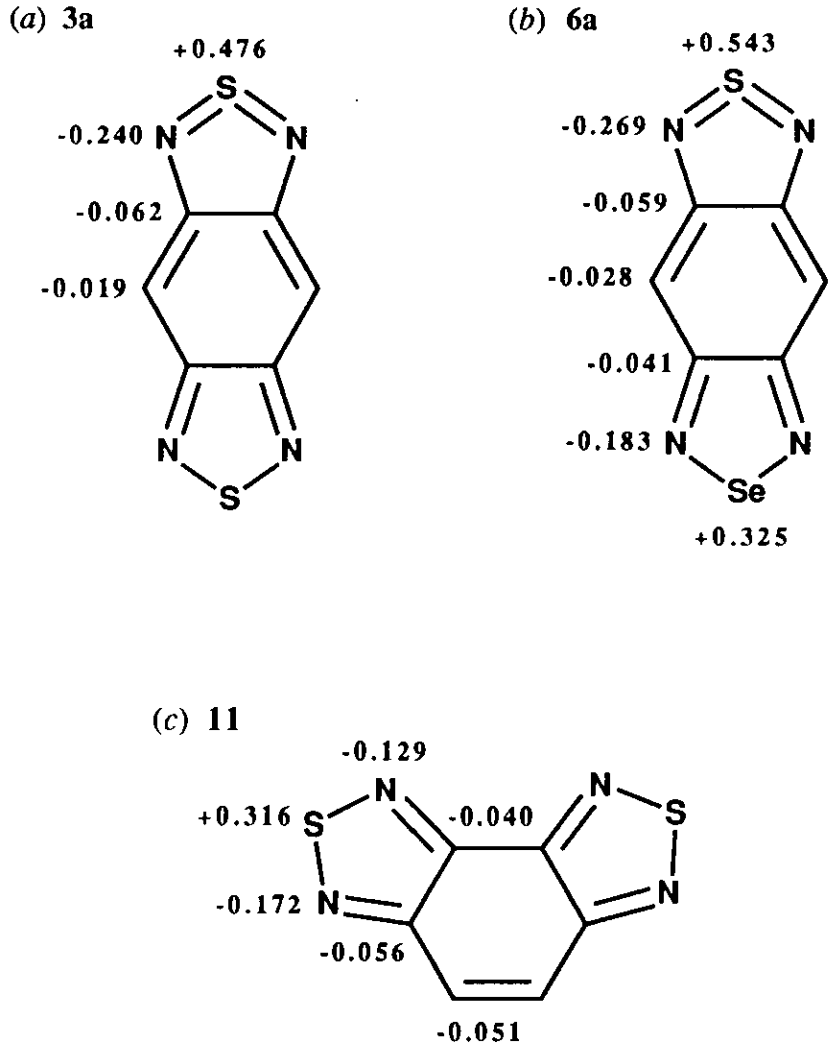

Figure 6. Net atomic charges of (*a*) **3a**, (*b*) **6a**, and (*c*) **11** calculated by the MNDO-PM3 method.

Optical Properties and Reactivities

Heterocycles **3**, **6**, and **12** display strong emission. Their fluorescence spectra were measured upon photoexcitation in dichloromethane at room temperature (Figure 7). These broad maxima are summarized in Table 3. Heterocycle **3c** is photochemically stable and has a relatively long lifetime, τ_f = 11.5 ns, which was determined from the decay curve shown in Figure 8. The lifetime extended to τ_f = 17 ns by a degassing procedure, and the value is longer than that of 9,10-diphenylanthracene (τ_f = 7.7 ns in cyclohexane). The laser-induced fluorescence (LIF) excitation spectrum of **3c** in supersonic free jets showed the 0-0 band at 589.809 nm, indicating that the energy gap between the HOMO and LUMO is small (2.10 eV).

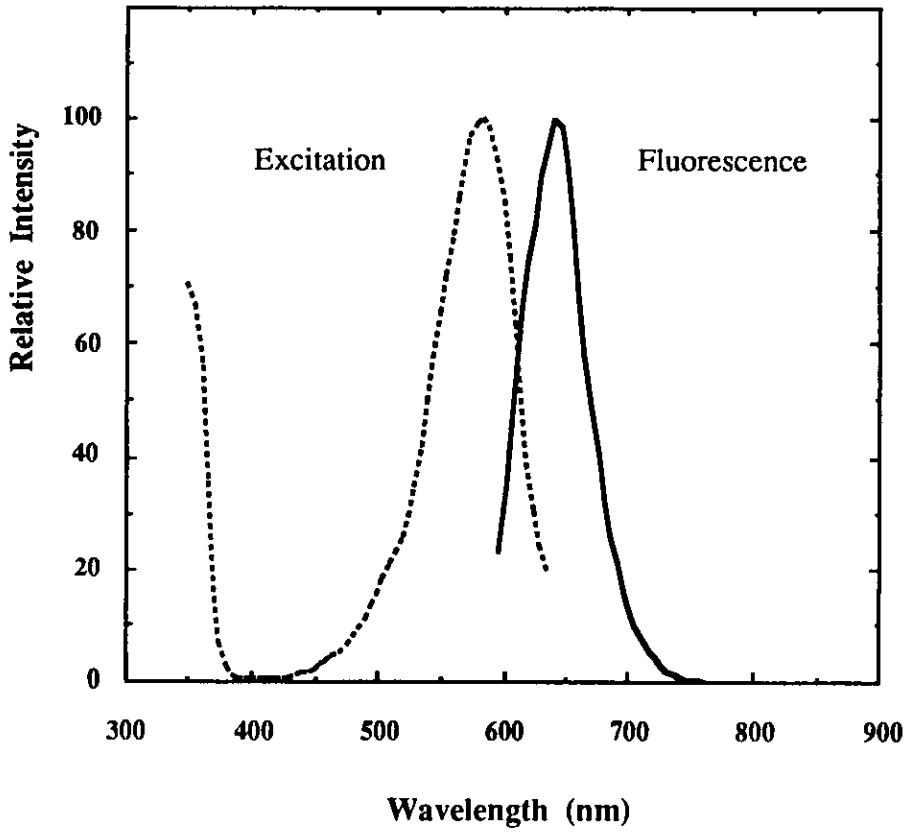

Figure 7. Fluorescence (——) and excitation (- - - -) spectra of **3c** (6 x 10^{-7} mol dm^{-3}) in dichloromethane.

Table 3. Fluorescence emission maxima[a] of heterocycles **3**, **6**, **11**, and **12**.

Heterocycle	$\lambda_{emission}$ / nm
3b	557
3c	642
6b	643
6c	689
11	367
12	561

[a] In CH_2Cl_2.

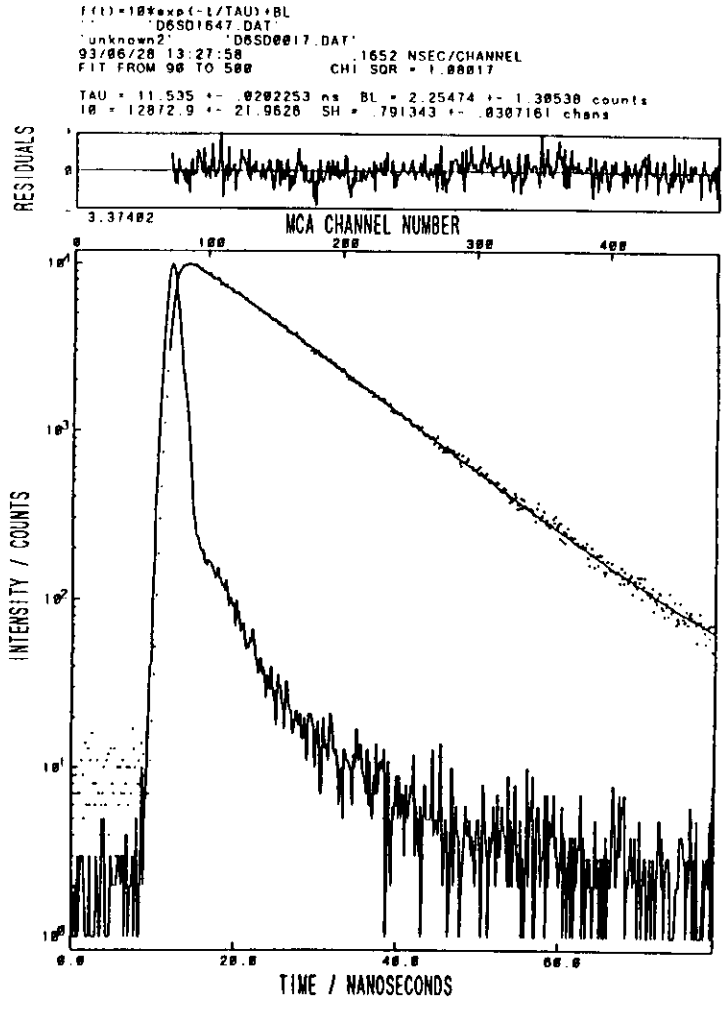

Figure 8. Fluorescence decay curve of **3c** in dichloromethane.

9,10-Diphenylanthracene and its derivatives, which are isoelectronic systems for **3c**, **6c**, and **12**, have been investigated as organic electroluminescence (EL) devices in the optoelectronic display field. The EL devices show emission on a thin film by an applied potential.[13] Although the quantum yields in solution and crystal have not been obtained yet, heterocycles **3**, **6**, and **12** may be applicable for EL devices. In addition, polar molecules such as organic dyes can be applied to photosensitive materials in the electrophotography field. Irradiation with visible light induces charge separation on the molecules, where carriers are generated and toner is adsorbed.[14] Heterocycles **3** are considered to be useful for this purpose owing to the advantages of their highly polarized structures and small molecular weights.

Heterocycles containing nonclassical thiophene rings are highly reactive, and some Diels-Alder reactions with dienophiles have been reported so far.[1] Heterocycle **3c** also reacted with *N*-phenylmaleimide **14** in refluxing xylene to give colorless needles in 89% yield (Scheme 3). Although the product dissociated to the starting materials in the EI mass measurement, the FAB mass spectrum showed the molecular weight for the 1 : 1 adduct **15**. The ^{1}H and ^{13}C NMR spectra exhibited a peak of the tertiary hydrogen atoms at δ 4.40 (s) and two peaks of the bridge and bridgehead carbon atoms at δ 49.7 and 55.3, and these spectra support the structure of the Diels-Alder-type adduct **15**. It is reasonable that **3c** reacts with a dienophile at the 4- and 8-positions because of the large atomic coefficients of the HOMO at these positions as shown in Figure 2. The adduct **15** reverted to **3c** and **14** by a retro-Diels-Alder reaction at its decomposition point (> 230 °C) with a large color change. The absorption spectra shown in Figure 9 display this color change. The broken line (*a*) shows the spectrum of **15** and the real line (*b*) indicates evolution of **3c**. This result suggests that the nonclassical heterocycle **3c** is also of interest as a functional dye.

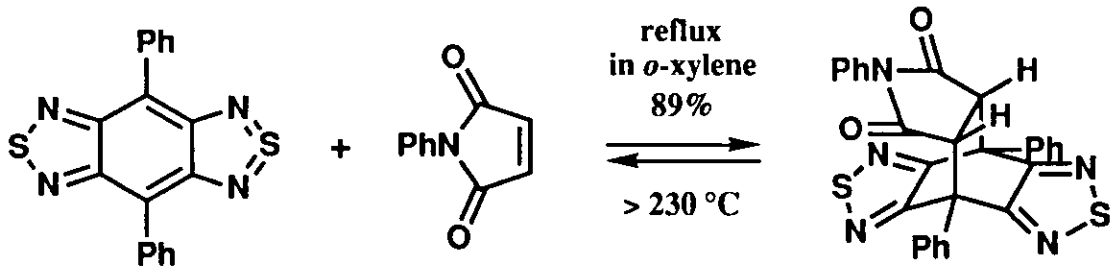

3c 14 15

Scheme 3

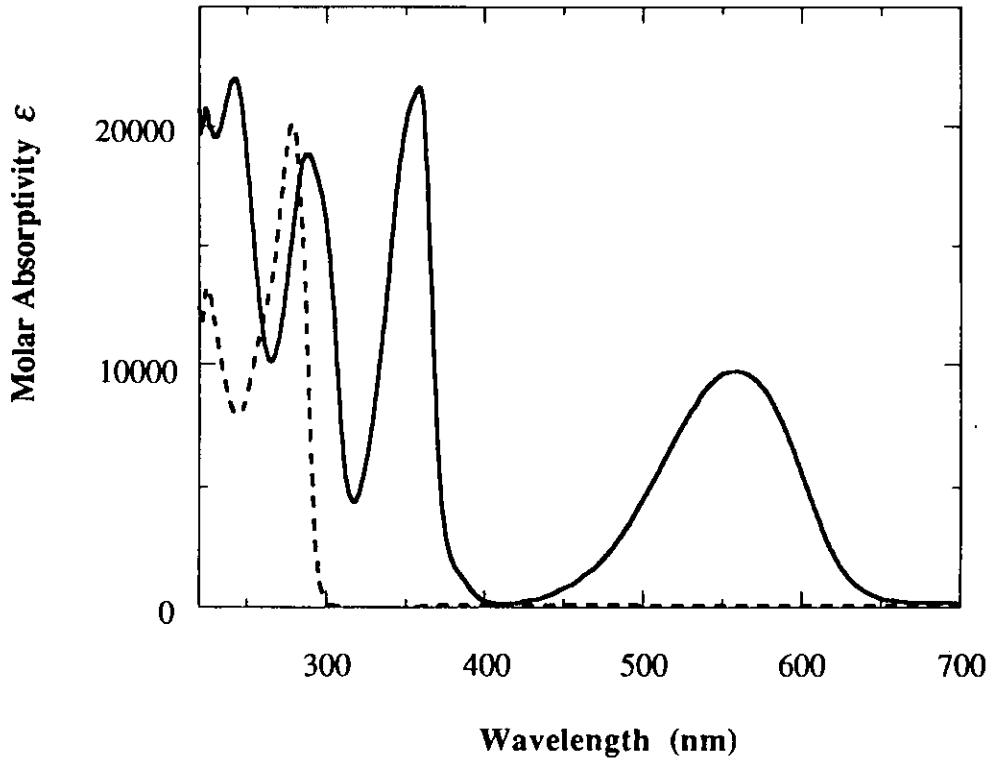

Figure 9. Absorption spectra of **15**. (*a*) Before heating (- - - -). (*b*) After heating at the decomposition point (——).

Reactions of **3b** with nucleophiles were investigated. Although compound **3b** reacted with morpholine or thiophenol to afford **3d** or **3e** (Scheme 4), the yields were very low after purification by sublimation. The reactions seemed to proceed together with side reactions such as desulfurization as judged by formation of diaminodibromobenzothiadiazole **9a**. The structures of **3d** and **3e** were determined by the high resolution mass spectra. The EI mass spectrum of **3e** showed some fragment peaks indicating the phenylthio group. The morpholino group of **3d** was supported by the ^{1}H NMR spectrum. Their absorption maxima listed in Table 4 (p. 87) are fairly red-shifted, suggesting that compounds **3d** and **3e** are enhanced amphoteric redox molecules.

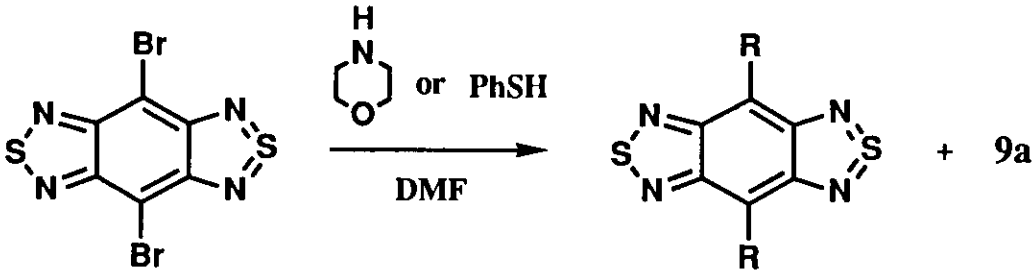

3b

3d R = –N O

3e R = SPh

Scheme 4

Properties of Donor-π-acceptor Systems

Because nucleophilic reactions of **3b** gave poor yields of products as mentioned above, introduction of electron-donating aryl groups into the benzobis(thiadiazole) skeleton was carried out. Compounds **3f** and **3g** were prepared through synthetic routes similar to that of **3c** (Scheme 2, p. 73) using the corresponding tin reagents **10b** and **10c** ($RSnBu_3$). These heterocycles were purified by sublimation (260 °C, 10^{-6} Torr), and their structures were determined by elemental analyses and their spectral data. Table 4 shows their decomposition points, color, and absorption maxima of **3c-g**.

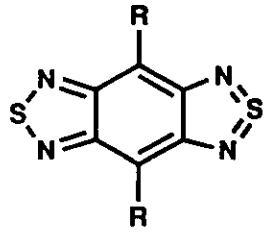

3d R = -N⟨ ⟩O

3e R = SPh

3f R = -⟨ ⟩-NMe$_2$

3g R = -⟨ ⟩(MeO)-OMe

3c R = Ph

Table 4. Decomposition points, color, and absorption maxima[a] of heterocycles **3**.

Heterocycle	Decomp / °C	Color	λ_{max} / nm (log ε)
3d	> 180	green	764 (3.70)
3e	237-238	blue	610 (3.90)
3f	301-303	green	732 (4.03)
3g	322-326	purple	564 (3.98)
3c	310-311	purple	558 (3.99)

[a] In CH_2Cl_2

The absorption maximum of **3f** is much red-shifted, and the value is comparable to that of **3d**. Moreover, the stability and yield were improved by incorporation of the benzene rings. On the other hand, the absorption maximum of **3g** is close to that of **3c**, indicating that the steric effect between the benzobis(thiadiazole) moiety and the methoxy groups disturbs the π-conjugation on the terphenyl moiety.

The CVs of **3d-g** all showed both oxidation and reduction waves. The second reduction waves are irreversible in contrast to that of **3c**. The half-wave potentials are given in Table 5, and the CV of **3d** is shown in Figure 10. Compounds **3d** and **3f** are strong electron donors due to the Wurster redox systems[15], and **3d** especially shows two reversible oxidation waves, whose potentials are lower than those of TTF. Their reduction potentials are generally high, and the effect of electron-donating groups is not so much. The E_{sum} values of **3d** and **3f**, which are the differences between the first oxidation potentials and the first reduction ones, are very small, indicating that they are good

3d R = -N O 3e R = SPh 3f R = -C6H4-NMe2

3g R = -C6H3(MeO)-OMe 3c R = Ph

Table 5. Oxidation and reduction potentials[a] of heterocycles 3.

	E_2^{ox} / V	E_1^{ox} / V	E_1^{red} / V	E_2^{red} / V	ΔE^{red}	E_{sum}
3d	+0.50	+0.28	-0.89	-1.58[b]	(0.69)	1.17
3e	-	+1.28[b]	-0.38	-1.04[b]	(0.66)	(1.66)
3f	-	+0.58	-0.75	-1.43[b]	(0.68)	1.33
3g	-	+1.22[b]	-0.74	-1.52[b]	(0.78)	(1.96)
3c	-	-	-0.61	-1.30	0.69	-

[a] 0.1 mol dm^{-3} n-Bu_4NClO_4 in CH_2Cl_2, Pt electrode, scan rate 100 mV s^{-1}, V vs. standard calomel electrode (SCE). [b] Irreversible waves. Calculated as E_p - 0.03 V.

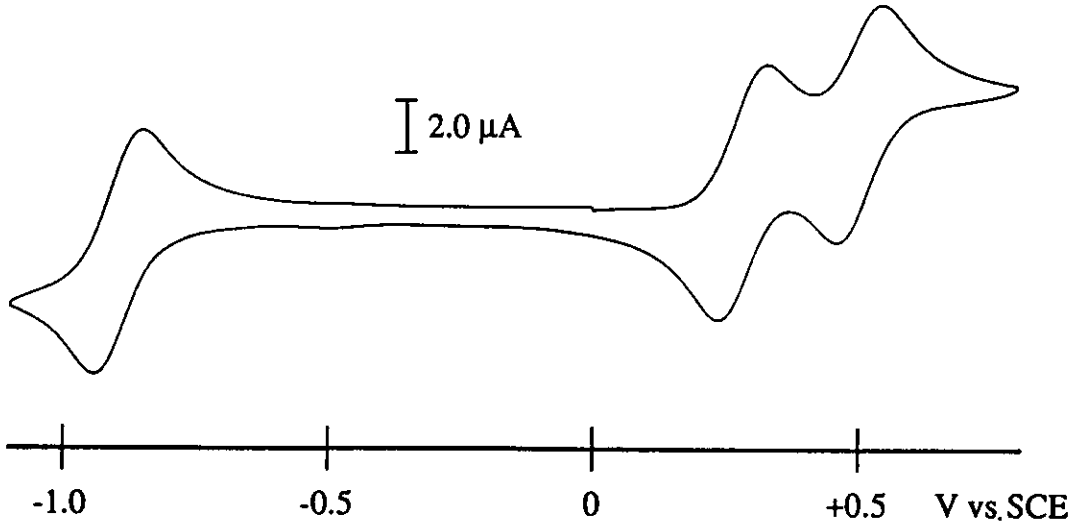

Figure 10. CV of **3d** in dichloromethane.

amphoteric redox systems. On the other hand, the oxidation state of **3g** is unstable and the potential is very high because of the steric hindrance. The oxidation potential of **3e** is similar to that of **3g**. However, the reduction potentials are remarkably high, and they are close to those of dibromide **3b** (E_1 = -0.35, E_2 = -1.10 V). The result suggests that oxidation and reduction take place at the phenylthio moiety and the benzobis(thiadiazole) unit, respectively, in **3e**. Therefore, **3e** is considered to have a character of a donor-σ-acceptor system. As mentioned above, donor-π-acceptor molecules could be obtained by introduction of amino groups into the nonclassical benzobis(thiadiazole) and its diphenyl-derivative. They are of interest as amphoteric redox systems with small molecular weights. According to the oxidation potentials, compounds **3d** and **3f** are also promising electron donors for organic conductors.

Summary

The novel nonclassical heterocycles **3** and **6** were synthesized and characterized. Their reduction potentials are comparable to that of *p*-benzoquinone, indicating their high electron affinities. Compounds **3** and **6** showed much high electron affinities and long absorption maxima in comparison with those of the Kekulé-type isomer **11**. These electronic properties are ascribable to the 14π-electron ring system containing a tetravalent sulfur atom. An X-ray crystal structure analysis was performed on a single crystal of **3b**. The molecule is planar and has a C_i symmetry. The molecular structure demonstrates the hypervalency on the sulfur atoms and the 14π-electron ring moiety. The crystal structure is composed of a set of two ribbon columns linked by short S•••N and N•••N contacts, and these columns interact with each other through short Br•••N contacts resulting in dense packing in the crystal. Heterocycles **3**, **6**, and **12** show strong fluorescence emission, and the lifetime of **3c** is relatively long. Compound **3c** reacted with *N*-phenylmaleimide **14** to afford the Diels-Alder-type adduct **15**, which reverted to **3c** and **14** at its decomposition

point. Although dibromide **3b** was reactive with nucleophiles to afford **3d** and **3e**, the reactions proceeded together with some side reactions. Novel donor-acceptor molecules were also prepared by introduction of strong electron-donating groups into the nonclassical framework, and their redox potentials were investigated in the CV study. Compounds **3d** and **3f**, which are substituted by amino groups, showed good amphoteric redox properties, and they are also promising electron donors for organic conductors.

Experimental

General. Melting points were measured on a YANACO MP-500D melting point apparatus and are uncorrected. IR spectra were determined on a PERKIN-ELMER FTIR 1600 spectrometer. ^{1}H and ^{13}C NMR spectra were obtained using a JEOL JNM-GX400 (400 MHz) spectrometer. Chemical shifts are reported in ppm from tetramethylsilane as an internal standard and are given in δ units. Mass spectra (EI) were obtained with a SHIMADZU GCMS-QP1000EX mass spectrometer operating at 70 eV by a direct inlet system. High resolution mass spectra (EI) and a FAB mass spectrum (Xe, 7 kV) using *m*-nitrobenzyl alcohol as a matrix were measured on a SHIMADZU KRATOS CONCEPT 1S mass spectrometer. UV / Vis absorption spectra and fluorescence spectra were determined on SHIMADZU UV-3101PC and SHIMADZU RF-1500 spectrometers, respectively. Elemental analyses were performed on YANACO MT-3 CHN CORDER. Purification of chromatography was performed using MERCK silica gel 60 (63-200 μm) or MERCK aluminium oxide 90 (activity I, neutral). All solvents were dried and purified by the usual methods.

General Procedure for Preparation of Aryltributyltin (10). Magnesium ribbon (1.46 g) in dry THF (30 ml) was activated with ultrasonic waves for 3 min under argon. A small amount of aryl bromide was added to the magnesium. After a reaction occurred exothermically, a solution of the aryl bromide (50 mmol) in THF (20 ml) was

added dropwise over 2 h. Then, to the Grignard reagent was slowly added a solution of tributyltin chloride (95%, 10.28 g, 30 mmol) in THF (20 ml) over 2 h, and the mixture was refluxed for 18 h. The reaction mixture was slowly poured into water (500 ml) and a yellow oil was extracted with ether (100 ml x 3). The ether solution was dried over $MgSO_4$ and concentrated. The residue was distilled at a reduced pressure using a Kugelrohr distillation apparatus to give the product.

Tributylphenyltin (10a):[9] colorless oil; yield 49%; bp > 140 °C, 3 Torr (lit. 145 °C, 2.5 Torr); ^{1}H NMR ($CDCl_3$) δ 0.88 (t, J = 7.3 Hz, 9 H, CH_3), 1.03-1.07 (m, 6 H, CH_2), 1.28-1.37 (m, 6 H, CH_2), 1.50-1.58 (m, 6 H, CH_2), 7.28-7.33 (m, 3 H), 7.44-7.47 (m, 2 H).

Tributyl[4-(dimethylamino)phenyl]tin (10b): pale yellow oil; yield 77%; bp > 160 °C, 1 Torr; ^{1}H NMR ($CDCl_3$) δ 0.88 (t, J = 7.3 Hz, 9 H, CH_3), 0.98-1.02 (m, 6 H, CH_2), 1.28-1.37 (m, 6 H, CH_2), 1.50-1.58 (m, 6 H, CH_2), 2.93 (s, 6 H, NCH_3), 6.74 (d, J = 8.5 Hz, 2 H), 7.32 (d, J = 8.5 Hz, 2 H).

Tributyl(2,4-dimethoxyphenyl)tin (10c): colorless oil; yield 91%; bp > 160 °C, 1 Torr; ^{1}H NMR ($CDCl_3$) δ 0.88 (t, J = 7.3 Hz, 9 H, CH_3), 0.99-1.03 (m, 6 H, CH_2), 1.27-1.36 (m, 6 H, CH_2), 1.48-1.55 (m, 6 H, CH_2), 3.73 (s, 3 H, OCH_3), 3.79 (s, 3 H, OCH_3), 6.41 (d, J = 2.0 Hz, 1 H), 6.51 (dd, J = 7.8, 2.0 Hz, 1 H), 7.24 (d, J = 7.8 Hz, 1 H).

5,6-Dinitro-4,7-diphenylbenzo[*c*][1,2,5]thiadiazole (8b). To a mixture of dibromide **8a**[7] (1.50 g, 3.9 mmol) and $PdCl_2(PPh_3)_2$ (0.55 g, 0.78 mmol) was added a solution of **10a** (3.15 g, 8.6 mmol) in dry THF (20 ml) under argon. The mixture was refluxed for 4 h, and it was stirred with aqueous KF solution. Dichloromethane (50 ml) was added and the organic layer was separated. The aqueous layer was extracted with dichloromethane (20 ml x 2). The combined organic solution was washed with aqueous NaCl solution and dried over Na_2SO_4. After removal of the solvent, the residue was chromatographed on silica gel (dichloromethane / *n*-hexane, 1 : 1) to give **8b** (0.97 g, 65%) as pale yellow prisms. mp 295-296 °C (from toluene); IR (KBr) 1552, 1382, 1356,

890, 753, 699 cm^{-1}; ^1H NMR (DMSO-d_6) δ 7.61 (s, 10 H, Ph); ^{13}C NMR (DMSO-d_6) δ 128.9, 129.16, 129.22, 130.1, 130.9, 141.3, 152.8; MS *m/z* (relative intensity) 378 (M^+, 54), 301 (35), 77 (100). Anal. Calcd. for $C_{18}H_{10}N_4O_4S$: C, 57.14; H, 2.66; N, 14.81. Found: C, 57.42; H, 2.95; N, 14.87.

4,7-Bis[4-(dimethylamino)phenyl]-5,6-dinitrobenzo[*c*][1,2,5]thiadiazole (8c). Similarly to the case of **8b**, **8a** (0.50 g, 1.3 mmol) was refluxed with **10b** (1.20 g, 2.9 mmol) and $PdCl_2(PPh_3)_2$ (0.19 g, 0.27 mmol) in THF (10 ml) for 20 h under argon. After cooling, the reaction mixture was stirred with aqueous KF solution and dichloromethane (40 ml) was added. The organic layer was separated and the aqueous layer was extracted with dichloromethane (20 ml x 2). The combined organic solution was washed with aqueous NaCl solution, dried over Na_2SO_4, and concentrated. The residue was washed with *n*-hexane and chromatographed on aluminium oxide (dichloromethane). Recrystallization from chloroform / *n*-hexane afforded **8c** (0.31 g, 50%) as purple crystals. decomp 294-296 °C; IR (KBr) 1612, 1570, 1545, 1446, 1377, 1206, 1154, 817 cm^{-1}; ^1H NMR (DMSO-d_6) δ 3.32 (s, 12 H, CH_3), 6.87 (d, J = 9.0 Hz, 4 H), 7.42 (d, J = 9.0 Hz, 4 H); MS *m/z* (relative intensity) 464 (M^+, 100), 372 (34). Anal. Calcd. for $C_{22}H_{20}N_6O_4S$: C, 56.88; H, 4.34; N, 18.10. Found: C, 56.88; H, 4.49; N, 17.83.

4,7-Bis(2,4-dimethoxyphenyl)-5,6-dinitrobenzo[*c*][1,2,5]thiadiazole (8d). Similarly to the case of **8b**, **8a** (1.00 g, 2.6 mmol) was refluxed with **10c** (2.50 g, 5.9 mmol) and $PdCl_2(PPh_3)_2$ (0.38 g, 0.54 mmol) in THF (20 ml) for 20 h under argon. After cooling, the reaction mixture was stirred with aqueous KF solution and dichloromethane (50 ml) was added. The organic layer was separated and the aqueous layer was extracted with dichloromethane (30 ml x 2). The combined organic solution was washed with aqueous NaCl solution, dried over Na_2SO_4, and concentrated. After short column chromatography on silica gel (dichloromethane), the obtained solid was repeatedly extracted with hot ethyl acetate until a pale yellow solid was left. The solution was cooled to give **8d** (0.81 g, 62%) as orange crystals. mp 302-303 °C (from chloroform / *n*-hexane); IR (KBr) 1610, 1543, 1461, 1358, 1302, 1263, 1212, 1027, 826, 769 cm^{-1}; ^1H

NMR (DMSO-d_6) δ 3.64 (s, 3 H, OCH_3), 3.71 (s, 3 H, OCH_3), 3.87 (s, 3 H, OCH_3), 3.88 (s, 3 H, OCH_3), 6.72-6.78 (m, 4 H), 7.32 (d, J = 8.2 Hz, 1 H), 7.55 (d, J = 8.6 Hz, 1 H); MS *m/z* (relative intensity) 498 (M^+, 100). Anal. Calcd. for $C_{22}H_{18}N_4O_8S$: C, 53.01; H, 3.64; N, 11.24. Found: C, 52.87; H, 3.73; N, 11.21.

5,6-Diamino-4,7-dibromobenzo[*c*][1,2,5]thiadiazole (9a).[8] A mixture of **8a** (1.54 g, 4.0 mmol) and iron powder (2.23 g, 40 mmol) in acetic acid (20 ml) was stirred at 100 °C for 1.5 h under nitrogen. Ethanol (4 ml) was added, and the reaction mixture was further stirred at 100 °C for 1.5 h. After cooling, the precipitate was filtered and washed with methanol. After drying *in vacuo*, the obtained solid was extracted with ethyl acetate using a Soxhlet extractor. Purification by sublimation (200 °C, 10^{-3} Torr) afforded **9a** (0.84 g, 64%) as yellow crystals. mp 258-260 °C (lit. mp 257-260 °C).

5,6-Diamino-4,7-diphenylbenzo[*c*][1,2,5]thiadiazole (9b). Reduction of **8b** (1.32 g, 3.5 mmol) with iron powder (1.95 g, 35 mmol) was carried out by a procedure like **9a**. After cooling, the precipitate was filtered and washed with methanol. The obtained solid was dissolved into hot ethyl acetate. The hot solution was treated with active carbon and filtered. The filtrate was cooled to give **9b** (0.74 g, 67%) as yellow needles. decomp 307-308 °C (from ethyl acetate); IR (KBr) 3423 (NH), 3324 (NH), 3239 (NH), 1636, 1456, 1432, 1365, 880, 824, 756, 700, 650, 518 cm^{-1}; ^1H NMR (DMSO-d_6) δ 5.35 (br s, 4 H, NH_2), 7.40-7.44 (m, 2 H), 7.48-7.56 (m, 8 H); ^{13}C NMR (DMSO-d_6) δ 109.1, 127.3, 128.9, 130.6, 135.7, 138.8, 150.6; MS *m/z* (relative intensity) 318 (M^+, 100), 317 (42). Anal. Calcd. for $C_{18}H_{14}N_4S$: C, 67.90; H, 4.43; N, 17.60. Found: C, 68.00; H, 4.61; N, 17.61.

5,6-Diamino-4,7-bis[4-(dimethylamino)phenyl]benzo[*c*][1,2,5]thiadiazole (9c). Reduction of **8c** (0.23 g, 0.50 mmol) with iron powder (0.28 g, 5.0 mmol) was carried out by a procedure like **9a**. After removal of the solvent, aqueous $NaHCO_3$ solution and dichloromethane (50 ml) were added to the residue. The organic layer was separated, dried over Na_2SO_4, and concentrated. The residue was chromatographed on short column of silica gel (dichloromethane / ethyl acetate, 1 : 1) to

afford a crude product of **9c** (decomp > 270 °C, 0.14 g, 68%), which was purified by sublimation (250 °C, 10^{-6} Torr) to give orange crystals. decomp > 300 °C; IR (KBr) 3433 (NH), 3360 (NH), 1613, 1525, 1442, 1360, 1188, 811, 587 cm^{-1}; ^1H NMR (DMSO-d_6) δ 2.97 (s, 12 H, NCH_3), 5.17 (br s, 4 H, NH_2), 6.88 (d, J = 8.7 Hz, 4 H), 7.32 (d, J = 8.7 Hz, 4 H); MS *m/z* (relative intensity) 404 (M^+, 100). Anal. Calcd. for $C_{22}H_{24}N_6S$: C, 65.31; H, 5.98; N, 20.78. Found: C, 65.57; H, 6.02; N, 20.69.

5,6-Diamino-4,7-bis(2,4-dimethoxyphenyl)benzo[*c*][1,2,5]thiadiazole (9d). Reduction of **8d** (0.15 g, 0.30 mmol) with iron powder (0.17 g, 3.0 mmol) was carried out by a procedure like **9a**. After cooling, the precipitate was filtered and washed with methanol. The obtained solid was chromatographed on short column of silica gel with a hot solution of chloroform and ethyl acetate (1 : 1). Evaporation of the solvent afforded a crude product of **9d** (mp > 275 °C, 0.11 g, 85%), which was purified by sublimation (250 °C, 10^{-6} Torr) to give yellow crystals. mp 302-309 °C; IR (KBr) 3416 (NH), 3339 (NH), 1608, 1574, 1512, 1464, 1434, 1414, 1297, 1210, 1157, 1134, 1028, 922, 840, 791, 608 cm^{-1}; ^1H NMR (DMSO-d_6) δ 3.69 (s, 3 H, OCH_3), 3.71 (s, 3 H, OCH_3), 3.84 (s, 6 H, OCH_3), 5.01 (br s, 4 H, NH_2), 6.65-6.69 (m, 2 H), 6.72 (t, J = 2.3 Hz, 2 H), 7.14 (t, J = 8.2 Hz, 2 H); MS *m/z* (relative intensity) 438 (M^+, 100). Anal. Calcd. for $C_{22}H_{22}N_4O_4S$: C, 60.25; H, 5.06; N, 12.78. Found: C, 60.30; H, 5.20; N, 12.73.

4,8-Dibromobenzo[1,2-*c*:4,5-*c*′]bis([1,2,5]thiadiazole) (3b). To a solution of diamine **9a** (0.33 g, 1.0 mmol) in dry pyridine (5 ml) was added thionyl chloride (1 ml) under argon. The reaction mixture was stirred for 20 h at room temperature. After removal of the solvent at a reduced pressure, water was added to the residue. The precipitate was filtered and washed with water and methanol. The crude product was sublimed at 200 °C and 10^{-6} Torr to give **3b** (0.26 g, 74%) as deep red crystals. decomp > 280 °C; IR (KBr) 1459, 1280, 1264, 924, 854, 604, 472 cm^{-1}; UV (CH_2Cl_2) λ_{max} 524 nm (log ε 3.64), 359 (4.26), 239 (4.33); MS *m/z* (relative intensity)

354 (55), 352 (M^+, 100), 350 (47), 273 (31), 271 (28), 192 (53), 96 (40), 70 (85). Anal. Calcd. for $C_6Br_2N_4S_2$: C, 20.47; N, 15.92. Found: C, 20.74; N, 16.10.

4,8-Diphenylbenzo[1,2-*c*:4,5-*c*´]bis([1,2,5]thiadiazole) (3c). A mixture of diamine **9b** (1.00 g, 3.1 mmol) and *N*-thionylaniline (0.74 ml, 6.5 mmol) in dry pyridine (12 ml) was stirred at 80 °C under argon. After stirring for 5 min, trimethylsilyl chloride (4 ml, 31 mmol) was added, and the reaction mixture was stirred for 5 h at the same temperature. The solvent was distilled off at a reduced pressure, and dichloromethane (50 ml) was added to the residue. The solution was washed with 1*N* hydrochloric acid, aqueous $NaHCO_3$ solution, and water. The organic layer was dried over Na_2SO_4 and concentrated. The residue was chromatographed on silica gel (toluene) to give **3c** (1.02 g, 95%) as purple prisms. decomp 310-311 °C (sublimation at 200 °C, 10^{-6} Torr); IR (KBr) 1449, 1364, 935, 868, 755, 687, 667, 506 cm^{-1}; ^1H NMR ($CDCl_3$) δ 7.54-7.58 (m, 2 H), 7.66 (t, J = 7.6 Hz, 4 H), 8.20 (d, J = 7.6 Hz, 4 H); ^{13}C NMR ($CDCl_3$) δ 121.6, 128.3, 129.0, 131.6, 134.9, 152.7; UV (CH_2Cl_2) λ_{max} 558 nm (log ε 3.99), 359 (4.33), 291 (4.25), 243 (4.30); MS *m/z* (relative intensity) 346 (M^+, 100), 313 (38). Anal. Calcd. for $C_{18}H_{10}N_4S_2$: C, 62.40; H, 2.91; N, 16.18. Found: C, 62.67; H, 3.11; N, 15.97.

4,8-Bis(4-morpholino)benzo[1,2-*c*:4,5-*c*´]bis([1,2,5]thiadiazole) (3d). To a solution of dibromide **3b** (35 mg, 0.10 mmol) in dimethylformamide (3 ml) was added morpholine (0.1 ml) at 80 °C under argon. The green solution was stirred for 25 min. The solvent was distilled off at a reduced pressure. Water was added, and the precipitate was filtered. After drying *in vacuo*, the obtained solid was sublimed at 170 °C and 10^{-6} Torr to give **3d** (4 mg, 10%) as a green solid. decomp > 180 °C; IR (KBr) 2872, 1460, 1433, 1368, 1277, 1120, 1105, 1003, 930, 871, 863, 563 cm^{-1}; ^1H NMR ($CDCl_3$) δ 3.64-3.68 (m, 8 H), 4.09-4.10 (m, 4 H), 4.56-4.58 (m, 4 H); UV (CH_2Cl_2) λ_{max} 764 nm (log ε 3.70), 350 (4.28), 277 (4.49); MS *m/z* (relative intensity) 364 (M^+, 100). Mass Calcd. for $C_{14}H_{16}N_6O_2S_2$: 364.07762. Found: *m/z* 364.07913.

4,8-Bis(phenylthio)benzo[1,2-*c*:4,5-*c*′]bis([1,2,5]thiadiazole) (3e). To a solution of dibromide **3b** (32 mg, 0.09 mmol) in dimethylformamide (2 ml) was added thiophenol (20 μl, 0.2 mmol) at 70 °C under argon. After stirring for 1 h, the reaction mixture was further stirred for 1 h with addition of thiophenol (20 μl, 0.2 mmol). After removal of the solvent, the residue was washed with *n*-hexane, ether, and methanol. The precipitate was filtered and washed with methanol. The obtained solid was sublimed at 200 °C and 10^{-6} Torr to give **3e** (4 mg, 11%) as a blue-black solid. decomp 237-238 °C; IR (KBr) 1578, 1477, 1437, 1294, 1022, 930, 878, 855, 737, 696, 687, 634, 531, 490 cm^{-1}; UV (CH_2Cl_2) λ_{max} 610 nm (log ε 3.90), 356 (4.36), 283 (4.21), 249 (4.42); MS *m/z* (relative intensity) 410 (M^+, 100), 377 (13), 333 (M^+ - Ph, 13), 301 (M^+ - SPh, 37). Mass Calcd. for $C_{18}H_{10}N_4S_4$: 409.97884. Found: *m/z* 409.97741.

4,8-Bis[4-(dimethylamino)phenyl]benzo[1,2-*c*:4,5-*c*′]bis([1,2,5]-thiadiazole) (3f). Similarly to the procedure of **3c**, a mixture of diamine **9c** (0.14 g, 0.34 mmol) and *N*-thionylaniline (46 μl, 0.41 mmol) in dry pyridine (5 ml) was stirred at 80 °C for 30 min under argon. Then, trimethylsilyl chloride (2 ml) was added, and the reaction mixture was refluxed for 17 h. After the usual workup, a crude product was separated by chromatography on silica gel (dichloromethane), and sublimation (260 °C, 10^{-6} Torr) afforded **3f** (0.13 g, 86%) as green crystals. decomp 301-303 °C; IR (KBr) 1604, 1428, 1373, 1206, 1135, 815 cm^{-1}; ^1H NMR ($CDCl_3$) δ 3.10 (s, 12 H, NCH_3), 6.97 (d, J = 8.9 Hz, 4 H), 8.23 (d, J = 8.9 Hz, 4 H); ^{13}C NMR ($CDCl_3$) δ 40.2, 111.9, 119.9, 123.5, 132.7, 150.5, 152.7; UV (CH_2Cl_2) λ_{max} 732 nm (log ε 4.03), 353 (4.42), 345 (4.41), 264 (4.12); MS *m/z* (relative intensity) 432 (M^+, 100), 417 (16), 216 (23). Anal. Calcd. for $C_{22}H_{20}N_6S_2$: C, 61.08; H, 4.66; N, 19.43. Found: C, 61.11; H, 4.72; N, 19.38.

4,8-Bis(2,4-dimethoxyphenyl)benzo[1,2-*c*:4,5-*c*′]bis([1,2,5]thia-diazole) (3g). Similarly to the procedure of **3c**, a mixture of diamine **9d** (110 mg, 0.25 mmol) and *N*-thionylaniline (34 μl, 0.30 mmol) in dry pyridine (3 ml) was stirred at 80 °C for 10 min under argon. Then, trimethylsilyl chloride (1 ml) was added, and the

reaction mixture was refluxed for 18 h. After the usual workup, a crude product was separated by chromatography on silica gel (dichloromethane), and sublimation (260 °C, 10^{-6} Torr) afforded **3g** (58 mg, 50%) as purple crystals. decomp 322-326 °C; IR (KBr) 1609, 1576, 1467, 1309, 1213, 1166, 1116, 1044, 1030, 921, 615 cm^{-1}; ^1H NMR ($CDCl_3$) δ 3.76 (s, 3 H, OCH_3), 3.77 (s, 3 H, OCH_3), 3.94 (s, 6 H, OCH_3), 6.75-6.79 (m, 4 H), 7.54-7.59 (m, 2 H); UV (CH_2Cl_2) λ_{max} 564 nm (log ε 3.98), 357 (4.41), 287 (4.27), 240 (4.47); MS *m/z* (relative intensity) 466 (M^+, 100), 343 (35). Anal. Calcd. for $C_{22}H_{18}N_4O_4S_2$: C, 56.63; H, 3.89; N, 12.01. Found: C, 56.77; H, 3.86; N, 12.14.

4,8-Dibromo[1,2,5]selenadiazolo[3,4-*f*]benzo[*c*][1,2,5]thiadiazole (6b). A mixture of diamine **9a** (65 mg, 0.20 mmol) and selenium dioxide (55 mg, 0.50 mmol) in ethanol (10 ml) was refluxed for 24 h. The precipitate was filtered and washed with hot water and hot ethanol. Purification by sublimation (220 °C, 10^{-6} Torr) gave **6b** (32 mg, 40%) as purple crystals. decomp > 280 °C; IR (KBr) 1451, 1351, 1276, 921, 860, 808, 776, 598 cm^{-1}; UV (CH_2Cl_2) λ_{max} 609 nm, 383, 250; MS *m/z* (relative intensity) 402 (53), 400 (M^+, 97), 398 (85), 319 (38), 240 (59), 238 (31), 177 (26), 175 (33), 96 (70), 80 (100), 70 (88). Anal. Calcd. for $C_6Br_2N_4SSe$: C, 18.06; N, 14.05. Found: C, 18.16; N, 13.98.

4,8-Diphenyl[1,2,5]selenadiazolo[3,4-*f*]benzo[*c*][1,2,5]thiadiazole (6c). A mixture of diamine **9b** (64 mg, 0.20 mmol) and selenium dioxide (22 mg, 0.20 mmol) in a solution of ethanol (7 ml) and water (3 ml) was refluxed for 15 min. After cooling, the precipitate was filtered and washed with water and methanol. Purification by chromatography on silica gel (dichloromethane) and sublimation (220 °C, 10^{-6} Torr) afforded **6c** (65 mg, 82%) as blue crystals. decomp 367-371 °C; IR (KBr) 1446, 1433, 1371, 940, 874, 834, 763, 751, 700, 688, 660 cm^{-1}; ^1H NMR ($CDCl_3$) δ 7.53-7.57 (m, 2 H), 7.63-7.67 (m, 4 H), 8.10-8.13 (m, 4 H); ^{13}C NMR ($CDCl_3$) δ 121.6, 128.2, 128.9, 131.8, 135.7, 152.8, 158.8; UV (CH_2Cl_2) λ_{max} 625 nm (log ε 4.01), 380 (4.46), 299 (4.29), 264 (4.13), 226 (4.27); MS *m/z* (relative intensity) 394 (M^+, 41), 392 (22),

314 (100), 313 (63), 157 (16), 141 (33), 114 (35), 77 (19). Anal. Calcd. for $C_{18}H_{10}N_4SSe$: C, 54.96; H, 2.56; N, 14.25. Found: C, 55.13; H, 2.81; N, 14.10.

4,9-Diphenyl[1,2,5]thiadiazolo[3,4-*g*]quinoxaline (12). A solution of diamine **9b** (70 mg, 0.22 mmol) and 1,4-dioxane-2,3-diol (130 mg, 1.1 mmol) in nitromethane (3 ml) was refluxed for 2 h under argon. After cooling, the orange precipitate was filtered and washed with nitromethane. The obtained solid was sublimed at 240 °C and 10^{-6} Torr to give **12** (57 mg, 76%) as orange crystals. decomp > 373 °C; IR (KBr) 1459, 1442, 1389, 1040, 897, 861, 756, 698, 652, 455 cm^{-1}; ^1H NMR ($CDCl_3$) δ 7.55-7.58 (m, 2 H), 7.64 (t, J = 7.6 Hz, 4 H), 7.85 (t, J = 7.6 Hz, 4 H), 8.87 (s, 2 H); UV (CH_2Cl_2) λ_{max} 471 nm (log ε 3.99), 363 (4.26), 349 (4.14), 254 (4.74); MS *m/z* (relative intensity) 340 (M^+, 100), 339 (77), 306 (71). Anal. Calcd. for $C_{20}H_{12}N_4S$: C, 70.56; H, 3.55; N, 16.46. Found: C, 70.41; H, 3.85; N, 16.47.

Diels-Alder reaction of 3c with *N*-phenylmaleimide. A mixture of **3c** (176 mg, 0.51 mmol) and *N*-phenylmaleimide **14** (173 mg, 1.0 mmol) in *o*-xylene (5 ml) was refluxed for 2 days under nitrogen. After cooling, the reaction mixture was chromatographed on a silica gel column with toluene. The first eluate was concentrated to give **3c** (23 mg, 13% recovery), and the second eluate gave **14** (84 mg). The elution with dichloromethane afforded a white solid, which was recrystallized from *n*-hexane / dichloromethane to give colorless needles (215 mg). ^1H NMR spectrum showed that the crystals contained 0.275 ratio of CH_2Cl_2 for **15** (89%). decomp > 230 °C; IR (KBr) 1716 (C=O), 1499, 1378, 1192, 753, 691, 651 cm^{-1}; ^1H NMR ($CDCl_3$) δ 4.40 (s, 2 H), 5.25 (s, 0.55 H, CH_2Cl_2), 6.63-6.66 (m, 2 H), 7.20-7.22 (m, 3 H), 7.52 (t, J = 7.5 Hz, 2 H), 7.61 (t, J = 7.5 Hz, 4 H), 8.15 (d, J = 7.5 Hz, 4 H); ^{13}C NMR ($CDCl_3$) δ 49.7, 55.3, 125.8, 128.3, 128.8, 128.9, 129.2, 130.4, 131.3, 161.5, 163.6, 170.2; UV (CH_2Cl_2) λ_{max} 279 nm (log ε 4.30), 225 (4.12); FAB-MS *m/z* 520 $[M + H]^+$. Anal. Calcd. for $C_{28}H_{17}N_5O_2S_2$: C, 64.72; H, 3.30; N, 13.48. Found: C, 64.63; H, 3.43; N, 13.29 (dried *in vacuo* at 110 °C for 7 h).

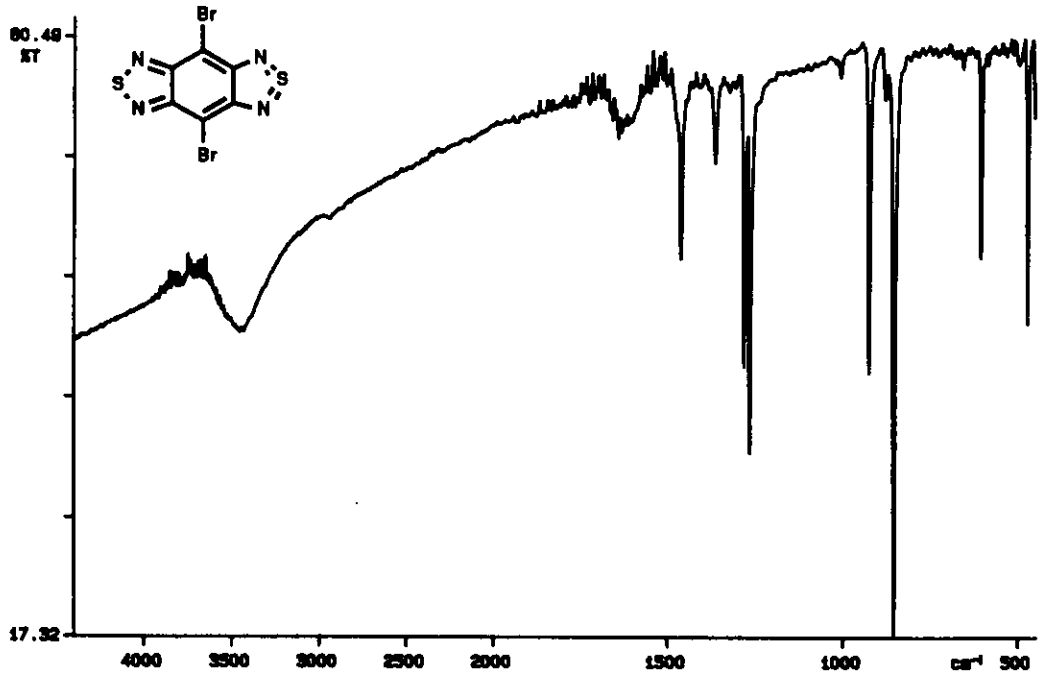

Figure 11. IR spectrum of **3b**.

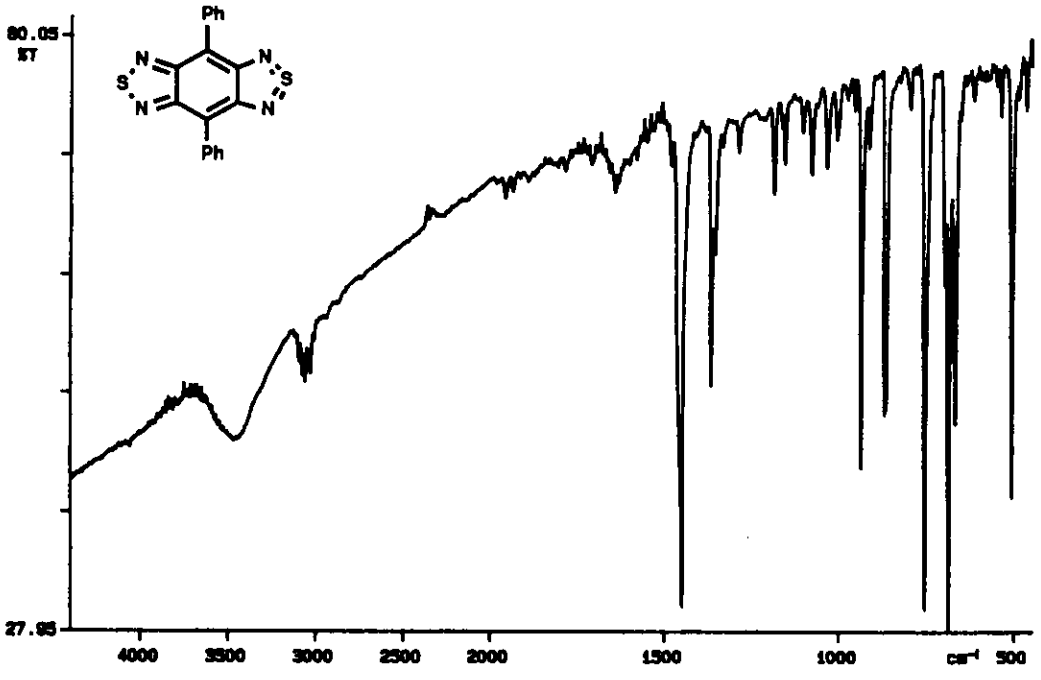

Figure 12. IR spectrum of **3c**.

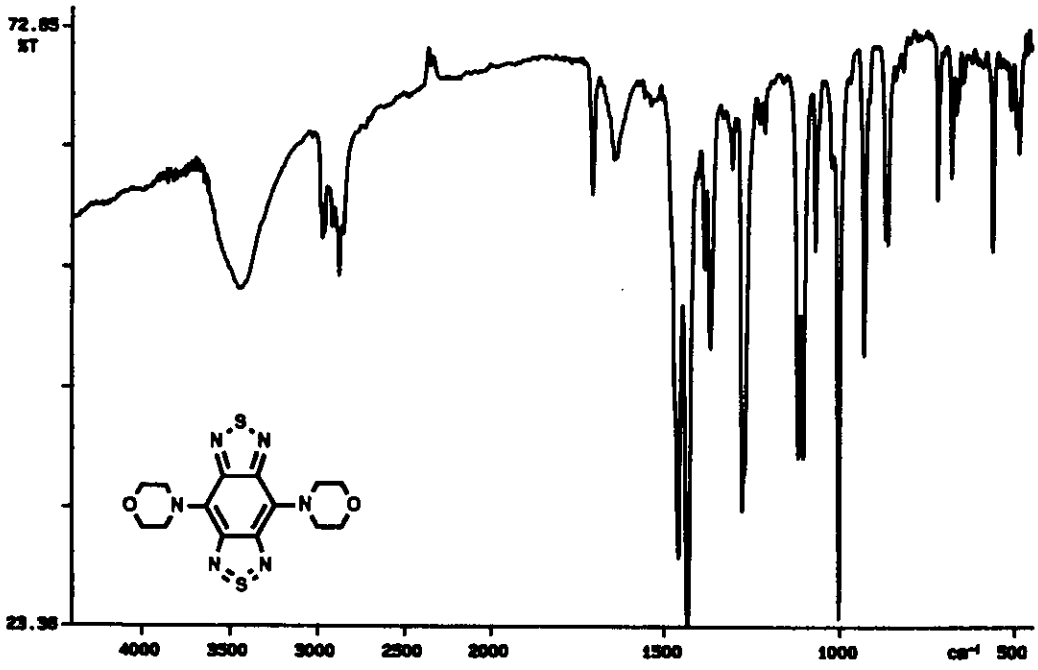

Figure 13. IR spectrum of 3d.

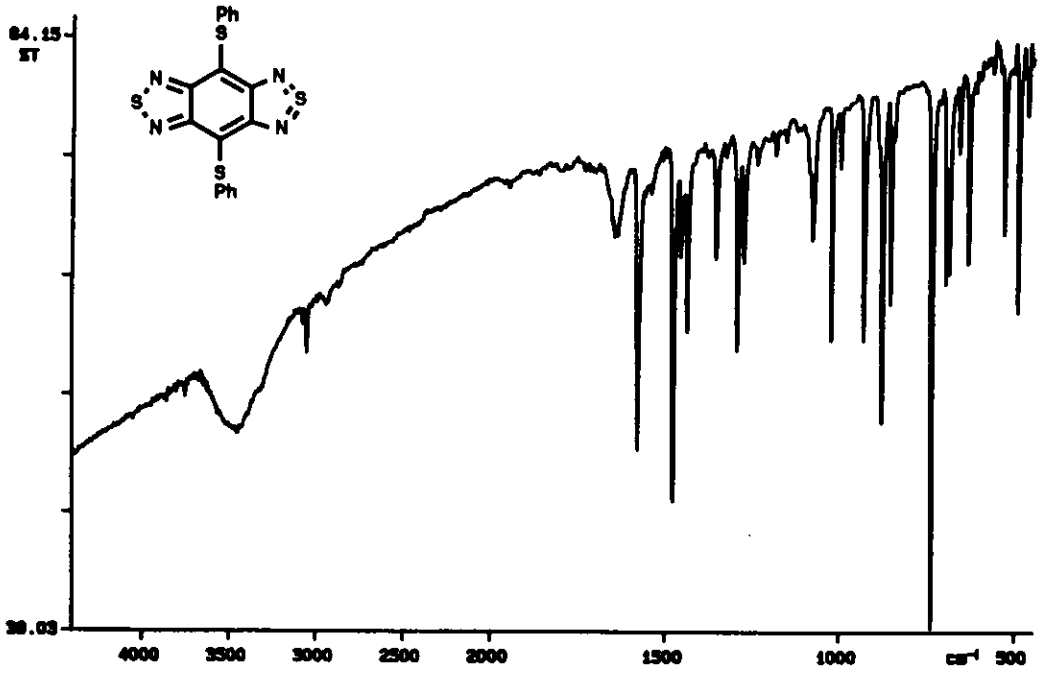

Figure 14. IR spectrum of 3e.

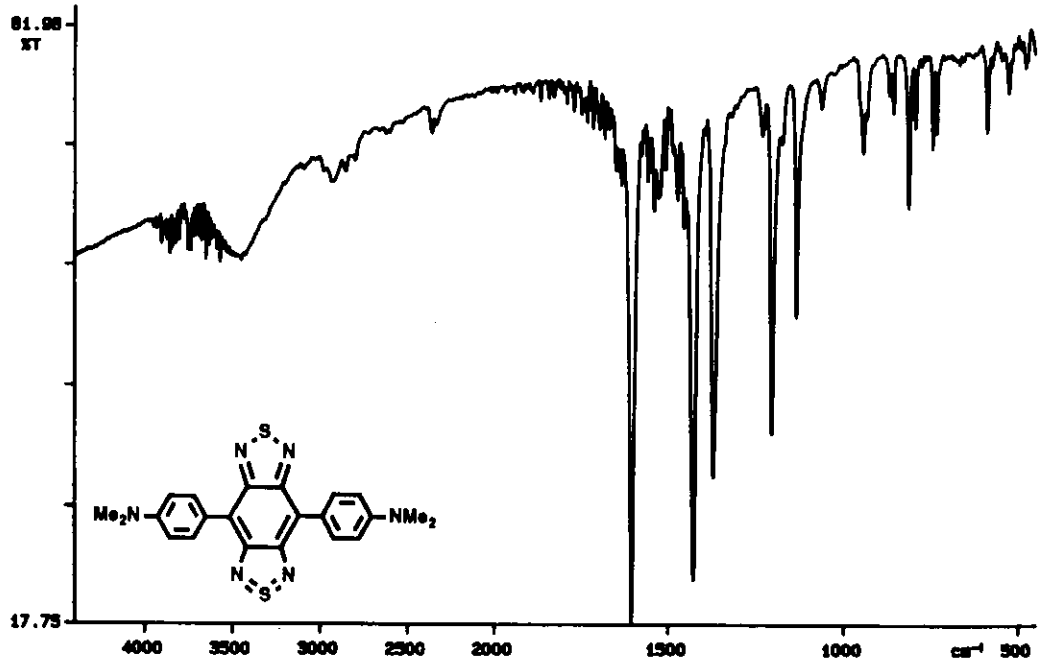

Figure 15. IR spectrum of 3f.

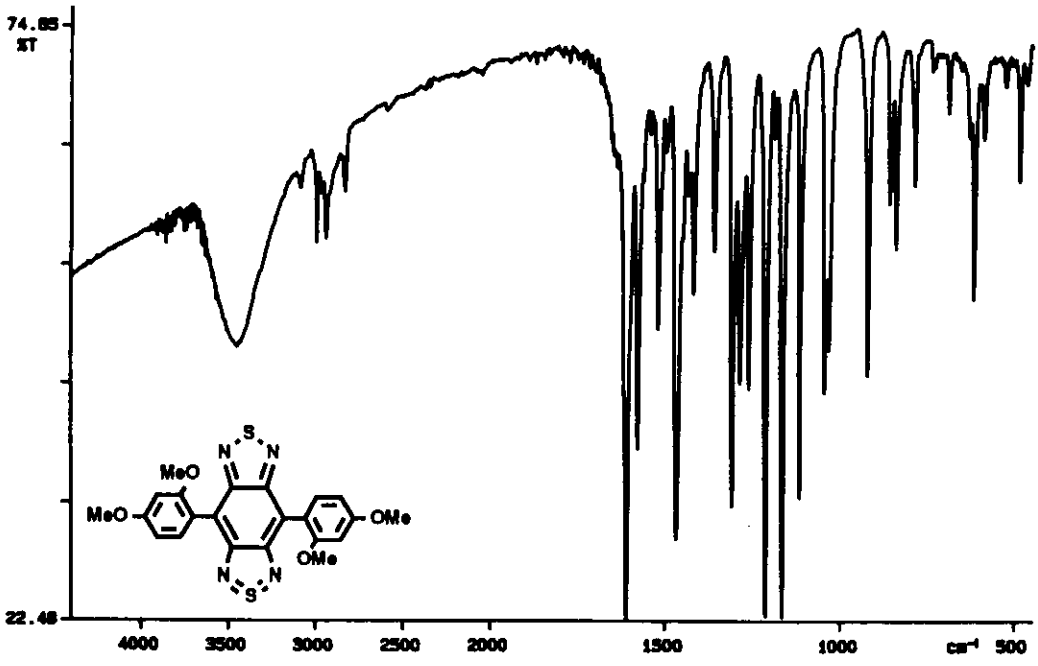

Figure 16. IR spectrum of 3g.

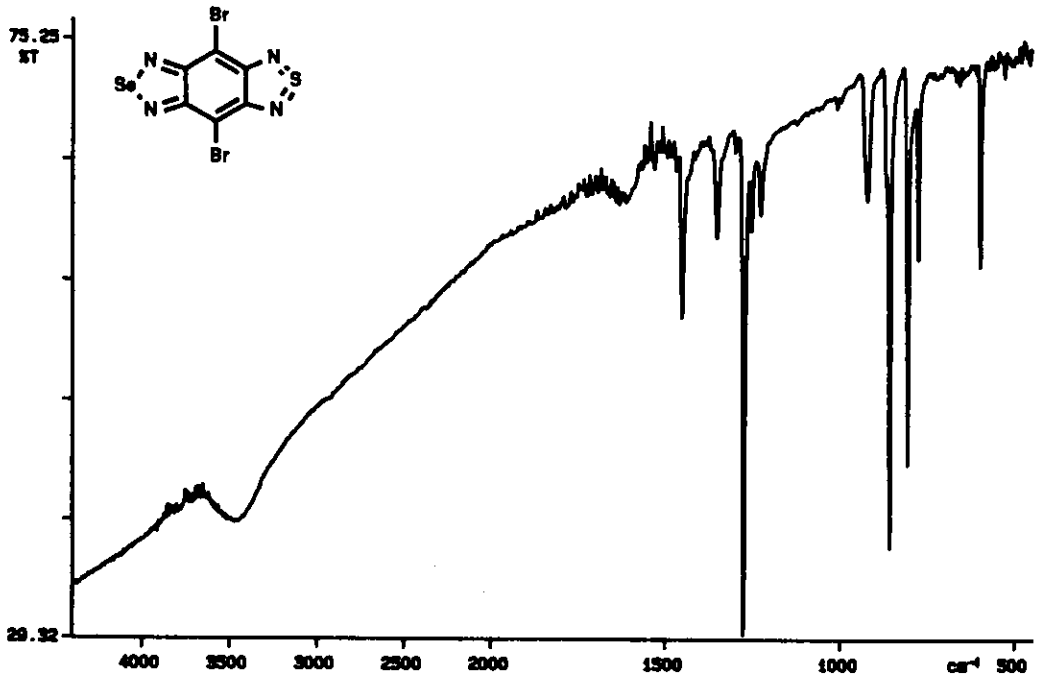

Figure 17. IR spectrum of **6b**.

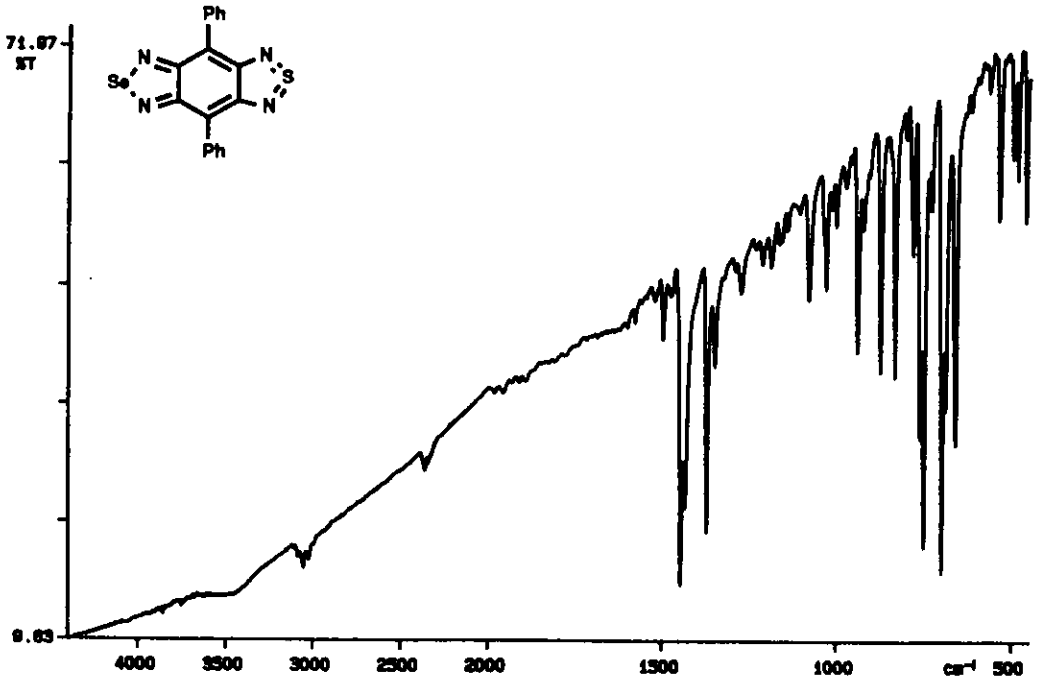

Figure 18. IR spectrum of **6c**.

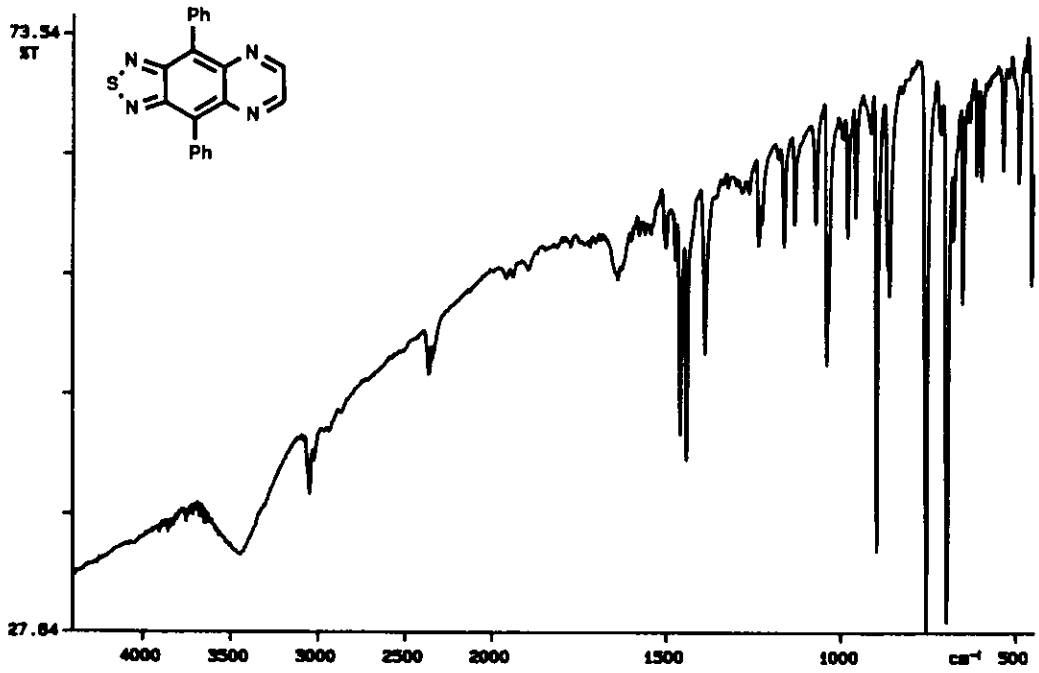

Figure 19. IR spectrum of **12**.

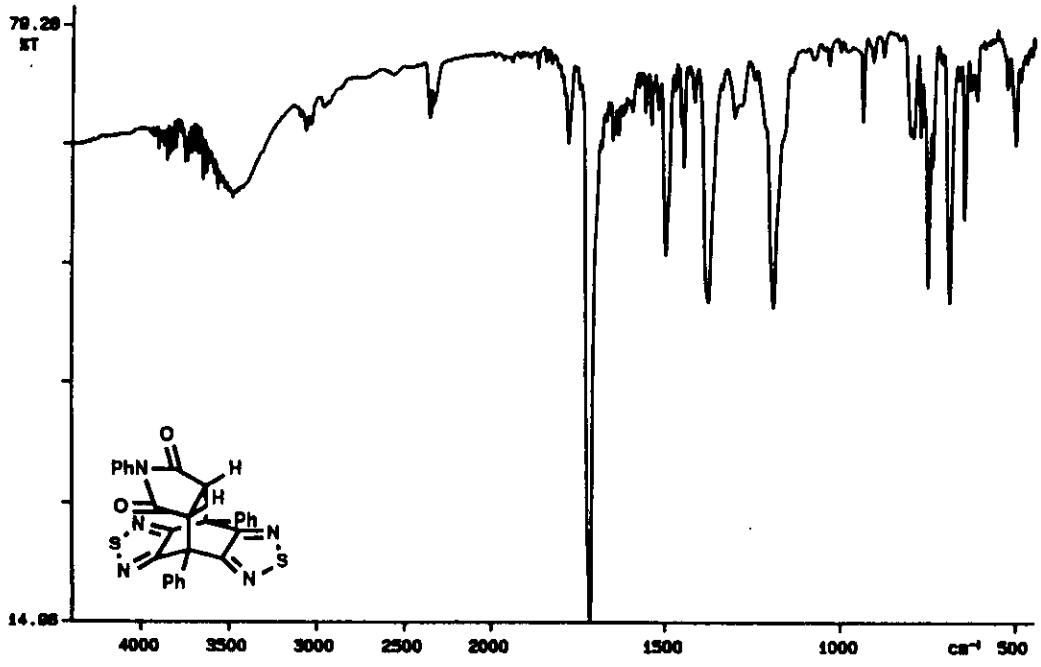

Figure 20. IR spectrum of **15**.

X-Ray Crystal Structure Analysis. A prism-like crystal with dimensions of 0.10 x 0.05 x 0.19 mm^3 along the *a*, *b*, and *c* axes was prepared by recrystallization from benzonitrile for the X-ray study. Crystal data are as follows: $C_6Br_2N_4S_2$, M = 352.04, monoclinic, space group $P2_1/n$, a = 15.569(1), b = 7.3990(4), c = 3.9405(3) Å, β = 90.192(4)°, V = 453.92(5) $Å^3$, Z = 2, D_c = 2.58 g cm^{-3}, $F(000)$ = 332, $\mu(Cu_{K\alpha})$ = 153.25 cm^{-1}, S = 3.40. An ENRAF-NONIUS CAD4 (40 kV, 32 mA) diffractometer was used with graphite-monochromated Cu K_α radiation (λ = 1.5418 Å); ω - 2θ scan technique. Cell parameters were determined by least-squares procedures on 25 reflections (44° < 2θ < 50°). A total of 1015 unique data was collected up to $2\theta_{max}$ = 140° at 296 K. No absorption correction was applied. The structure was solved by the heavy-atom Patterson methods and expanded using Fourier techniques. All the parameters were refined by the full-matrix least-squares method anisotropically. The final R and R_w values are 0.024 and 0.030 for 859 reflections with $|F_o| > 3\sigma|F_o|$. The maximum and minimum residual peaks on the final difference Fourier map corresponded to 0.37 e $Å^{-3}$ and -0.39 e $Å^{-3}$, respectively. All calculations were performed using the teXsan programs. The atomic coordinates and thermal parameters (Table 6), bond lengths (Figure 3, p. 77), and bond angles (Table 7) are presented.

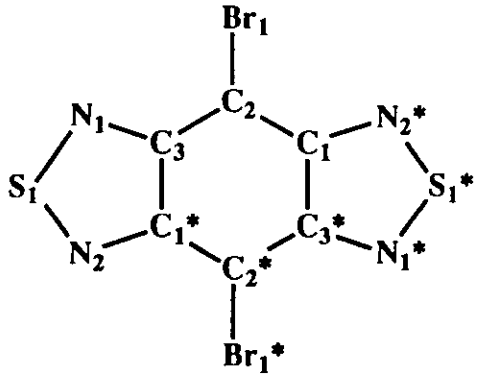

Table 6. Final atomic coordinates and equivalent isotropic thermal parameters[a] (Å2).

Atom	x	y	z	B_{eq}
Br1	0.18653 (2)	0.16149 (6)	-0.2783 (1)	2.79 (1)
S1	0.10043 (6)	-0.3869 (1)	0.2874 (3)	2.88 (2)
N1	0.1412 (2)	-0.2158 (4)	0.099 (1)	2.52 (7)
N2	0.0011 (2)	-0.3312 (4)	0.311 (1)	2.58 (8)
C1	0.0058 (2)	0.1673 (5)	-0.161 (1)	2.10 (8)
C2	0.0819 (2)	0.0688 (5)	-0.122 (1)	2.06 (8)
C3	0.0760 (2)	-0.0986 (5)	0.037 (1)	2.03 (8)

[a] $B_{eq} = (4/3)\Sigma_i\Sigma_j\beta_{ij}\boldsymbol{a}_i\cdot\boldsymbol{a}_j$.

Table 7. Bond angles (degree).

Atom	Atom	Atom	Angle	Atom	Atom	Atom	Angle
N1	S1	N2	102.0 (2)	S1	N1	C3	106.9 (3)
S1	N2	C1	106.3 (3)	N2	C1	C2	125.5 (4)
N2	C1	C3	113.0 (3)	C2	C1	C3	121.5 (3)
Br1	C2	C1	120.7 (3)	Br1	C2	C3	122.2 (3)
C1	C2	C3	117.1 (3)	N1	C3	C1	111.8 (3)
N1	C3	C2	126.8 (3)	C1	C3	C2	121.4 (3)

Electrochemical Measurements. Cyclic voltammetry was performed on a TOHO TECHNICAL RESEARCH Polarization Unit PS-07 potentiostat / galvanostat. The electrochemical measurements were carried out in distilled dichloromethane containing 0.1 mol dm^{-3} tetrabutylammonium perchlorate using Pt working and counter electrodes and a standard calomel electrode (SCE). The concentration of each sample was *ca.* 0.5 mmol dm^{-3}. The solution was degassed by argon bubbling. The scan rate was 100 mV s^{-1}. All values are given in V vs. SCE.

References and Notes

(1) (a) M. P. Cava and M. V. Lakshmikantham in *Comprehensive Heterocyclic Chemistry, Vol. 4* (Eds. : C. W. Bird, G. W. H. Cheeseman), Pergamon Press, New York, **1984**, p. 1037. (b) C. A. Ramsden in *Comprehensive Heterocyclic Chemistry, Vol. 6* (Ed. : K. T. Potts), Pergamon Press, New York, **1984**, p. 1027. (c) A. Ishii, J. Nakayama, J. Kazami, Y. Ida, T. Nakamura, and M. Hoshino, *J. Org. Chem.*, **1991**, *56*, 78. (d) A. Tsubouchi, N. Matsumura, and H. Inoue, *J. Chem. Soc., Chem. Commun.*, **1991**, 520.

(2) Y. Yamashita, K. Saito, T. Suzuki, C. Kabuto, T. Mukai, and T. Miyashi, *Angew. Chem., Int. Ed. Engl.*, **1988**, *27*, 434. Half-wave reduction potentials of **1**: E_1 = +0.10 V, E_2 = -0.82 V vs. SCE; measured at a Pt electrode in acetonitrile with 0.1 mol dm^{-3} Et_4NClO_4, scan rate 100 mV s^{-1}.

(3) (a) A. P. Komin, R. W. Street, and M. Carmack, *J. Org. Chem.*, **1975**, *40*, 2749. (b) J. Kane and R. Schaeffer, *Cryst. Struct. Commun.*, **1981**, *10*, 1403.

(4) T. Suzuki, H. Fujii, Y. Yamashita, C. Kabuto, S. Tanaka, M. Harasawa, T. Mukai, and T. Miyashi, *J. Am. Chem. Soc.*, **1992**, *114*, 3034; C. Kabuto, T. Suzuki, Y. Yamashita, and T. Mukai, *Chem. Lett.*, **1986**, 1433.

(5) Y. Yamashita, T. Suzuki, and T. Mukai, *J. Chem. Soc., Chem. Commun.*, **1987**, 1184.

(6) Only one of the possible resonance forms (e.g. **3a**) is shown for each compound. For **6** the contribution of the structure containing a tetravalent selenium atom is small.

3a:

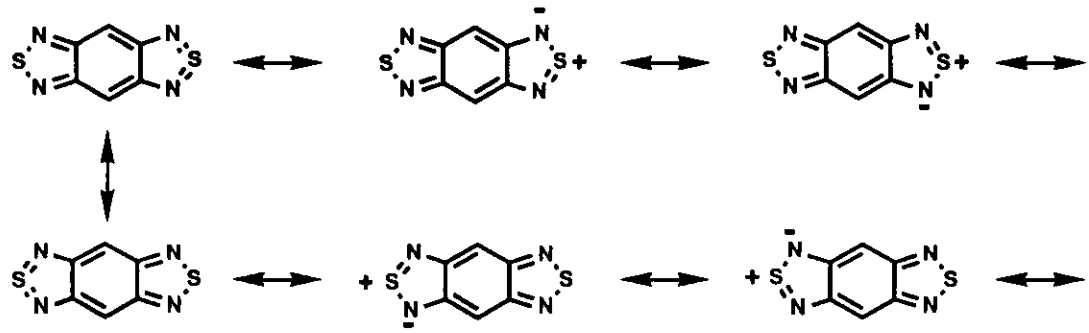

(7) T. Uno, K. Takagi, and M. Tomoeda, *Chem. Pharm. Bull.*, **1980**, *28*, 1909.

(8) Y. Tsubata, T. Suzuki, Y. Yamashita, T. Mukai, and T. Miyashi, *Heterocycles*, **1992**, *33*, 337.

(9) M. Kosugi in *Jikken Kagaku Koza*, 4th ed., *Vol. 24* (Ed.: The Chemical Society of Japan), Maruzen, Tokyo, **1992**, p. 189; J. L. Wardell and S. Ahmed, *J. Organomet. Chem.*, **1974**, *78*, 395.

(10) A. P. Komin and M. Carmack, *J. Heterocycl. Chem.*, **1975**, *12*, 829; V. G. Pesin, A. M. Khaletskii, and V. A. Sergeev, *Zh. Obshch. Khim.*, **1962**, *32*, 181.

(11) Calculated by the MNDO-PM3 method, MOPAC program, J. J. P. Stewart, *J. Comput. Chem.*, **1989**, *10*, 209, 221.

(12) A. Gieren, H. Betz, T. Hübner, V. Lamm, R. Neidlein, and D. Droste, *Z. Naturforsch. B*, **1984**, *39*, 485.

(13) S. Saito in *Jikken Kagaku Koza*, 4th ed., *Vol. 12* (Ed.: The Chemical Society of Japan), Maruzen, Tokyo, **1993**, p. 206.

(14) M. Okawara, M. Matsuoka, T. Hirashima, and T. Kitao, *Kinosei Shikiso*, Kodansha, Tokyo, **1992**, p. 134.

(15) K. Deuchert and S. Hünig, *Angew. Chem., Int. Ed. Engl.*, **1978**, *17*, 875.

Conclusion

The present thesis describes various novel types of donors and donor-π-acceptor molecules containing fused thiadiazole rings.

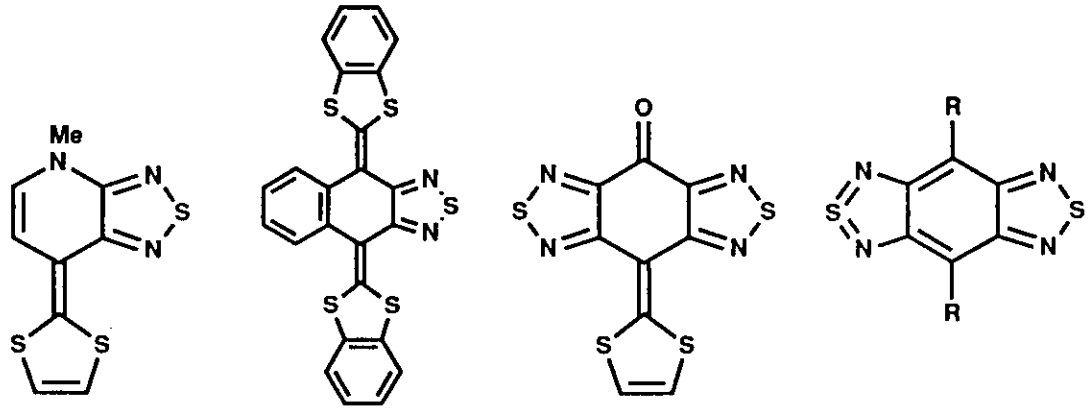

1 **2** **3** **4**

Novel electron donor, 7-(1,3-dithiol-2-ylidene)-4-methyl-4,7-dihydro[1,2,5]-thiadiazolo[3,4-*b*]pyridine **1**, was synthesized and investigated. Compound **1** was designed by introduction of a fused thiadiazole ring into an unstable electron system. It has a highly polarized structure, and the intramolecular CT bands due to the donor-π-acceptor system were observed in the absorption spectrum. The crystal has a unique columnar structure connected by short S•••S contacts. The electron-donating ability is stronger than that of TTF. The strong electron donor **1** and its derivatives gave highly conducting CT complexes and cation radical salts. The analogous compound containing two fused thiadiazole rings is of interest as an electron donor for organic conductors.

The crystal structure of nonplanar donor, 4,9-bis(1,3-benzodithiol-2-ylidene)-4,9-dihydronaphtho[2,3-*c*][1,2,5]thiadiazole **2**, was studied. The butterfly-shaped structure, which is caused by the steric hindrance between the dithiole groups and the fused benzene

ring, was demonstrated. The conformational change between the neutral and the cation radical states is small because of the intramolecular S•••N contacts arising from an electrostatic effect. The molecules uniformly make columnar stacks, and the molecular shape seems to act as a kind of template. The good electrical conductivities in the neutral and the cation radical states are ascribable to the effective molecular overlap. The intercolumnar interaction of the PF_6 salt suggests a new type of molecular network formed by nonplanar molecules.

The crystal structure and electrical behavior of 4*H*,8*H*-8-(1,3-dithiol-2-ylidene)-benzo[1,2-*c*:4,5-*c*´]bis([1,2,5]thiadiazol)-4-one **3** were investigated. Compound **3** is characterized by the highly polarized structure containing both donor and acceptor units. In the crystal the molecules are uniformly stacked, and the molecular overlap is in accord with the most effective interaction between the HOMO and LUMO, suggesting an intermolecular CT interaction. Furthermore, the molecules are three-dimensionally connected with each other through short heteroatom contacts owing to the highly polarized molecular structure. The electrical conducting behavior fails to obey Ohm's law. The current increased approximately in proportion of the third power of voltage. This result suggests that a highly polarized molecule shows unique electrical behavior in an electric field.

Novel heterocycles, benzobis(thiadiazole)s **4** and the monoselenium analogues **5** which contain a tetravalent sulfur atom, were synthesized and investigated. Compounds **4** and **5** showed high electron affinities comparable to that of *p*-benzoquinone. They were also characterized by the high electron affinities and long absorption maxima compared with those of the Kekulé-type isomer. These electronic properties are ascribable to the 14π-electron ring system containing a tetravalent sulfur atom. The crystal structure is composed of ribbon-type columns linked by heteroatom contacts to form a unique molecular network. Heterocycles **5** and **6** are expected to be applicable as organic EL devices and photosensitive materials because of their strong fluorescence emission and highly polarized structures. The nonclassical benzobis(thiadiazole) derivatives substituted

with various types of functional groups are considered to be attractive redox systems for organic conductors.

Introduction of the 1,2,5-thiadiazole rings into electron donors results in large polarization, which is helpful to stabilize the ring systems. Highly polarized molecules show interesting physical properties. Unique molecular assemblies are constructed by intermolecular interactions between polarized heteroatoms. Control of physical properties and crystal structures of such molecules seems possible by changing the polarizability affected by the charge densities on the heteroatoms.

Acknowledgments

The present work has been carried out under the supervision of Professor Yoshiro Yamashita (The Graduate University for Advanced Studies and Chemical Materials Center, Institute for Molecular Science). The author would like to express his sincere gratitude to Professor Yamashita for his kind guidance and continuous encouragement. One of the deepest impressed things is his endless and attractive ideas in research works. He introduced the author to the interesting world of the organic conductors. The author also wishes to express his deep thanks to Dr. Shoji Tanaka and Dr. Masaaki Tomura (Chemical Materials Center, Institute for Molecular Science) for their helpful advice and valuable suggestions. He studied the present work in comfort. The author is greatly indebted to Miss Sachiyo Nomura (Chemical Materials Center, Institute for Molecular Science) for her kind service of elemental analyses and mass spectra measurements. Dr. Masatoshi Kozaki, Mr. Chitoshi Kitamura, Mr. Akira Ohta, Mrs. Mari Aoyagi, and Miss Takako Kokue in the center gave him fruitful suggestions and much help. He wishes to express his heartfelt thanks to them.

The author is grateful to Dr. Kenichi Imaeda (Institute for Molecular Science) for the measurements of the electrical conductivities of the single crystals in Chapter 2 and 4. The author is greatly indebted to Professor Mizuka Sano (International Christian University) for growing the single crystals in Chapter 4. The author also would like to express his gratitude to Dr. Takanori Suzuki (Tohoku University) for his fruitful suggestions throughout this work and for conducting the X-ray crystallographic study in Chapter 3. The author wishes to express his thanks to Professor Satoshi Hirayama (Kyoto Institute of Technology) and Mr. Mitsuhiko Kono (The Graduate University for Advanced Studies) for the measurements of the fluorescence spectra in Chapter 5 and their fruitful comments. He especially had valuable discussions with Mr. Kono. The author

would like to thank Professor Koji Tanaka and Dr. Hirotaka Nagao (Institute for Molecular Science) for conducting the X-ray crystallographic study in Chapter 5.

The author is grateful to Professor Hiroshi Kato and Dr. Tomoshige Kobayashi (Shinshu University) for their valuable suggestions and encouragement.

My research work was in part supported by research fellowships from the Japan Society for the Promotion of Science for Young Scientists.

Thanks are due to all friends for supporting his life.

Finally, the author would like to express sincere gratitude to his parents, Mr. Muneaki Ono and Mrs. Takako Ono, and grandmother, Ms Kikue Ono, for their continuous support and encouragement.

November 1994

Katsuhiko Ono

List of Publications

(1) "Preparation and Properties of 7-(1,3-Dithiol-2-ylidene)-4-methyl-4,7-dihydro-[1,2,5]thiadiazolo[3,4-*b*]pyridines: Novel Donor Molecules containing a 1,2,5-Thiadiazole Unit" K. Ono, S. Tanaka, K. Imaeda, and Y. Yamashita, *J. Chem. Soc., Chem. Commun.*, **1994**, 899-900.

(2) "Nonplanar Bis(1,3-dithiole) Donors Affording Novel Cation Radical Salts" Y. Yamashita, K. Ono, S. Tanaka, K. Imaeda, and H. Inokuchi, *Adv. Mater.*, **1994**, *6*, 295-298.

(3) "Dithio-derivatives of *p*-Quinodimethanes Fused with 1,2,5-Thiadiazoles: a Novel Type of π-Donor-Acceptor System" Y. Yamashita, K. Ono, S. Tanaka, K. Imaeda, H. Inokuchi, and M. Sano, *J. Chem. Soc., Chem. Commun.*, **1993**, 1803-1805.

(4) "Benzobis(thiadiazole)s Containing Hypervalent Sulfur Atoms: Novel Heterocycles with High Electron Affinity and Short Intermolecular Contacts between Heteroatoms" K. Ono, S. Tanaka, and Y. Yamashita, *Angew. Chem., Int. Ed. Engl.*, **1994**, *33*, 1977-1979.